Contrails

AMRL-TR-68-8

DESIGN STUDY FOR RADAR LAND MASS SIMULATION SYSTEM

IVAN H. SHIM

JON I. WIGBY

ALFRED E. MLETZKO

Distribution of this document is unlimited. It may be released to the Clearinghouse, Department of Commerce, for sale to the general public.

Approved for Public Release

Contrails

FOREWORD

This study was initiated by the Behavioral Sciences Laboratory of the Aerospace Medical Research Laboratories, Wright-Patterson Air Force Base, Ohio.

The research was conducted under project 6114, "Simulation Techniques for Aerospace Crew Training," Task 611414, "Electromagnetic Systems Simulation". The research was conducted by CBS Laboratories, a Division of Columbia Broadcasting System, Inc., Stamford, Connecticut, under Contract No. F33615-67-C-1400. The Systems Development Branch, headed by Mr. I. Shim of the Intelligence Systems Department, was responsible for the effort. The principal investigator for CBS Laboratories was Mr. J. Wigby who designed the mechanical systems presented. Mr. A. Mletzko contributed the control system design. Mr. William L. Foley of the Simulation Techniques Branch, Training Research Division was the contract monitor for the Aerospace Medical Research Laboratories.

The research was started in February 1967, and was completed in October 1967.

This technical report has been reviewed and is approved.

WALTER F. GRETHER, PhD
Technical Director
Behavioral Sciences Laboratory
Aerospace Medical Research Laboratories

Approved for Public Release

Contrails

ABSTRACT

A design study and investigation to determine the requirements for the mechanical and electrical components of a Radar Land Mass Transparency System has been performed. The technique consists of moving a laser beam across a 122 cm square transparency to simulate the side-looking radar system of an aircraft. The most promising system of those considered from accuracy, complexity and cost considerations is shown to be a horizontally driven transparency with a vertically driven flying spot scanner. The spot, in its vertical heading, scans out a strip 5 cm wide. Spot size can be kept to 2.5 microns over the 5 cm scan length at any location on the transparency. Smoothness of motion to simulate an aircraft is achieved through a feedback control system designed to move at constant velocity. An overriding position loop will correct for any accumulated errors which could result from environmental or load condition changes. A position accuracy of $\pm$ 0.00127 cm over the entire transparency is shown to be quite feasible. In addition, the speed range from low flying aircraft to satellites of approximately 100:1 is also shown to be feasible using the same system. Mechanical and electrical components chosen for performance calculations and tolerance determinations are off-the-shelf. These parts are easier to acquire and lower in cost than equivalent custom made components.

Approved for Public Release

Contrails

TABLE OF CONTENTS

	PAGE
SECTION I - INTRODUCTION	1
SECTION II - SYSTEM DESIGN SELECTION	3
SYSTEM DESIGN CHARACTERISTICS	4
SECTION III - MECHANICAL SYSTEM ANALYSIS	7
SYSTEM A	7
SYSTEM B	7
SYSTEM C	11
SYSTEM D	11
SYSTEM D SELECTED	17
SECTION IV - MECHANICAL SYSTEM COMPONENTS	19
LASER	19
MIRRORS	19
GAS BEARING	19
HEADING CONTROL BEARINGS	21
LINEAR BEARINGS AND GUIDEWAYS	21
SWIVEL COUPLING	23
LEAD SCREW	23
HEADING CONTROL	24
OPTICAL WINDOW	24
GUIDEWAYS	24
PMT AND LIGHT PIPE	27
LUBRICATION	27
LINEAR CONTROLLER	31
STRUCTURES	31
OPTICAL FOCUS CONTROL	33

Approved for Public Release

Contrails

TABLE OF CONTENTS (continued)

	PAGE
Factors Affecting Focus in the x Drive System	33
Factors Affecting Focus in the y Drive System	33
Conclusion to Focus Control	34
POSITION ACCURACY IN THE X DIRECTION	34
POSITION ACCURACY IN THE Y DIRECTION	40
FILM HANDLING	43
TEMPERATURE AND HUMIDITY EFFECTS	43
PMT DRIVE SYSTEM	45
Conclusion On Position Accuracy	46
SECTION V - SYSTEM MAINTAINABILITY	47
SELECTION OF BEARINGS, COMPONENTS, AND MECHANISMS	47
Component Service Life	47
Periodic Maintenance	47
Alignment and Adjustment	47
Conclusions	49
SECTION VI - DUAL TRANSPARENCY READOUT SYSTEM	49
SECTION VII - CONTROL SYSTEM DESIGN	51
CONTROL REQUIREMENTS	51
SYSTEM DESIGN	51
Constants and Variables	53
VELOCITY SENSITIVE SYSTEM DESIGN	53
Motor Transfer Function	57
Tachometer Transfer Function	59
Compensation Networks	67
Torque Rejection Characteristic	69

Approved for Public Release

Contrails

TABLE OF CONTENTS (continued)

	PAGE
Step Torque Response	75
POSITION SENSITIVE SYSTEM DESIGN	81
Loop Gain Calculations	81
APPENDIX I - LOAD TORQUE ANALYSIS OF X-Y MOTION SYSTEMS	89
GENERAL	89
TORQUE ANALYSIS - HORIZONTAL MOTION SYSTEM	89
TORQUE ANALYSIS - VERTICAL MOTION SYSTEM	93'
TORQUE ANALYSIS - HEADING CONTROL MOTOR	95
TORQUE LOAD CAUSED BY CENTER OF GRAVITY	97
WINDAGE TORQUE ON SCANNER DISC	100
APPENDIX II - STRUCTURAL LOADS AND DEFLECTIONS	101
GENERAL	101
DEFLECTION OF HORIZONTAL I-BEAM BY FILM TRANSPARENCY SUPPORT	101
DEFLECTION OF VERTICAL I-BEAM BY SCANNER CARRIAGE	107
HORIZONTAL AND VERTICAL RECTANGULAR GUIDEWAY DEFLECTION	111
ELONGATION OF SCANNER TOP SUPPORT STRUCTURE	113
ELONGATION OF SCANNER LOWER STRUCTURE	115
LATERAL DEFLECTION OF TOP SCANNER SUPPORT MEMBER	115
DEFLECTION OF OPTICAL WINDOW DURING LOADING	117
APPENDIX III - INERTIA	119
LEAD SCREW INERTIA	119
SCANNER CARRIAGE INERTIA	119
FILM TRANSPARENCY SUPPORT INERTIA	120
VERTICAL GUIDEWAY ASSEMBLY CENTROID AND INERTIA CALCULATION	121
HORIZONTAL GUIDEWAY ASSEMBLY CENTROID AND INERTIA CALCULATION	122

Approved for Public Release

Contrails

TABLE OF CONTENTS (concluded)

	PAGE
APPENDIX IV - WEIGHT	123
WEIGHT OF GLASS	123
WEIGHT OF FRAMEWORK	123
WEIGHT OF STEEL CHANNEL	123
WEIGHT OF HORIZONTAL GUIDEWAY ASSEMBLY	124
WEIGHT OF VERTICAL GUIDEWAY ASSEMBLY	125
APPENDIX V - SYSTEM VIBRATION	127
GENERAL	127
VIBRATION ANALYSIS OF SCANNER SHAFT AND DISC	127
SCANNER GAS BEARING NATURAL FREQUENCY	130
NATURAL FREQUENCY OF HORIZONTAL GUIDEWAY ASSEMBLY	130
NATURAL FREQUENCY OF VERTICAL GUIDEWAY ASSEMBLY	131
LINEAR BEARING NATURAL FREQUENCY	132
LEAD SCREW NATURAL FREQUENCY	133

Approved for Public Release

Contrails

LIST OF ILLUSTRATIONS

FIGURE NUMBER	TITLE	PAGE
1	SIMPLIFIED RADAR SIMULATOR DIAGRAM	5
2	SYSTEM A X-Y TRANSLATING SCANNER	9
3	SYSTEM B X-Y TRANSLATING TRANSPARENCY	10
4	SYSTEM C X-Y TRANSLATING SCANNER	13
5	SYSTEM D X TRANSLATING TRANSPARENCY Y TRANSLATING SCANNER	14
6	TRANSPARENCY READOUT SYSTEM	17
7	MIRROR CONFIGURATION	18
8	LINEAR ROLLER BEARING	20
9	MODIFIED ACME LEAD SCREW THREADS	22
10	TRANSPARENCY DRIVE AND LEAD SCREW ASSEMBLY	25
11	VERTICAL LEAD SCREW AND SCANNER MODULE ASSEMBLY	26
12	PHOTOMULTIPLIER AND GUIDEWAY ASSEMBLY	28
13 (1 of 2)	STRUCTURE ASSEMBLY	29
13 (2 of 2)	STRUCTURE ASSEMBLY	30
14	CUTAWAY VIEW OF SCANNER AND HEADING CONTROL ASSEMBLY	32
15	SCANNER ASSEMBLY	35/36
16	DYNAMIC DEFLECTION PLOT OF THE VERTICAL GUIDEWAY IN THE X DIRECTION	39
17	DYNAMIC DEFLECTION PLOT OF THE HORIZONTAL GUIDEWAY IN THE Y DIRECTION	42
18	SIMULATOR WITH WINDOW LOWERED FOR CHANGE OF FILM TRANSPARENCIES	44
19	DUAL TRANSPARENCY READOUT SYSTEM	48
20	CONSTANT SPEED FEEDBACK CONTROL SYSTEM	50
21	BASIC VELOCITY SERVO	52

Approved for Public Release

Contrails

LIST OF ILLUSTRATIONS (continued)

FIGURE NUMBER	TITLE	PAGE
22	DETERMINATION OF AMPLIFIER GAIN K_A	60
23	INERTIA WHEEL DIAMETER VS. LENGTH FOR CONSTANT INERTIA OF 2365 GM-CM-SEC^2 (33 OZ-IN.-SEC^2)	64
24	BODE PLOTS OF LOOP RESPONSE AND CORRECTIVE NETWORK RESPONSE	66
25	BODE PLOT OF LOOP RESPONSE WITH CORRECTIVE NETWORKS ADDED TO LOOP	68
26	BODE PLOT OF OPEN LOOP RESPONSE	70
27	UNCOMPENSATED VELOCITY SENSITIVE SERVO LOOP	72
28	VELOCITY SENSITIVE SERVO WITH LOAD TORQUE DISTURBANCE	73
29	BODE PLOT OF $1 + 2\xi \frac{s}{w} + (\frac{s}{w})^2$	74
30	TORQUE REJECTION CHARACTERISTIC	76
31	VELOCITY SYSTEM RESPONSE TO UNIT STEP TORQUE DISTURBANCE OF 72.1 GM-CM (1 OZ-IN.)	77
32	DISPLACEMENT OF SPOT DUE TO 72.1 GM-CM (1 OZ-IN.) STEP TORQUE DISTURBANCE	78
33	DISPLACEMENT DUE TO 72.1 GM-CM (1 OZ-IN.) STEP TORQUE VELOCITY SERVO LOOP	79
34	POSITION CORRECTION LOOP	80
35	DIGITAL TO ANALOG CONVERTER OUTPUT	82
36	FRICTION TORQUE BACK EMF MOTOR CHARACTERISTIC	84
37	BODE PLOTS FOR POSITION LOOP	86
38	LOOP FOR DETERMINATION OF AMPLIFIER CONSTANT $K_A K'_A$	88
39	LEAD SCREW TORQUE VS. LOAD	90
40	OFF-CENTER LEAD SCREW MOUNTING	98
41	OPTICAL WINDOW DEFLECTION	102
42	HORIZONTAL I-BEAM LOAD DIAGRAM	103

Approved for Public Release

Contrails

LIST OF ILLUSTRATIONS (concluded)

FIGURE NUMBER	TITLE	PAGE
43	VERTICAL I-BEAM LOAD DIAGRAM	106
44	GUIDEWAY SECTION LOAD DIAGRAM	110
45	SCANNER TOP SUPPORT STRUCTURE LOAD DIAGRAM	112
46	SCANNER BOTTOM SUPPORT STRUCTURE LOAD DIAGRAM	114
47	SCANNER TOP SUPPORT SIDE MEMBER LOAD DIAGRAM	116
48	SCANNER DRIVE MOTOR SHAFT DISPLACEMENT	126

LIST OF TABLES

TABLE	TITLE	PAGE
I	SYSTEM A: RADAR LAND MASS SIMULATOR TRADE-OFF STUDY	8
II	SYSTEM B: RADAR LAND MASS SIMULATOR TRADE-OFF STUDY	12
III	SYSTEM C: RADAR LAND MASS SIMULATOR TRADE-OFF STUDY	15
IV	SYSTEM D: RADAR LAND MASS SIMULATOR TRADE-OFF STUDY	16
V	FOCUS CONTROL	37
VI	HORIZONTAL DRIVE SYSTEM - SYSTEMATIC ERRORS	38
VII	VERTICAL DRIVE SYSTEM ERRORS	41
VIII	LIST OF CONSTANT USED	54
IX	SYSTEM NATURAL FREQUENCIES	128

Approved for Public Release

Contrails

SECTION I

INTRODUCTION

The operational usefulness and economy of radar simulation is only realized if the simulations achieve a realism that is representative of actual sensor performance. This has been the case with the plan position indicator (PPI) system simulations. The advent of side-looking radar with its greatly increased resolution coupled with the greater speed and range of host aircraft has, however, invoked the need for new and better simulation techniques.

Radar system technology has made rapid progress in recent years as a result of technological advances that have permitted the development of efficient high power transmitters, low noise receivers, compact antennas, and improved signal processing techniques. Operational system capabilities have advanced from the simple low resolution PPI systems to the sophisticated side-looking systems capable of resolving, with fidelity adequate for detection and identification purposes, targets of greater military significance.

The PPI radar systems were developed and extensively used as an aid to navigation where the relatively low system resolution was adequate for detecting the relatively large and permanent features of the terrain necessary for navigation purposes. It became apparent, however, that under certain conditions of weather and/or darkness, the radar system would be the only sensor usable for weapon launch purposes. Thus, procedures were established using the PPI sensor with its gross resolution to establish target reference points, aiming points, and bomb release points in order that successful bombing runs could be carried out regardless of darkness or inclement weather conditions.

While the all weather, day-night nature of the radar sensor was thereby demonstrated and successfully employed, it is within the last few years that its ground resolving capability has approached that necessary for the detection and identification of military targets. With greater resolvency power, the identification of military targets, whose nature and location were not known beforehand, carries the degree of confidence necessary to warrant responsive action.

The fact that radar is an all weather sensor and that the resolving capability of the then existing systems was not limited by basic physical laws provided the impetus for an extensive and comprehensive development program which resulted in the side-looking airborne radar systems now in operation. The basic objectives of that program were to develop radar systems capable of collecting needed intelligence under adverse lighting and weather conditions and, eventually, with the development of suitable display and support systems, to provide the foundation for an all weather, day or night reconnaissance strike capability. That the first objective has been met is amply demonstrated in the intelligence collected daily by operational SLAR systems employed by all of the military services. Experience gained with those systems, together with continued improvements in resolution, dynamic range, geometrical fidelity, and

Approved for Public Release

Contrails

stand-off range, have shown that the second objective, that of an all weather reconnaissance-strike capability using radar as the basic sensor, will be feasible in the near future. In fact, programs for the development of auxiliary subsystems (e.g., in-flight signal processing, mensuration, and displays) and support systems (e.g., precise navigation and guidance systems, weapon systems) are underway to bring this much needed capability closer to operational reality.

Since a radar system depicts information within its field of "view" as a function of the reflective properties of the constituent elements at radar wavelengths, the scene rendition differs considerably from that normally perceived by the human eye when the field is illuminated by light. Thus the operator of a radar system must be trained in the use and interpretation of information presented by a radar display. Effective techniques for simulating PPI radar returns and displays have been developed and are in extensive use. These techniques prove economical because they permit simulation of a wide range of flight conditions. They are operationally necessary because they permit simulation of terrain areas not normally accessible to aircraft overflight.

Approved for Public Release

Contrails

SECTION II

SYSTEM DESIGN SELECTION

The feasibility of the components and techniques employed in the radar simulation system has been evaluated and demonstrated under previous study programs. The objective of the program is, through the study and analysis of alternative approaches, to recommend methods of radar simulation system implementation that will permit the following:

- Simulation of side-looking radar imagery for use in training image interpreters in the characteristics and uses of SLAR imagery.
- Simulation of a real-time side looking radar display. This display would be used as a part-task trainer for air crew members slated for assignment to reconnaissance-strike aircraft or other vehicles requiring in-flight analysis of side-looking radar imagery.
- Simulation of a real-time side looking radar display which is a component part of a total system simulator. This display would be used, in concert with the controls and displays associated with all support systems, in the training of operator personnel who will be crew members of reconnaissance-strike vehicles.

The basic criteria for the evaluation of the alternative approaches was that the resulting system be equally applicable to each phase of radar simulation. For example, the simulator must be able to produce simulated radar strip maps which would find immediate operational use in the training of image interpreters. The same basic simulator must be usable in the simulation of in-flight displays which will be necessary when the in-flight display of side looking radar data becomes an operational capability. Likewise, the same basic simulator must be usable as a subsystem in a total system simulator for a reconnaissance-strike vehicle wherein the operator and all other crew members are exposed, in realistic work station environments, to all situations likely to be encountered in a mission. Thus, the simulator must have inherent within its design, a range of mechanical, optical, and electronic capabilities that will permit its adaptation to the simulation situation for which it is employed. The nature of side looking radar and the requirements for realistic simulation were recognized as problem areas which could not be solved by available technology. Sensor resolution, resolution elements per return, and area of coverage were problems which did not seem to have solutions. A series of study programs were undertaken by the Aerospace Medical Lab with CBS Laboratories, to study and breadboard techniques which would offer suitable means to simulate display presentation of SLAR systems.

The first problem undertaken was the investigation of a suitable high resolution scanning technique. This program, the "Optical Spot Size Study for Data Extraction from a Transparency" under Contract number AF 33(615)-2355, demonstrated that a focused laser beam can be employed in a scanning configuration to resolve 256 lp/mm, and discern 30 shades of gray. The system consisted of a laser, beam expander, rotating lens scanner, light collector and photomultiplier tube. A subsequent program, the "Development of High-Speed Low

Approved for Public Release

Contrails

Jitter Scanning Technique for Application to Radar Simulation" under contract number AF 33(615)-3458, demonstrated that the scanner can meet the stringent jitter requirements necessary for an undistorted display. At a scan rate of 500 scans per second and a bandwidth of 5 MHz, longitudinal and transverse jitter could be held to less than one-fourth of a resolution element. This system employed a six-lens rotating disk supported by a hydrostatic air bearing. Resolution and signal-to-noise ratio were comparable with the initially developed system.

Even though the scanner fulfilled the requirements initially set forth, there was a void in the area of transparency preparation. This problem was two-fold. There was the recorder itself which had to transfer input data onto the transparency and encode each data element in the form of a gray shade. Secondly, there was the problem of obtaining source data at the desired resolution, and processing it to obtain the necessary format, scale, and continuity required by the transparency. The first of these two problems was studied under Contract AF 33(615)-5408. The system that resulted from this study was a rotating drum recorder fed by an input digital tape or other forms of digital inputs. A preliminary study of the second problem showed that a great deal of source data exists, but not in a form lending itself to a simple method of combination and collation.

The purpose of this study effort is to incorporate the rotating disk laser scanner into a transparency motion system and thereby effect a relative x-y-ψ motion of the scan line relative to the transparency. Not only must the motion be near measuring system accuracy, but smoothness must be such that line banding effects are not present. The mechanical structure must be designed to maintain focus over the entire 122 cm x 122 cm (48 in. x 48 in.) transparency area. Scanner resolution must be retained at the 200 lp/mm level and free of vibrations. In addition the system must allow operator access for loading and unloading transparencies and of course, be reasonable in cost.

SYSTEM DESIGN CHARACTERISTICS

The design characteristics of the system is 1) to move a scanner over the surface of a large transparency, and 2) extract encoded data in the form of grey shade variations. The general overall parameters of such a system are:

Film Transparency size and range of motion	122 cm x 122 cm (48 in. x 48 in.)
Motion accuracy	0.00254 cm (0.001 in.)
Speed range of simulated flight over transparency	100:1
Inputs to simulator	Heading (ψ), x, y Position, V_x, V_y Velocity components

Approved for Public Release

Contrails

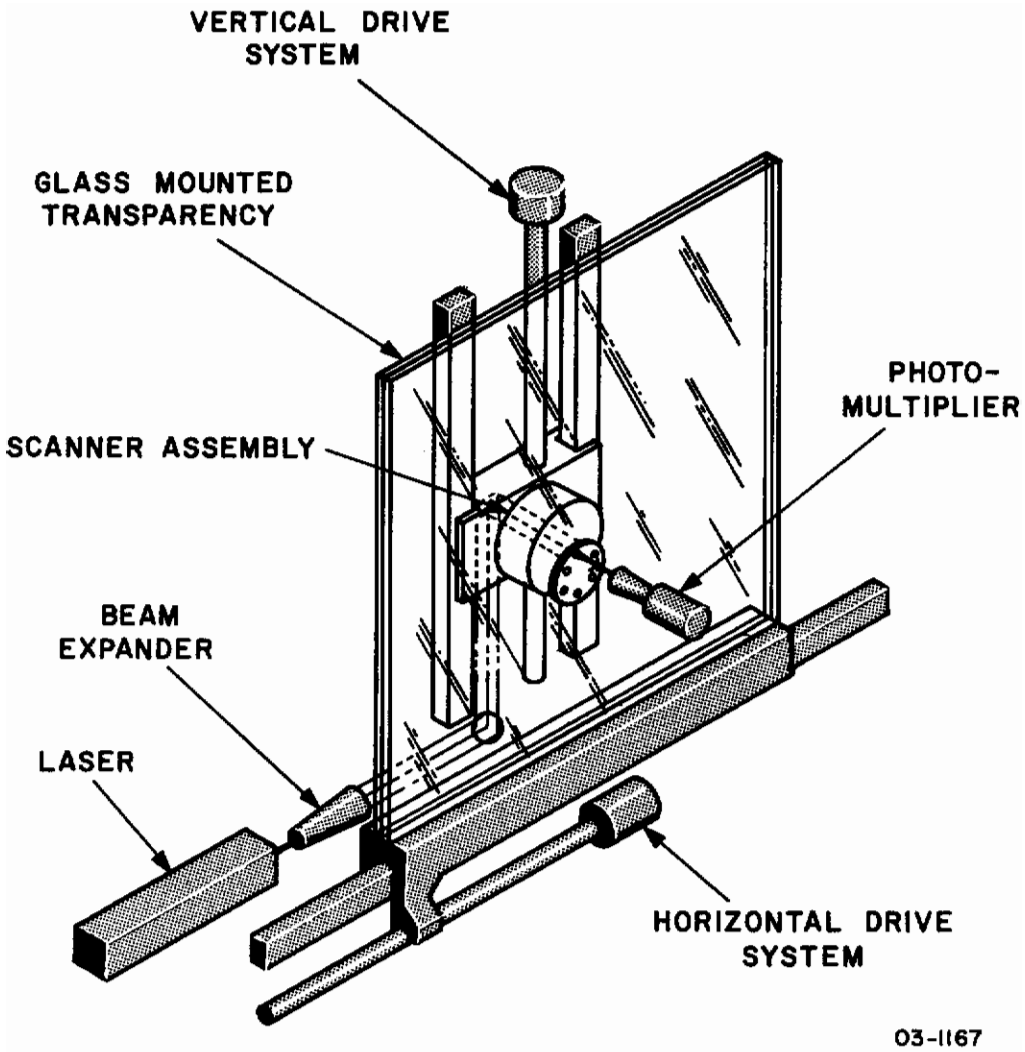

Figure 1 SIMPLIFIED RADAR SIMULATOR DIAGRAM

Approved for Public Release

Contrails

Line Pitch Variation	10% max.
Scan Jitter	one-fourth resolution element

The design which evolved from a study of a number of configurations is not markedly different from presently adopted configurations as illustrated in Figure 1. The transparency is sandwiched between glass plates and supported in the vertical plane by a horizontal motion transport system. The laser scanner faces the transparency and is mounted on a vertically directed transport. The scanner is rotatable about its optical axis to simulate aircraft heading. The vertical motion of the scanner is coupled to the light collecting photo-multiplier tube and follows the path of the scanner over the plane of the transparency.

The approach to this study was to develop a modular building block concept rather than utilize highly rigid structure material such as large cast iron frameworks or granite base or tables. The system constraints established at the outset of the program and a preliminary analysis showed that the requirements could be met by this approach. The bulk of the study examined the mechanical rigidity and the electronic sensor stability of the entire system design.

Information is encoded on transparencies in terms of a density value for each discrete data point. The number of density values permissible is a function of the system noise consisting principally of film and detector noise. For this particular system, it was assumed that 20 gray levels would be encoded and the density range would be greater than 2.0.

Approved for Public Release

Contrails

SECTION III

MECHANICAL SYSTEM ANALYSIS

The first portion of this report is devoted to a discussion of system configurations which may be employed to fulfil the overall objective. Each approach was studied from an analytical basis. Comparison tables were generated to show the advantages and disadvantages of one system with respect to another. A configuration was selected on the considerations shown in these tables. Among these are x and y drive accuracy, friction and frictional variations, temperature and humidity effects, dynamic speed range, human factor considerations, alignment, maintainability, and cost.

The basic function of the radar simulation system is to electromechanically move a laser generated line scan across the film transparency to simulate side-looking radar of an aircraft. This line scan, which is continuously moving, is simulating an aircraft both in heading and speed over a transparency. A scale of approximately 1:3,000,000, simulates aircraft range and field of maneuver. A two inch wide scan simulates the side looking radar range. This scan is generated by a rotating disc scanner which utilizes f/2 lenses focused to 2.5 micron spots. Each 5 cm (2 in.) line is laid down at 500 cycles per second. Transmitted light is collected by a light pipe photomultiplier tube combination. The output of the photo-multiplier tube is fed to video amplifying circuits.

The study program was evolved from the three basic system configurations proposed in the initial CBS proposal. The schematic representations of these basic configurations in turn evolved into four system concepts. Each system was considered in a number of critical areas and the results listed in tabular form. A description of each system is discussed in the following paragraphs.

SYSTEM A

The configuration illustrated in Figure 2 employs a concept where the transparency is fixed on a horizontal plane and the scanner is translated in two directions. Both tables would be driven by lead screws and supported by conventional VEE guide ways with rollers for smooth and precise tracking. The transparency is easily handled and positioned on the horizontal glass table. Thus, its basic advantages are the ease of loading film, and the greater operator accessibility. Its key disadvantages lie in unequal x and y driving torque requirements due to the pyramid table construction. The glass support deflects 50 microns (0.002 in.) even with a one inch glass section. The f/2 lenses utilized to achieve a 2.5 micron spot limits focal depth variations to $\pm$ 5 microns. The 50 microns deflection places an additional focus control requirement on the system. Table I presents the essential characteristics of this design.

SYSTEM B

System B is very similar to system A except the transparency is x-y controlled. As in other systems, the scanner rotates about the optical axis to achieve a heading change. This system configuration is extremely large. It has

Approved for Public Release

Contrails

TABLE I

SYSTEM A

RADAR LAND MASS SIMULATOR TRADE-OFF STUDY

FACTORS	HORIZONTAL TRANSPARENCY TRANSLATING X-Y SCANNER
Size/Weight/Inertia:	137 cm x 221 cm x 178 cm (54 in. x 87 in. x 70 in.) Very heavy - low inertia
Guide Ways:	"V" Guides with rollers Very accurate but expensive
Driving Mechanism:	1-1/4 in. dia. Moore Lead Screws
Scanner Mechanism:	6 Objective lenses mounted on an air bearing supported disc whole unit supported on Heading controlled mount.
Supply Lines, Air & Electric:	6 ft long x - y traversing supply lines with swivel coupling & slip rings
Optical System:	
Laser Position	335 cm (132 in.) from scanner (max)
Beam Expander	12 in. lg telescopic unit
Mirrors	3 mirrors-unstable-high loss
Objective Lenses	super ground to compensate for window thickness and deflection
Optical Window	1-3/8 in. total thickness - high degree of imperfection - sags 0.0025 in. due to its own weight.
Film Handling:	Operator needs but to move hinged PMT & open top glass & lay print down flat, easy to load.
Spot Position Accuracy:	
X Direction	0.0025 cm (0.000970 in.) — Perturbations due to PMT rods, air & electric line, and scanner gyroscopic motions.
Y Direction	0.0025 cm (0.000970 in.)
ψ Heading	1/10° - fairly stable
Focus Control:	Difficult to maintain $\pm$ 5 μ due to optical window sag
Ease of Fabrication:	Large special castings required - alignment difficult
Cost of Fabrication:	High cost - long lead time
Temperature Effects:	Stratification uniform on lead screws & film
Torque:	Unequal load torque on drive motors

Approved for Public Release

Contrails

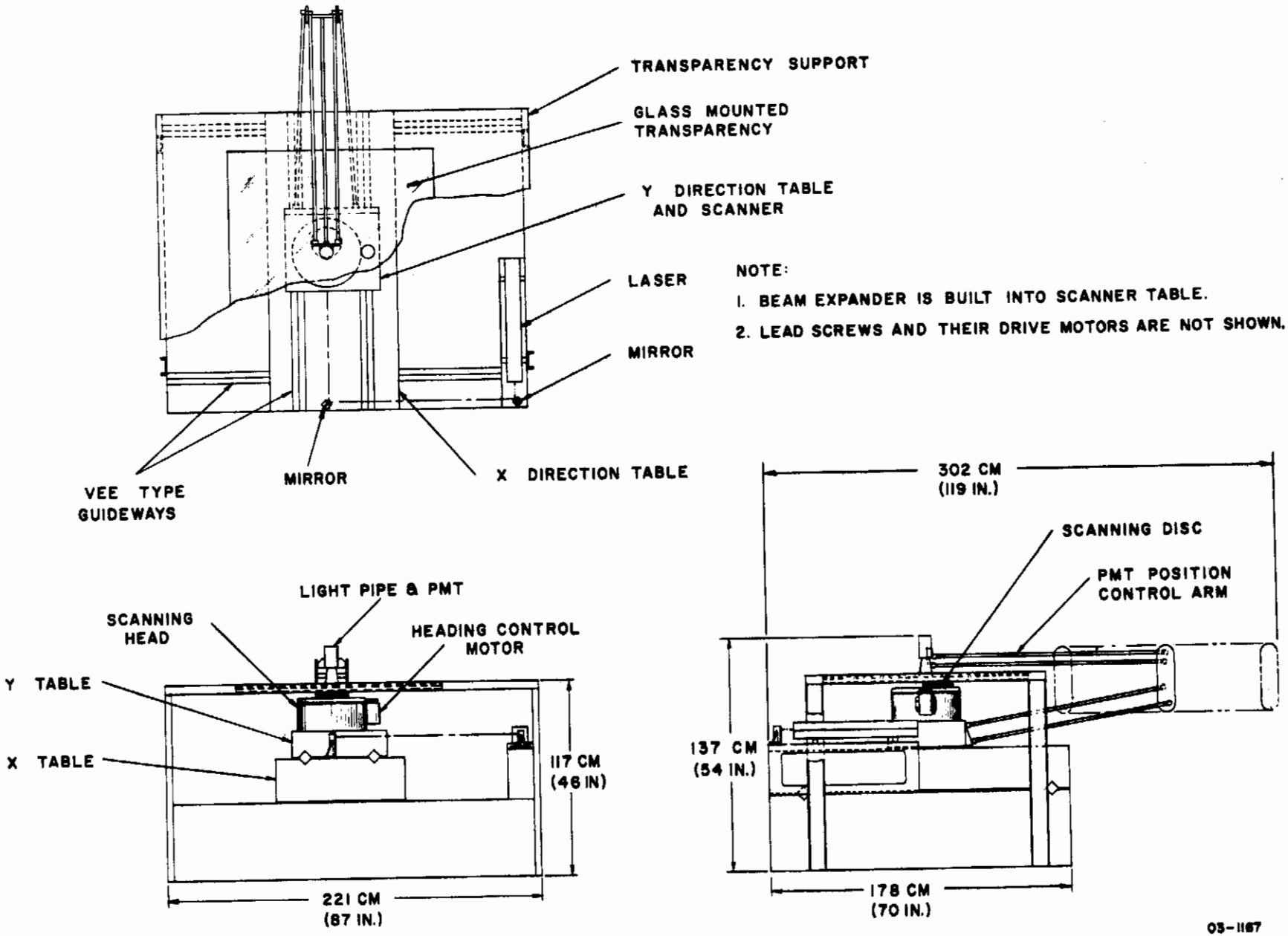

Figure 2 SYSTEM A X-Y TRANSLATING SCANNER

Approved for Public Release

Contrails

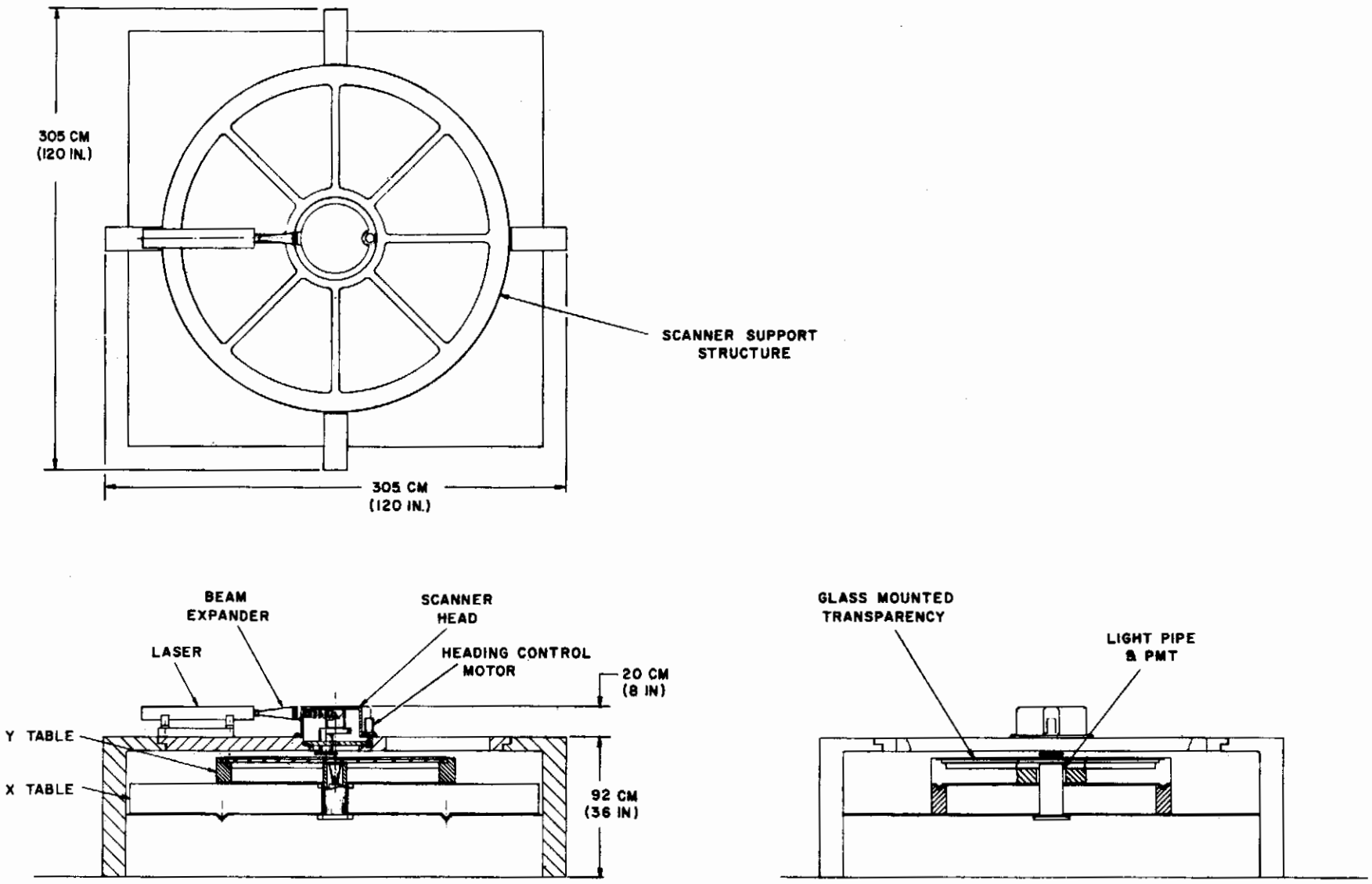

Figure 3 SYSTEM B X-Y TRANSLATING TRANSPARENCY

03-1167

Approved for Public Release

Contrails

overall dimensions of 305 cm (120 inches) square and approximately 112 cm (44 in.) high, and consequently has a high load inertia. The guide ways and drive system is similar to system A. Loading of this system is complicated by the overhead mounting of the scanner, as illustrated in Figure 3. This simulator is less complex in design since supply gas lines, electrical lines and the photomultiplier are stationary. This system, however, suffers from unequal x-y drive torques and complexity of focus control to account for film support sag. In addition, the top table must have two driving lead screws or be counter balanced to account for the offset center of gravity. Frictional perturbations can also arise due to higher frictional loads. Table II gives pertinent design characteristics.

SYSTEM C

System C features a vertically mounted transparency with a translating x-y scanner. The overall size is approximately 196 cm (77 inches) deep, 228 cm (90 inches) wide and 287 cm (113 inches) high. Its scanner is driven and guided in a similar manner to that of system A. Coordinated control of PMT is attained by a mechanical link for the vertical drive and a lead screw horizontal drive. The horizontal coupling between scanner motion and lead screw is a source of trouble. The height of the unit presents a stability problem in addition to long optical focal path and lengthy gas and electric supply lines. As in system A, pyramiding of x - y drive tables creates torque inequalities between the two directions of motion. This system is illustrated in Figure 4 and the design characteristics are listed in Table III.

SYSTEM D

This system is depicted in Figure 5. The transparency is mounted vertically to eliminate film sag in the focal plane, and is driven horizontally by a precision acme lead screw and drive motor similar to system A. Horizontal guiding is achieved by rectangular guide ways and linear roller bearings. The scanner is driven vertically in the y-direction by a precision acme lead screw and drive motor and is also guided by rectangular guide ways and linear roller bearings. Since the drives are not stacked one on the other, they are mechanically independent, resulting in equal x-y driving torques. In addition, the maintenance of focus, low inertia, ease of film handling, ease of fabrication and the reasonable size 76 cm x 203 cm x 305 cm (30 in. x 80 in. x 120 in.) make this a desirable configuration. Table IV summarizes the essential characteristics of this system and Figure 6 illustrates a transparency readout system.

One of the main attributes of this configuration is that it is expandable to a dual transparency scanner. Essentially, the depicted configuration is one-half of the expanded system. Scanning, heading control, scanner translation, laser, and beam expander would be common while transparency mount, transparency drive and light collector would be duplicated. The expanded system remains attractive in all aspects of evaluation. Transparency loading, alignment and accuracy are superior to other configurations.

Approved for Public Release

Contrails

TABLE II

SYSTEM B

RADAR LAND MASS SIMULATOR TRADE-OFF STUDY

FACTORS	HORIZONTAL TRANSPARENCY TRANSLATING X - Y TRANSP.	
Size/Weight/Inertia:	112 cm x 305 cm x 305 cm (44 in. x 120 in. x 120 in.) very heavy - medium inertia	
Guide Ways:	Same as System A	
Driving Mechanism:	Same as System A	
Scanner Mechanism:	Same as System A	
Supply Lines, Air & Electric:	Stationary lines swivel air coupling & electrical slip rings.	
Optical System:		
Laser Position	76 cm (30 in.) from scanner	
Beam Expander	Same as System A	
Mirrors	1 Mirror - very stable - low loss	
Objective Lenses	Same as System A	
Optical Window	Same as System A	
Film Handling:	Difficult to load - Scanner structure is in the way thus reducing opening to slip print in place	
Spot Position Accuracy:		
x Direction	0.0025 cm (0.000970 in.)	Possible perturbations due to eccentric mounting of lead screws
y Direction	0.0025 cm (0.000970 in.)	
ψ Heading	1/10 in. - fairly stable	
Focus Control:	Same as System A. Systems A & B require glass support or a focus control system. A focus control system adds mech. errors.	
Ease of Fabrication:	Same as System A	
Cost of Fabrication:	Same as System A	
Temperature Effects:	Same as System A	
Torque:	Unequal load torques on motors	

Approved for Public Release

Contrails

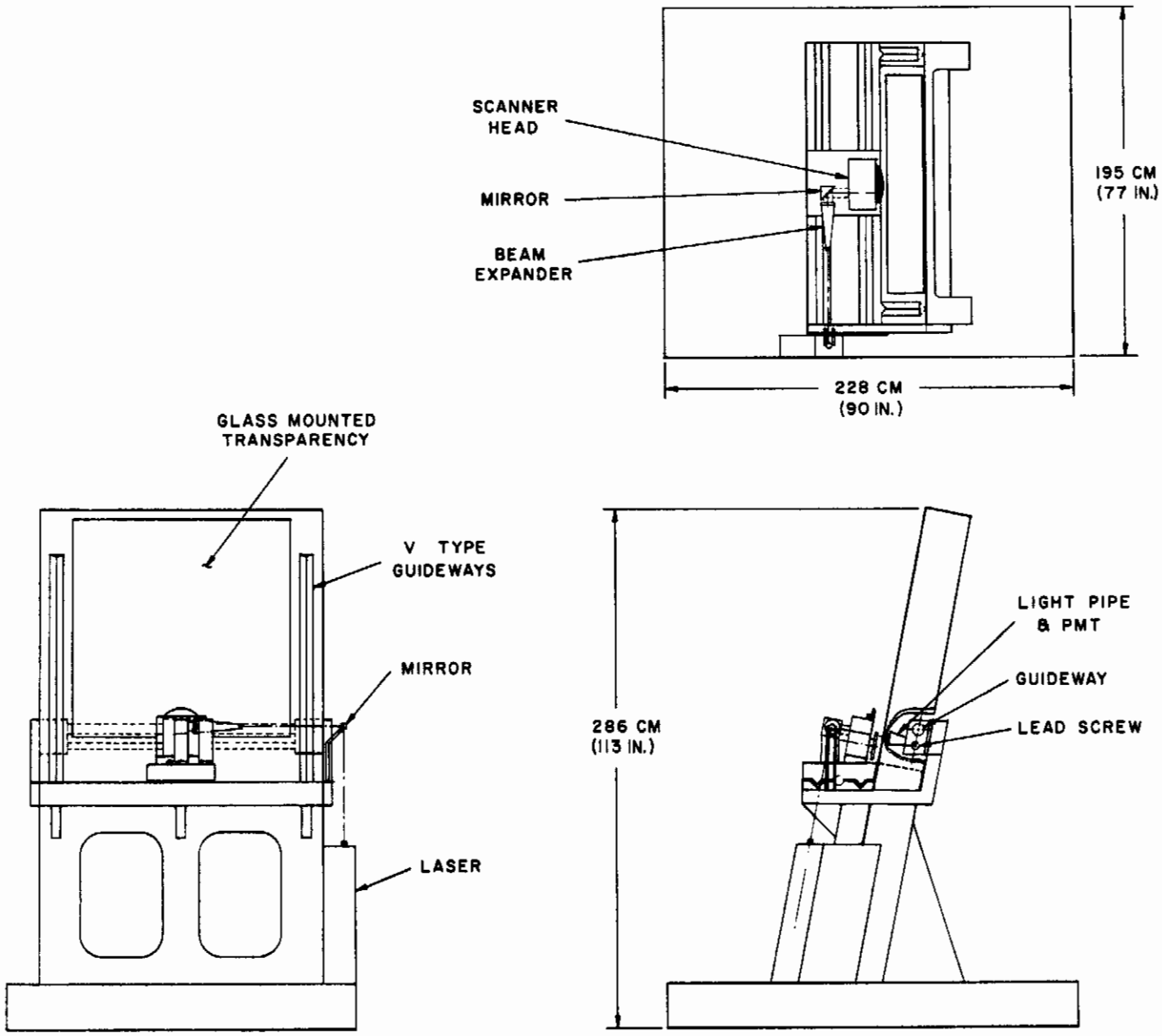

Figure 4 SYSTEM C X-Y TRANSLATING SCANNER

Approved for Public Release

Approved for Public Release

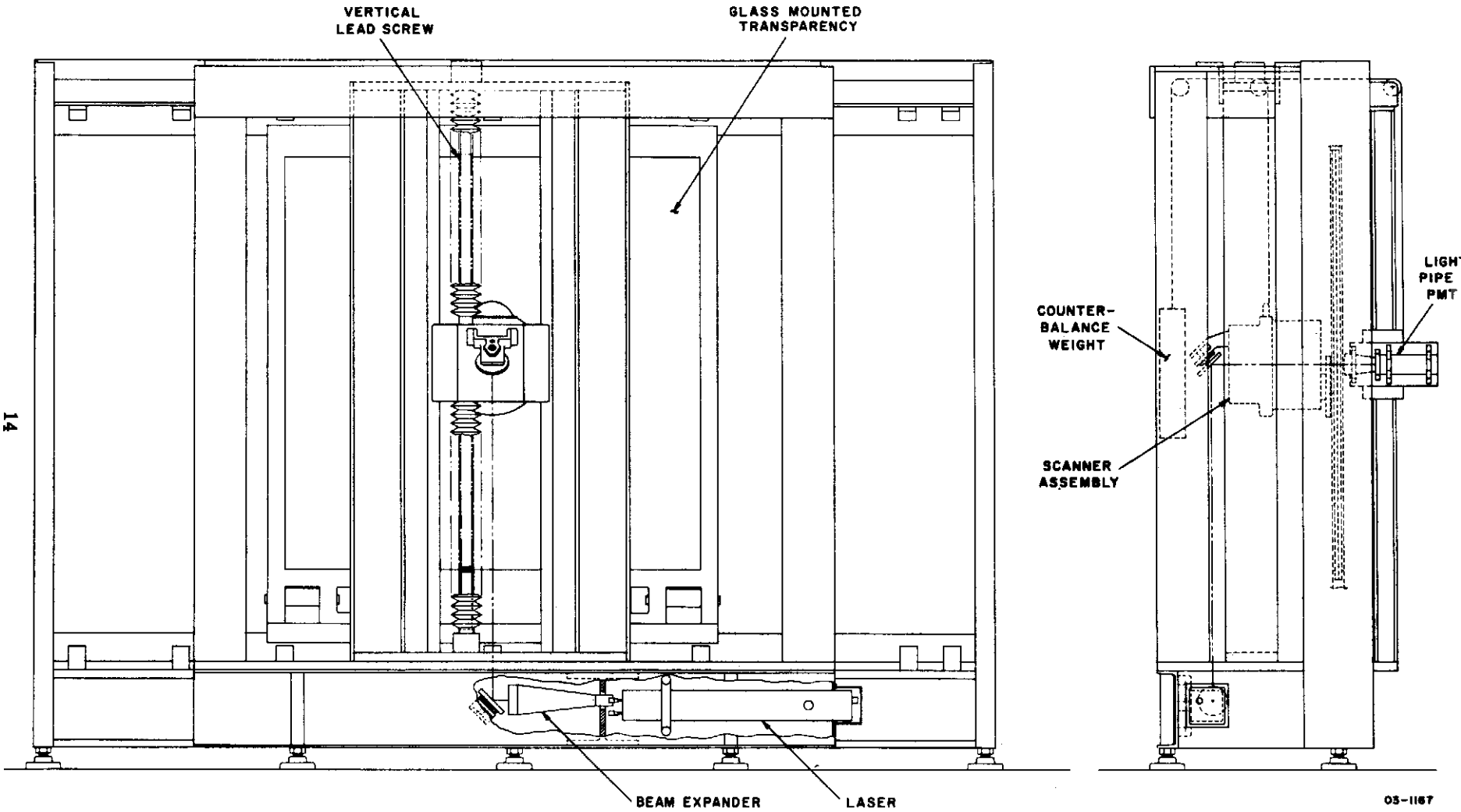

Figure 5 SYSTEM D X TRANSLATING
TRANSPARENCY
Y TRANSLATING SCANNER

Contrails

TABLE III

SYSTEM C

RADAR LAND MASS SIMULATOR TRADE-OFF STUDY

FACTORS	VERTICAL TRANSPARENCY TRANSLATING X - Y SCANNER
Size/Weight/Inertia:	195 cm x 228 cm x 286 cm (77 in. x 90 in. x 113 in.) very heavy - high inertia
Guide Ways:	Similar to System A
Driving Mechanism:	X Drive uses 1-1/4 Moore Lead Screw. Y Drive 2-1/2* Saginaw Ball Screw
Scanner Mechanism:	Same as System A
Supply Lines, Air & Electric:	Similar to System A
Optical System:	
Laser Position	131 in. Max from Scanner
Beam Expander	Same as System A
Mirrors	2 Mirrors - unstable - medium loss
Objective Lenses	carefully ground not as critical as System A
Optical Window	7/8 in. total thickness less imperfections - no sag
Film Handling:	easier than System B. Glass Frame pivots horizontally permitting flat mounting of transparency then tilt up
Spot Position Accuracy:	
x Direction	0.001 in. — good parallelity between scanner & transparency deflections. In transparency support increase position tolerance.
y Direction	0.0015 in.
ψ Heading	1/10° - not as stable due to mounts
Focus Control:	Sag minimized - focus simplified - good scanner transparency parallel
Ease of Fabrication:	Similar to System A
Cost of Fabrication:	Same as System A
Temperature Effects:	Non uniform effects on film & lead screw
Torque:	Unequal load torques on motors

* Might use smaller lead screw with 500 micron in. tol. red

Approved for Public Release

Contrails

TABLE IV

SYSTEM D

RADAR LAND MASS SIMULATOR TRADE-OFF STUDY

FACTORS	HORIZONTAL TRANSLATING TRANSPARENCY & VERTICAL TRANSLATING SCANNER (VERTICAL TRANSPARENCY)
Size/Weight/Inertia:	76 cm x 203 cm x 305 cm (30 in. x 80 in. x 120 in.) lightest - low inertia
Guide Ways:	rectangular guide ways - not so accurate, inexpensive, easy to line up
Driving Mechanism:	Similar to System A
Scanner Mechanism:	Same as System A
Supply Lines, Air & Electric:	Similar to System A with shorter supply lines
Optical System:	
Laser Position	152 cm (60 in.) max from scanner
Beam Expander	Same as System A
Mirrors	2 mirrors - fairly stable - medium loss
Objective Lenses	Same as System C
Optical Window	3/4 in. total thickness - no sag
Film Handling:	Similar to System C. Both System C & D require spring loading glass against transparency to avoid transparency slippage during readout
Spot Position Accuracy:	
x Direction	0.0010 in.
y Direction	0.0015 in.
ψ Heading	1/10° - not as stable due to vertical mounting
Focus Control:	Sag avoided - focus maintained - parallelism of components is fair
Ease of Fabrication:	Standard Material used - such as rods & I Beams, Alignment simplified.
Cost of Fabrication:	Lower cost - lead time reduced due to use of standard parts
Temperature Effects:	Nonuniform effects on lead screw & film
Torque:	Equal load torques on motors

Approved for Public Release

Contrails

SYSTEM D SELECTED

This system has been selected as the most desirable in meeting the performance objectives. The following discussion contains a detailed design and analysis, and describes the systems performance. Included are discussions of the mechanical components of the system such as bearings, lead screws, guideways and optical focus control, of system maintenance, and of the feedback control system for x and y motion.

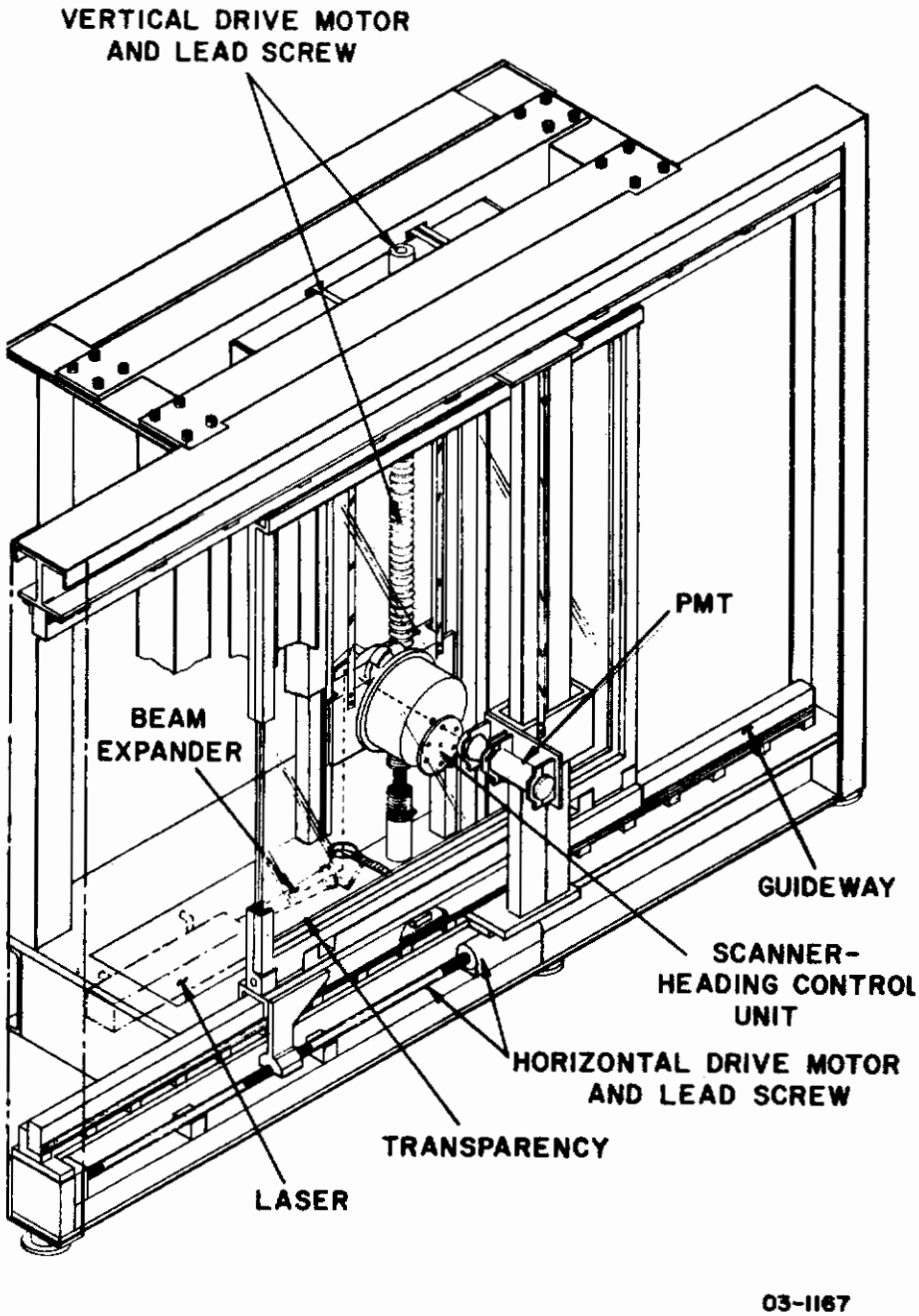

Figure 6 TRANSPARENCY READOUT SYSTEM

Approved for Public Release

Contrails

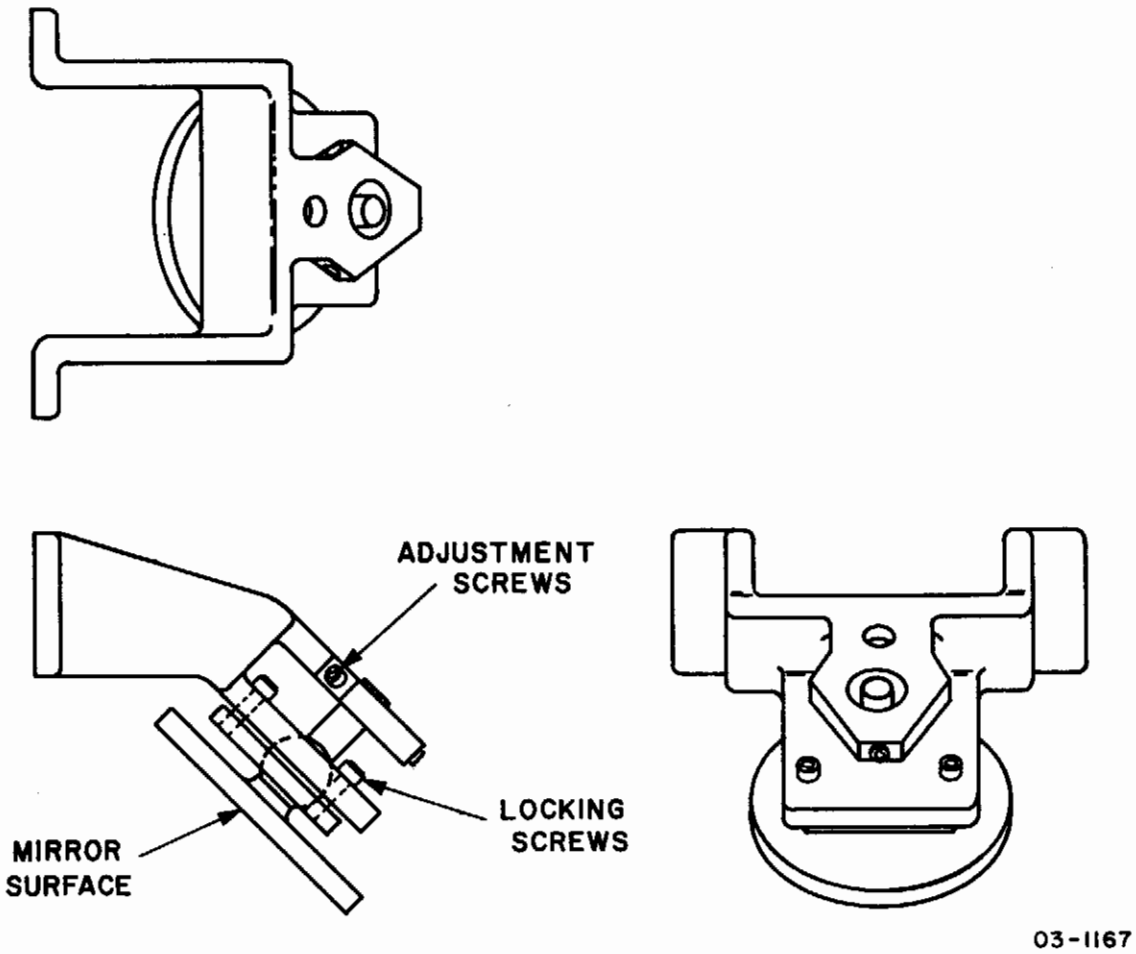

Figure 7 MIRROR CONFIGURATION

Approved for Public Release

Contrails

SECTION IV

MECHANICAL SYSTEM COMPONENTS

A brief description of systems A thru D have been described and illustrated as to their characteristics, advantages, and disadvantages. Each system will have variations in those specific components utilized. For instance, all of the optical systems discussed are very similar. The same laser, beam expander, approximate number of lenses, and the same scanning disc with f/2 objective lenses are used. Yet the objective lenses are more complex for systems A and B due to the heavier film support. Mirror losses are higher for system A using 3 mirrors. The drive motors, tachometers, rotary as well as linear encoders and lead screws are about the same for each system. Each system requires a similar glass frame to support and align the film transparency. The resulting structural configurations vary according to each approach. However, the more practical approach uses off-the-shelf components such as I-beams, channels, angles and tubes. These parts are readily available and provide ease of fabrication and alignment. The large castings shown for the horizontal system present long lead delays and require precision machining which delays delivery and raises the cost of the end item. The following discussion attempts to give some insight into the components selected, their quality, finish, accuracy, and life. This is followed by a more intensive look at overall system errors and their effects on system accuracy.

LASER

A helium neon gas laser is used to provide a uniform intensity light source. This laser operates at 6328Å wavelength, featuring built in beam pointing for ease of beam alignment. It is ruggedly built, has a sealed-beam plasma tube for maintenance free operation. A beam expander is utilized with the laser to expand the beam to its working diameter of 2 inches. Beam expansion also serves to reduce beam angular divergence as well as to avoid optical degradation by micron sized dust particles. The beam expander produces filtered wavefronts with a smooth Gaussian intensity profile.

MIRRORS

The two mirrors used in this system are similar to the configuration illustrated in Figure 7. This configuration facilitates rigid stationary mounting of the laser. Each mirror deflects the expanded laser beam 90°. The mirrors are "first surface mirrors" such as electroless nickle over steel with 90% reflectivity. Each mirror is fully adjustable about its optical axis.

GAS BEARING

The scanner gas bearing supports both the optical scanner disc and its drive motor directly by eliminating an intermediate coupling and its angular error. This gas bearing is hydrostatic and exhibits low starting torque and practically infinite life. Axial and radial bearing runout is maintained with-

Approved for Public Release

Contrails

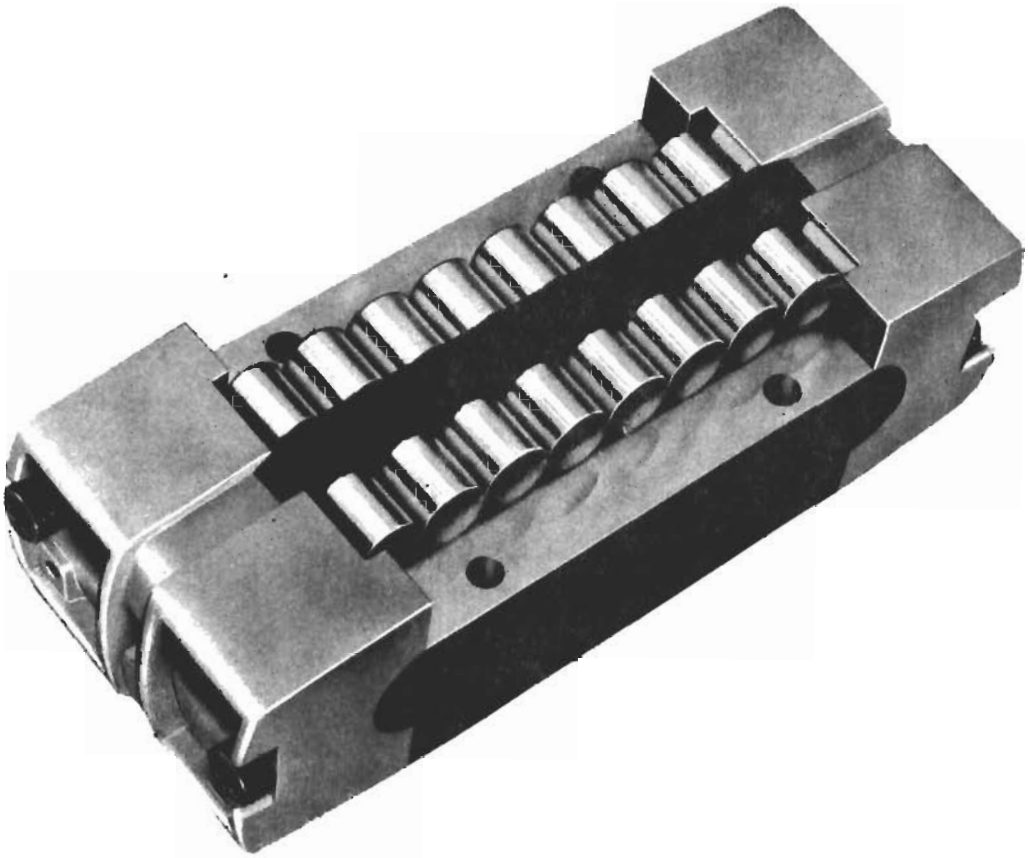

03-1167

Figure 8 LINEAR ROLLER BEARING

Approved for Public Release

Contrails

in 0.38 micron (15 micro-inches). The complete absence of metal to metal contact allows this bearing to operate at 5000 revolutions per minute, and at this speed there is no mechanical noise or vibration. The stiffness approaches 17,900 kilograms per cm (250,000 pounds per inch), making it very insensitive to outside perturbations. The bearing material is corrosion resistant steel providing maximum resistance to corrosive elements and humidity. The bearing will operate reliably on dehumidified air filtered down to 5 micron particles.

HEADING CONTROL BEARINGS

The nature of the scanner configuration requires open center design to allow the laser beams to pass through the center. For this reason large bore slim profile bearings are used. Two unequal size angular contact bearings are back loaded against each other, thereby taking out axial as well as radial clearance in each bearing. The angular contact bearing has a higher complement of rollers than the deep groove contact bearing or four point contact bearing with a subsequently higher load capability. The base grooves are honed to a precise geometry for quiet operation. Balls and races are made from AISI 52100 steel. The ball sphericity is held to 0.635 microns (25 micron-inches). Bearing runout, both axial and radial, is held within 2.5 microns ($\pm$ 100 micro-inches). Additional runout control can be achieved by building the scanner to fit the bearing inner races as well as phasing the outer races in the housing. This may not be necessary since most of the error is systematic and can be compensated for electronically. Furthermore, these bearings are stationary during actual scanning, therefore, bearing jitter is not present.

These bearings are grease lubricated for the life of the bearings. Labyrinth sealing is provided to protect scanner componentry from contamination.

LINEAR BEARINGS AND GUIDEWAYS

Linear rough bearings and rectangular guideways are used both on the horizontal transparency drive system, as well as on the vertical scanner drive. These bearings, shown in Figure 8, exhibit smooth, friction-free motion under load. They feature a built-in damper which minimizes structural vibrations and serves to guide the rollers in the load zone. The antifriction characteristics of the bearings significantly reduce the power demand on the drive system. Low friction means less wear on lead screws and allows greater position control accuracy. The rugged design of the bearings permits greater high load carrying capability and consequently, a high spring rate.

These bearings require only a minimum amount of lubrication. Therefore, grease lubrication for the life of the bearing is practical. The bearing and lubricant are protected from contaminants by using either surface wipers or covers. A surface wiper would be sufficient in this case since there is no generation of contaminants.

The bearing races and rollers are made from hardened AISI 52100 steel. The guideway surface on which the linear bearing operates is one of the bearing races. Rockwell "C" scale (R_c58) hardness is maintained.

Approved for Public Release

Contrails

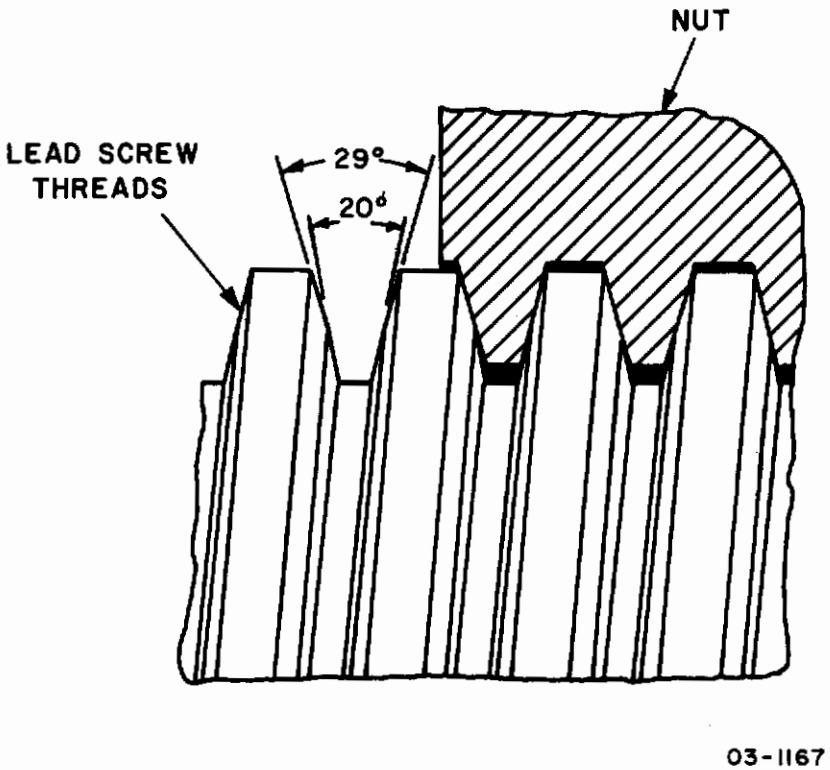

Figure 9 MODIFIED ACME LEAD SCREW THREADS

Approved for Public Release

Contrails

Preloading pads are used, one per pair of opposing bearings to preload the bearings and establish a primary reference surface. Accuracy is not critically dependent upon guideway parallelism, since the preloading compensates for variations in thickness along the guideway length. The guideways are supplied with a surface parallelity of $\pm$ 2.5 microns ($\pm$ 0.0001 inch). The accuracy of the linear bearing perpendicular to guideway is within $\pm$ 0.635 micron ($\pm$ 25 microinches).

The life for a linear roller bearing properly mounted, kept clean, and properly lubricated is determined by fatigue of the materials. The fatigue life, based on B-10 life, is expressed by the following equation:

$$\text{Life} - (C/P)^{3.33} = \text{Ten Million Inches of Travel}$$

C = Dynamic Capacity

P = Working Load on Bearing

SWIVEL COUPLING

The gas bearing must receive a continuous supply of gas to provide smooth accurate support of the scanning disc. A rotating coupling is necessary to accomplish this. Therefore, a dynamic gas coupling is built directly into the scanner support housing. This is accomplished using graphite filled teflon seals backed up with a garter load spring. This seal configuration provides extremely smooth action, with a coefficient of friction lower than that of common neoprene O-rings. They have unlimited shelf life, work in most corrosive environments, have the high pressure range of up to five times the dynamic life of O-rings and are size competitive with O-rings as well.

LEAD SCREW

The lead screws used in both the horizontal and vertical servo systems feature modified acme screw threads (See Figure 9). The particular lead screw selected provides the ultimate in position accuracy and smoothness of operation. The lead screw has the following features.

1) Near carbide hardness and dimensional stability

2) The lead screw is accurately thread ground, inspected, then lapped to a high microfinish, all under temperature controlled conditions.

3) The lead screw assembly assures perfect alignment and support in the system to within 0.25 micron accuracy.

4) The lead screw is carefully machined and inspected to reference blocks exceeding Bureau of Standard requirements.

Approved for Public Release

Contrails

The lead screw therefore provides a very high degree of accuracy, one that responds to minutely small movements, as small as 1/40 of a micron (1 or 2 millionths of an inch). This smoothness of control, together with the high magnification of movement that is unique with a lead screw (approximately 150 to 1) produces excellent repeatability. The modified acme tooth form gives perfect angular fit, and the tightly fitting nut is burnished until it runs free along the full length of the mating screw. Lead error is corrected and periodic error eliminated due to refined lapping techniques. The cyclic error of the lead screw is held to $\pm$ 0.39 micron ($\pm$ 15 microinches). To compensate for heat generation during operation, the lead screw has a linearly cumulative error built-in which amounts to -7.5 micron (-300 microinches).

HEADING CONTROL

Simulation of aircraft heading is achieved by supporting the scanner on a large shaft. The scanner is rotated about the optical center to simulate aircraft heading. A dc torque motor, coupled by one-to-one ratio antibacklash gear set to a sine-cosine potentiometer, provides closed loop heading control. The sine-cosine potentiometer provides a 360° electrical function with better than 0.1% linearity. The life of the potentiometer exceeds 30 million cycles. The antibacklash spurgear set is designed for infinite life and low angular error less than one tenth of a degree. The drive motor consists of a direct shaft coupled dc torque motor with a wound armature and permanent magnetic field. It is designed for high torque positioning systems exhibiting high torque at low speeds for speed control systems. Since the armature is attached directly to the shaft/load, there are no backlash errors and servo stiffness is high. In addition, the motor exhibits a high linearity whereby torque increases directly with the input current, independent of speed or angular position. This provides excellent electrical control characteristics.

OPTICAL WINDOW

The optical windows provide a rigid means of supporting the film transparency. The windows facilitate microinch levels of accuracy in film transparency positioning and focus control. The glass windows are fabricated from a high optical grade glass nearly free from seeds, stones, bubbles, and striae. The transparency mounts between the two pieces of 0.95 cm (3/8 in.) thick optical glass. The glass is supported verically in frames which in turn are supported top and bottom by linear bearings and are guided on rectangular guide ways attached to the frame work of the radar land mass simulator.

The high quality of window fabrication assures the transmission of a powerful and uniform beam of light to the photomultiplier tube located on the back side of the glass. For a complete picture, see Figure 10.

GUIDEWAYS

Vertical position control of the scanner and uniformity of focus are, as shown in Figure 11, accomplished using two vertically mounted rectangular guide ways. Three pairs of linear roller bearings on each side of the scanner

Approved for Public Release

Contrails

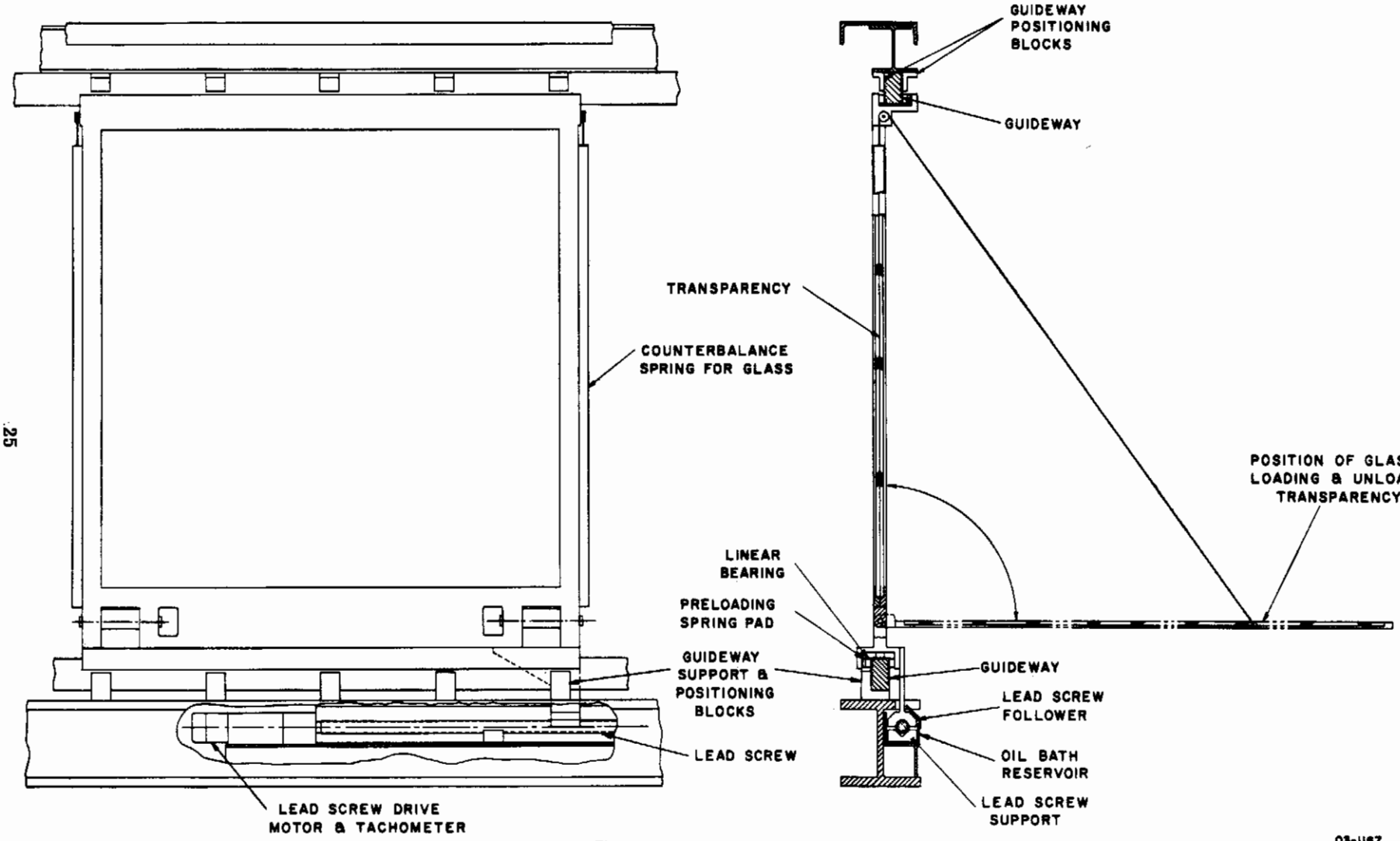

Figure 10 TRANSPARENCY DRIVE AND LEAD SCREW ASSEMBLY

Approved for Public Release

Contrails

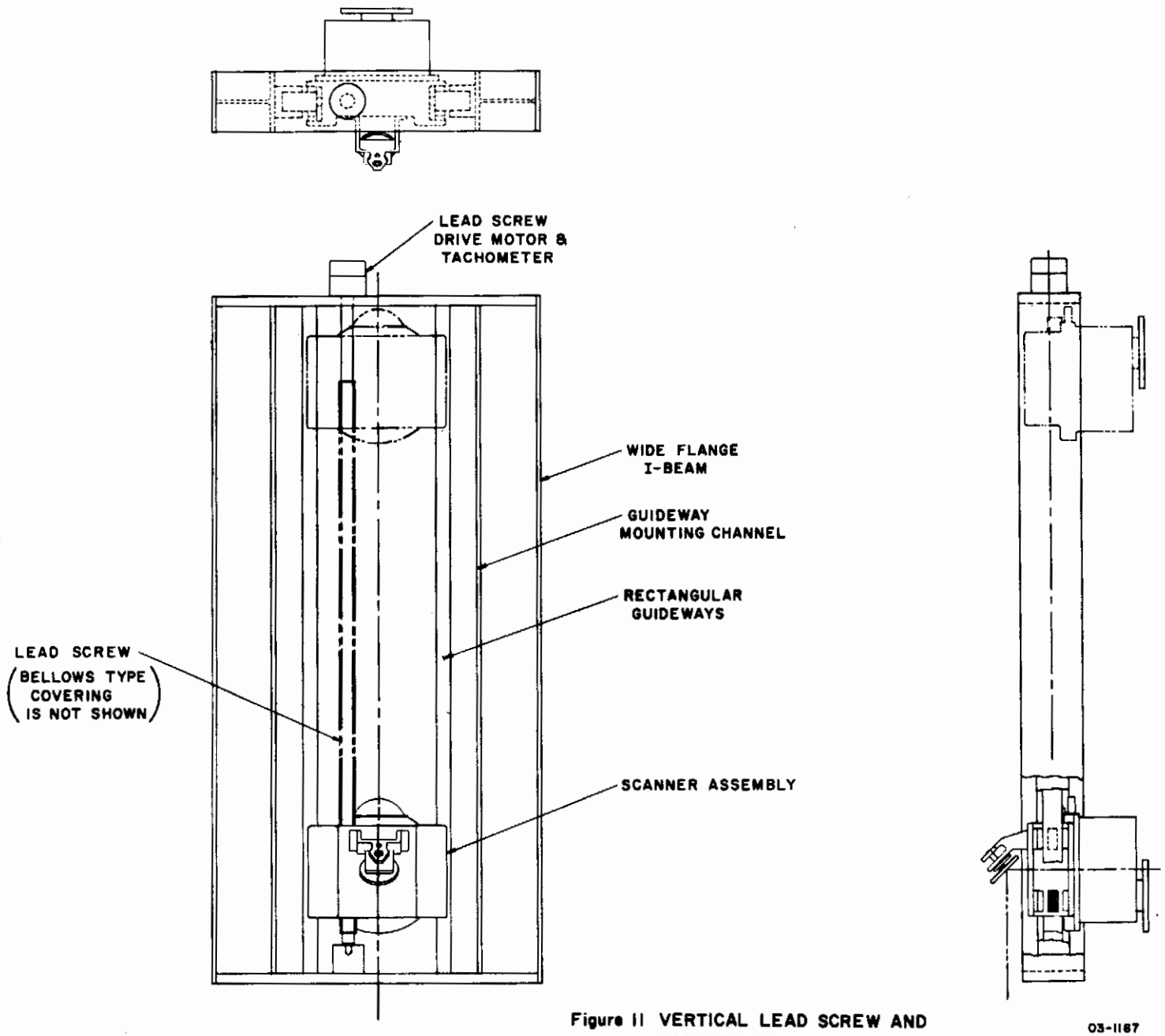

Figure 11 VERTICAL LEAD SCREW AND SCANNER MODULE ASSEMBLY

03-1167

Approved for Public Release

Contrails

frame serve to guide the scanner along the guide ways. There is no direct loading of the guide ways other than the preload on the linear rollers. A preload on these bearings serves to smooth out the rolling action and establish one reference plane for each pair of opposed loaded bearings. The preloading and relaxation of guideways flatness after machining necessitates the adjustment of the guideways along their lengths. This is accomplished by using an adjustment block in the form of a channel which has push-pull adjustment screws approximately every six inches along its length. The guideway is fitted to this channel and both pieces are attached to a structural I-beam. The guideway is autocollimated and adjusted until it is aligned. The adjusted guideway is then assembled in the unit.

The horizontal guideway consists of a similar configuration and its accuracy is comparable to that of the vertical unit. The bottom guideway is supported on accurately ground blocks every twelve inches. The guideway is autocollimated and shimmed until it is accurately aligned. The blocks are then ground to fit precisely and both blocks and guideway are tightened down. The upper guideway is laterally aligned since the film transparency is vertically guided by the lower guideway.

All the guideways used are hardened steel (R_c58 minimum). The hardened precision ground way surfaces provide high load capability, eliminate surface brinnelling, increase smoothness of operation and offer high reliability.

PMT AND LIGHT PIPE

The light signal transmitted through the film is collected via a conical light pipe on the emulsion side of the film. The light pipe serves to reduce the two inch scanned line to approximately one inch required at the photomultiplier face. In addition the light is diffused over the photocathode surface thereby smoothing out sensitivity irregularities in the tube. The light pipe and photomultiplier are side mounted on a small bearing carriage, as shown in Figure 12. The carriage is mounted to two back-to-back vertical guideways. It is driven up or down by a pulley mechanism and counterweight slaved to the scanner lead screw. The response and accuracy of this method of driving the photomultiplier is excellent and presents a simple, inexpensive, compact unit.

LUBRICATION

The radar land mass simulator does not have a lubrication maintainability problem. All of its bearings are sealed, self lubricated types. Because of the slow rate of motion in the x and y drives, sealed grease lubrication is the best choice. The horizontal lead screw has a shielded oil bath system. This provides two advantages: it gives the best lubrication to the lead screw and stabilizes the lead screw against thermal variants, thereby eliminating short time temperature effects. The vertical lead screw has a number of disadvantages at first glance; it is difficult to lubricate uniformly, it is subject to thermal gradient and it supports the full weight of the scanner.

These problems complicate lubrication which serves two purposes: to hydrodynamically separate metallic surfaces from dry running and, to

Approved for Public Release

Contrails

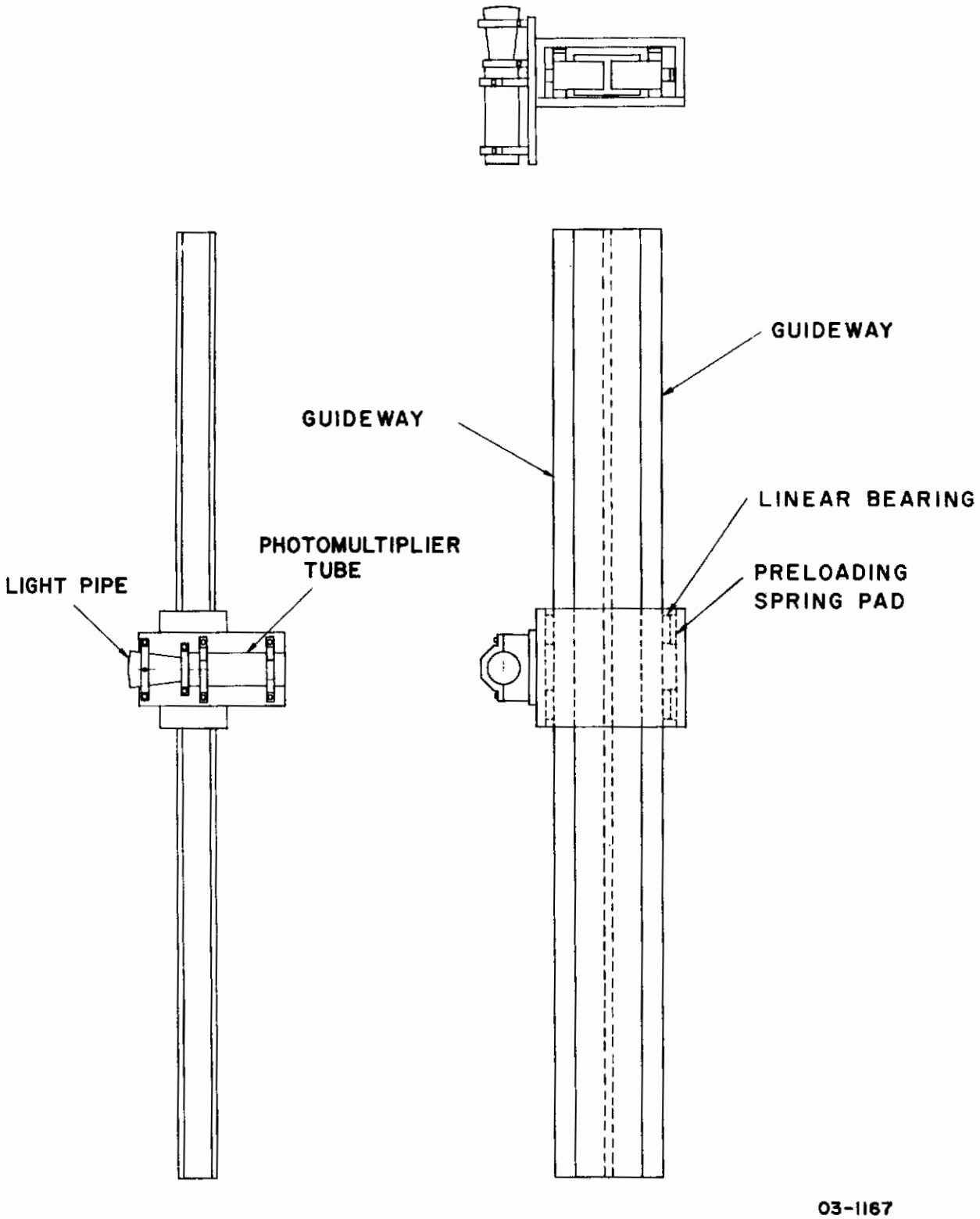

Figure 12 PHOTOMULTIPLIER AND GUIDEWAY ASSEMBLY

Approved for Public Release

Contrails

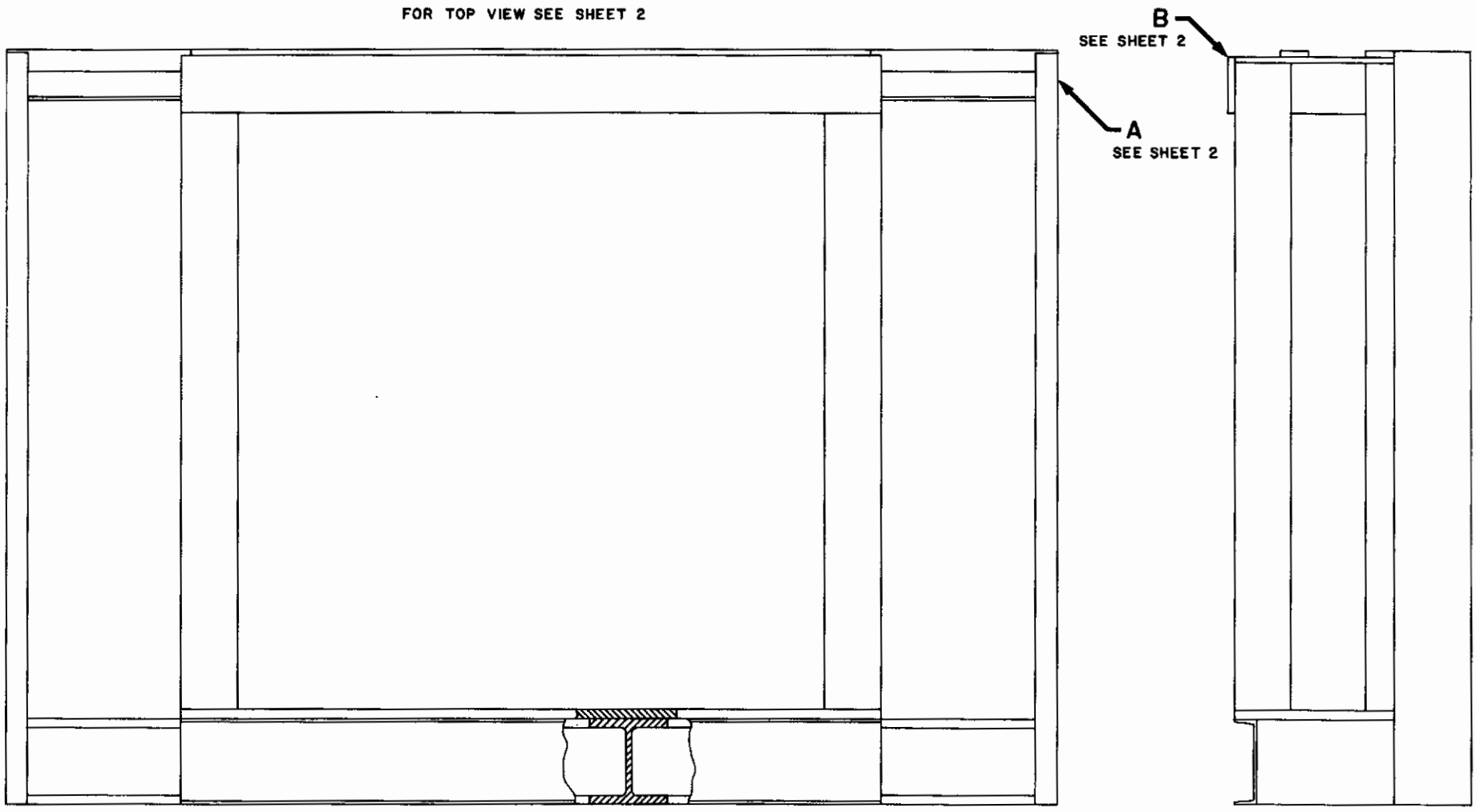

Figure 13 (1 of 2) STRUCTURE ASSEMBLY

03-1167

Approved for Public Release

Contrails

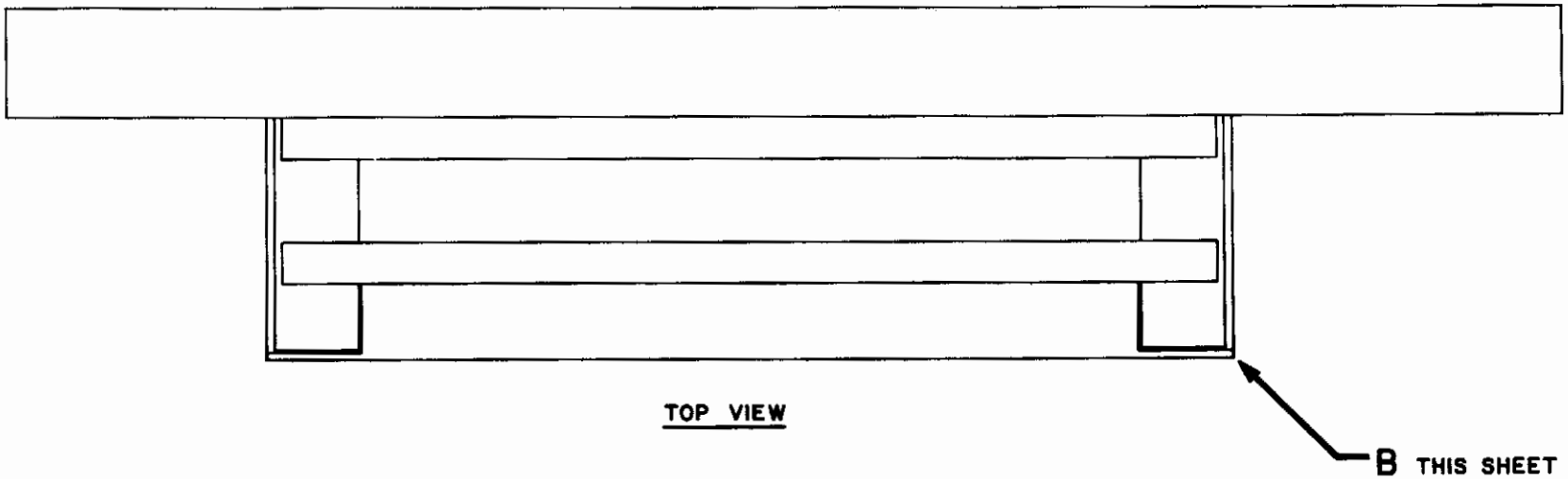

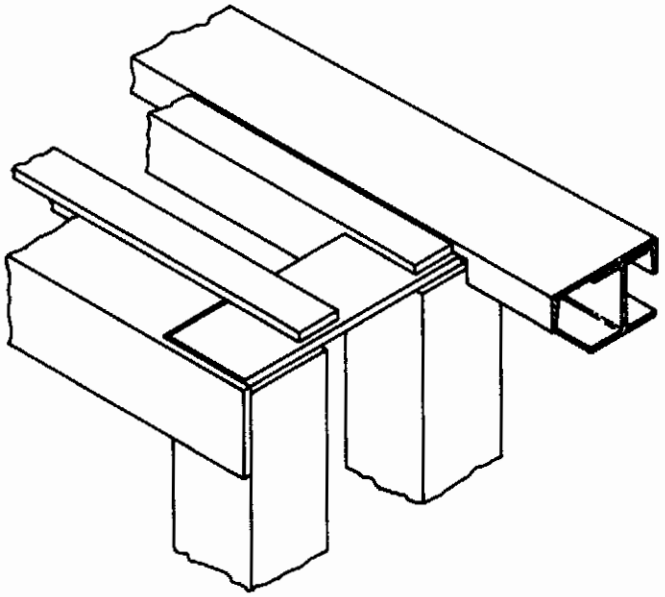

DETAIL - B THIS SHEET & SHEET 1

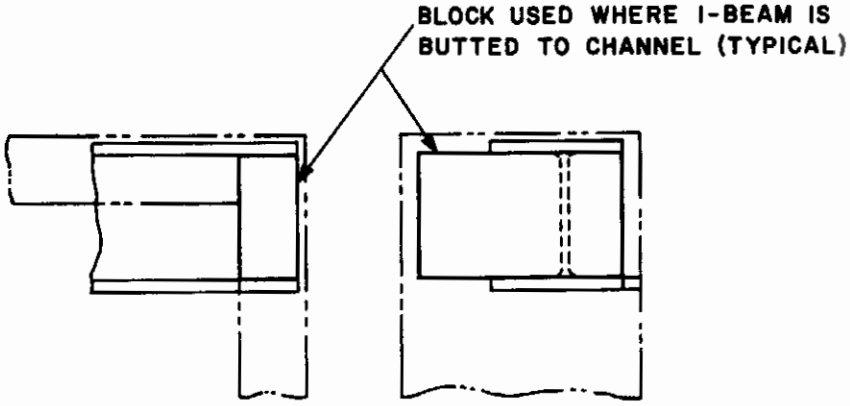

PHANTOM LINES INDICATE OUTLINE OF CHANNELS

- SCALE ENLARGED -

DETAIL - A SHEET 1

03-1167

Figure 13 (2 of 2) STRUCTURE ASSEMBLY

Approved for Public Release

Contrails

remove heat generated between dynamically loaded components. These difficulties are overcome by the following approaches. The lead screw nut is drip lubricated at an extremely low rate to avoid oil buildup and refill problems. The screw is protected from thermal variants and dirt by boots which have air conditioning capability by tapping off room conditioned air directly from the supply. The loads are effectively removed from the screw by counter weighting the scanner via a pulley dead weight system. This, in no way, affects system accuracy. In addition, the lead screw itself is held and driven at the top to avoid sag or deflection due to its own weight.

LINEAR CONTROLLER

A linear position pick-off is mounted to a vertical and to a horizontal guideway to provide optimum position feedback control. The system to be used consists of strips of inductive material placed on accurately ground flats. These flats are mounted to guideways in each direction of motion and a pick-off of mounted on the moving part of the scanner and film support. The pick-off does not touch the inductors and there are no wearing parts or degradation of signal. The pick-off generates a sinusoidal waveform which is split up into fine increments resulting in measurable position accuracies one order of magnitude smaller than the overall accuracy of the machine. This position pick-off method is easily adaptable to this machine, it is economical, accurate, does not add perturbation to the system and is extremely reliable based on machine tool industry acceptance.

STRUCTURES

The structural components that make up the radar land mass simulator constitute the foundation for optimum system operation. The structural configuration selected for this study, as illustrated in Figure 13, evolved from system x and y motion requirements. In addition to a high degree of accuracy required, the system must be easily fabricated from reasonably active materials (short lead time raw stock), and it must be easily aligned and maintained. I-beams, channels, and angles are readily available as opposed to cast meehanite, the widely used machinery base material. Inquiries were made at local foundries and casting houses. Lead times of 6 months or greater are necessary to obtain raw castings. On the other hand, off-the-shelf components, which are available on short lead times, lend themselves to ease of fabrication and alignment. Steel is used throughout the structure to take advantage of its higher modulus of elasticity than aluminum alloys, and its ability to maintain uniform thermal expansion. I-beams are used to support all the guideways due to their high strength-to-size ratio and high, bi-directional strength. Channels which tie into the large I-beams are used to effect some weight reduction where I-beams are not necessary. The structures are conceived as modular units which provide bench assembly capability to facilitate final assembly and alignment. In addition, packaging of subcomponents is held to a compactness which permits shipment or movement within a facility, since the unit fits through standard door openings. The structure sets on five adjustable feet which permit leveling and horizontal alignment.

A structural skin is installed over the framework to protect the user from laser exposure, the equipment from dust, and to enhance the finished quality of the equipment.

Approved for Public Release

Contrails

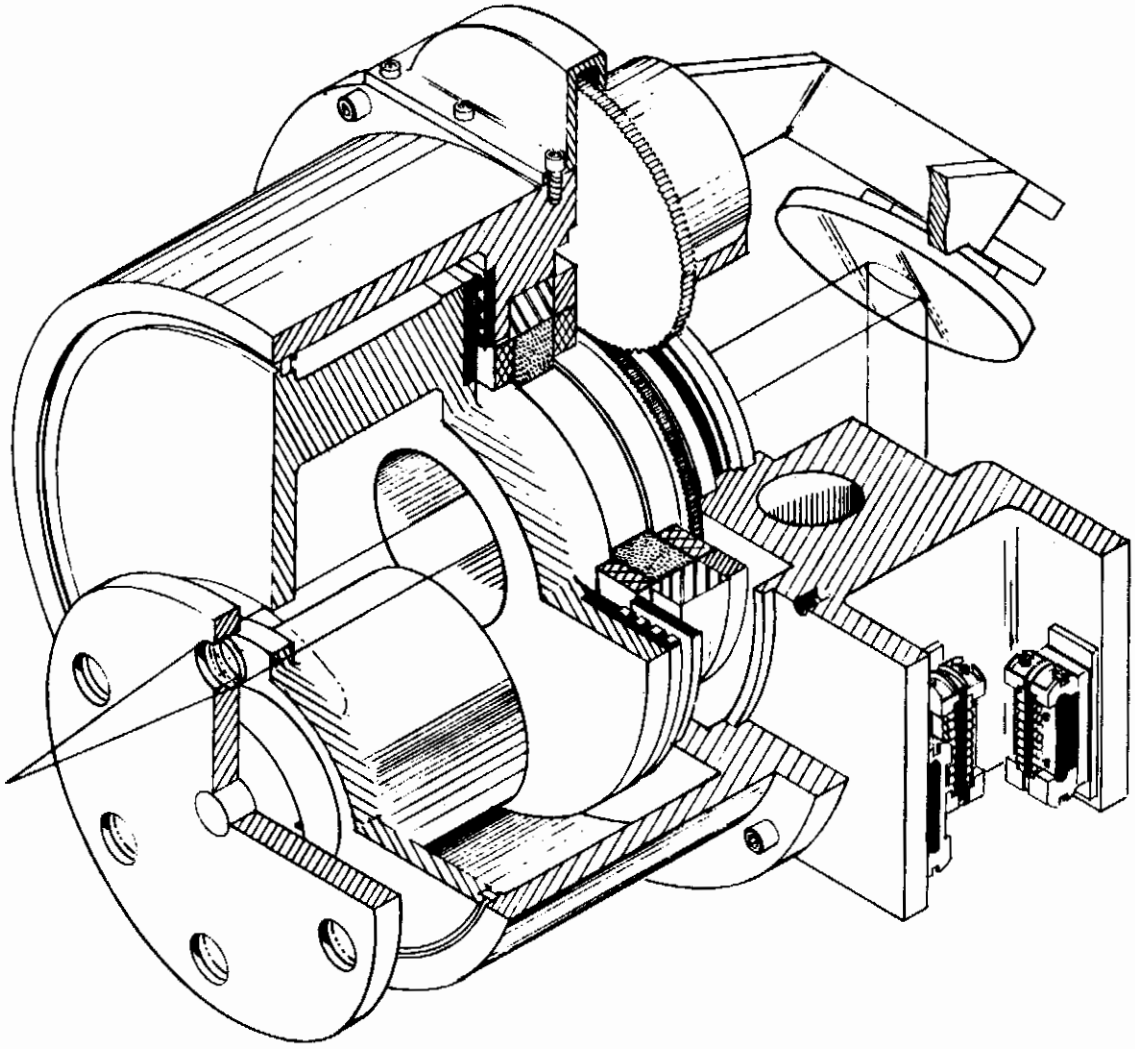

03-1167

Figure 14 CUTAWAY VIEW OF SCANNER AND HEADING CONTROL ASSEMBLY

Approved for Public Release

Contrails

OPTICAL FOCUS CONTROL

Precision antifriction bearings are utilized in both the x and y drives to assure uniformity of focus. Frame members are deflection analyzed for low deflection rates and subcritical vibratory modes. Guideways directly affecting x-y drive componentry are precision machined, straightened, and optically aligned for maximum repeatability and focus control. The associated mechanical parts will not be affected by humidity.

CBS Laboratories has developed a scanner optical system under contract AF 33(615)-3458. This system is nearly identical to the Land Mass Simulator System, as shown in Figures 14 and 15. The differences exist in the scanning head which rotates about its optical axis to simulate aircraft heading; the film is rigidly affixed between two 0.95 cm (three-eights inch) thick optical windows; and a conical light pipe is required to collect the scanned lines under any scanner heading position. The heading positioning requires a separate control system and a direct drive motor which maintains a heading within 1/10 of a degree.

The optical windows present some aberrations due to glass thickness. However, this is corrected in the scanner objective lens. The light pipe provides an efficient means of transmitting the scanned line to the photomultiplier tube. It also serves to diffuse the light intensity over the face of the tube.

Factors Affecting Focus in the x Drive System

The horizontally driven transparency will contribute some minute defocusing caused by its support bearings, the guideways, glass and framework. The bearings will vary ± 0.64 microns (± 25 microinches). The guideways can create as much as ± 2.5 microns (± 0.0001 in. lateral deviation) from true dimension. The air bearing contributes ± 0.2 micron (± 8 microinches). The glass will not deflect due to its vertical mounting but is subject to optical imperfections. Flatness can be held to within ± 25 micron (± 1000 microinches). The frame will deflect somewhat but will not affect focusing unless it twists. Initial twisting of the frame can be corrected during installation and alignment. In general all the aforementioned factors are systematic errors, and window flatness and guideway variations can be removed by careful alignment.

Appendix II presents a detailed analysis of structural loads and deflections and Appendix IV discusses the weight factors. Vibrations, which can also be a factor in any precision motion systems, are analyzed in Appendix V.

Factors Affecting Focus in the y Drive System

The vertically driven scanner assembly will cause defocussing through bearing runout, scanner heading control assembly errors, and scanning disc nonuniformities. Each of these factors contribute ± 0.64 micron, ± 2.5 micron, and ± 0.2 micron (± 25 microinches, ± 100 microinches, and ± 8 microinches) defocus respectively. The guideways contribute ± 2.5 microns (± 0.0001 inch). These errors are systematically repeatable, and the guideway errors can be removed by alignment.

Approved for Public Release

Contrails

Appendix II presents a detailed analysis of structural loads and deflections and Appendix IV discusses the weight factors. Vibrations, which can also be a factor in any precision motion system, are analyzed in Appendix V.

Conclusion to Focus Control

A summation of factors contributing to defocusing is outlined in Table V. The gross defocus under all worst case conditions indicates the system has up to ± 4.87 microns (± 193 microinches) of defocusing error. An additional possible ± 30 microns (± 1200 microinches) are removed at initial buildup by proper alignment of optical window frames and guideways. The lenses used permit some flexibility as demonstrated by the following equation, where the depth of focus tolerance is calculated.

$$\pm \Delta z = 2f^2\lambda$$

where

Δz = allowable depth of focus tolerance

f = lens no is f/2

λ = 6328 Å wavelength of He-Neon Laser

$$\Delta z = (2)(2)^2(0.0000006328)$$

$$= \pm 5.1 \times 10^{-6} \text{ meters}$$

$$= \underline{\pm 5.1 \text{ microns}}$$

As can be seen the f/2 lens depth of focus variation exceeds ± 4.87 microns. Further reductions of this tolerance appear achievable and should be relizable in the hardware program.

POSITION ACCURACY IN THE X DIRECTION

Positioning of the laser spot along the x-axis of the system is accomplished by continuous traversing of a motor driven lead screw nut. Spot position accuracy is a direct function of guideway and structure deflection, guideway bearing runout, lead screw errors, scanner gas bearing runout and scanner heading control bearing runout. Structural deflections cause the spot to deviate from its true position by as much as 20 microns (800 microinches), and vary predictably at any point of transparency traverse. An error budget contained in Table VI shows magnitudes as a function of distance along the axis. Figure 16 shows a plot of dynamic deflection vs vertical position. Linear roller bearings are used to support the scanner from lateral motion. These bearings have a systematic error of ± 0.5 microns (± 20 microinches)

Approved for Public Release

Contrails

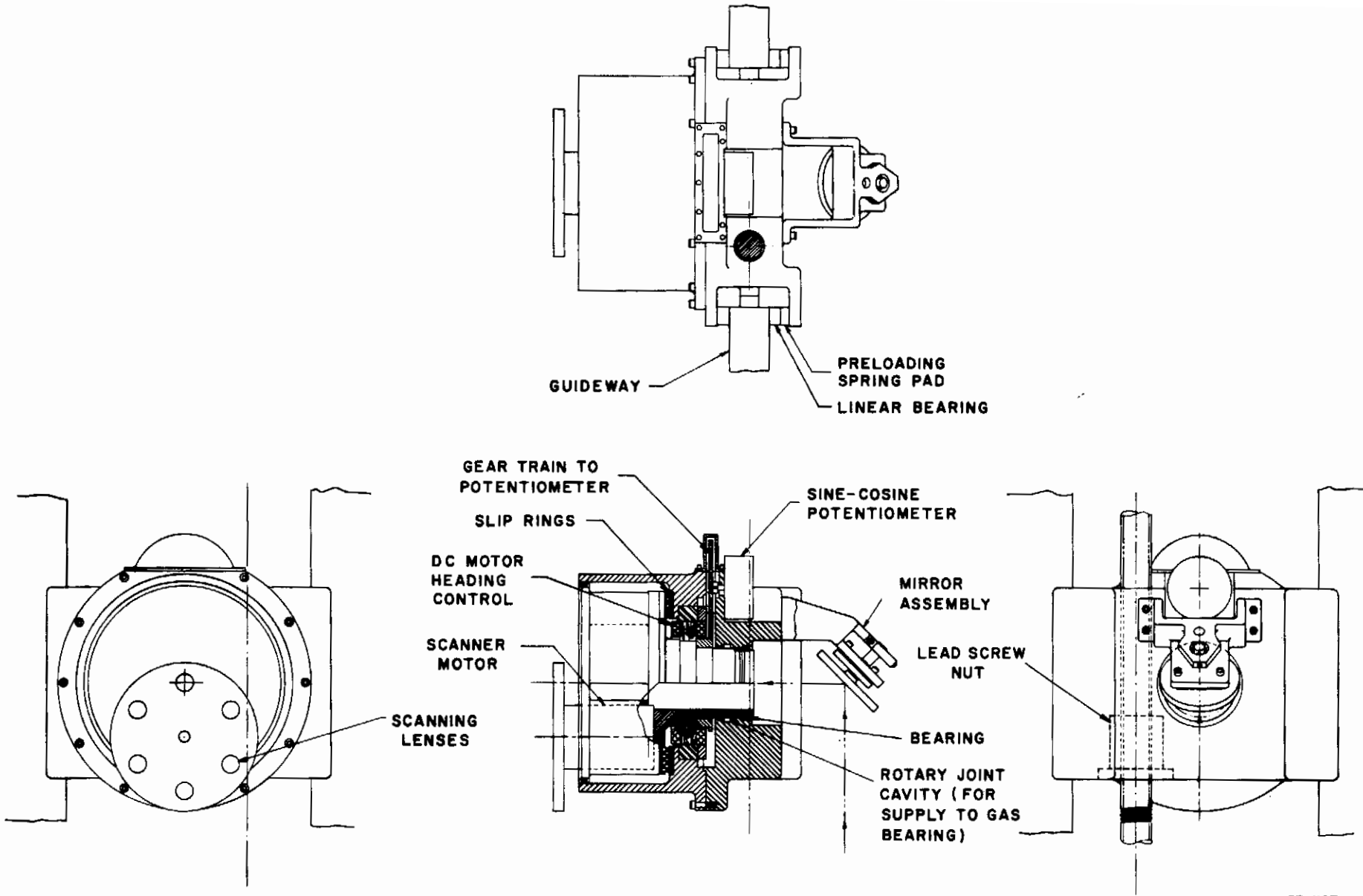

Figure 15 SCANNER ASSEMBLY

Approved for Public Release

Contrails

Approved for Public Release

Contrails

TABLE V

FOCUS CONTROL

FACTORS CAUSING DEFOCUS	MAGNITUDE MICRONS	MAGNITUDE MICRO INCHES
Transparency Thickness	± 0.25	± 10
Glass Frame Linear Bearings	± 0.64	± 25
Axial Mounting or Scanner Lenses	± 0.64	± 25
Scanner Gas Bearing Axial Runout	± 0.20	± 8
Heading Control Bearing Axial Runout	± 2.50	± 100
Scanner Traverse Linear Bearings	± 0.64	± 25
TOTAL DEFOCUSING	± 4.87	± 193
The Following Factors are Non Contributing Since They are Removed by Proper Alignment		
Optical Window Flatness	± 25.00	± 1000
Horizontal Guideway Straightness	± 2.50	± 100
Vertical Guideway Straightness	± 2.50	± 100
TOTAL NON CONTRIBUTING ERROR	± 30.00	± 1200

Approved for Public Release

Contrails

Table VI

HORIZONTAL DRIVE SYSTEM - SYSTEMATIC ERRORS

MAXIMUM VALUES OF ERRORS ALONG VERTICAL AXIS FROM FLOOR

SYSTEMATIC ERROR SOURCE	0	6	12	18	24	30	33	36	42	48	54	60	66
1. Vertical Guideway Deflection	0	*1.65 *(65)	0	1.65 (65)	0	1.65 (65)	0	1.65 (65)	0	1.65 (65)	0	1.65 (65)	0
2. Vertical I-Beam Deflection (6 x 6 x .320)	0	2.5 (100)	6.5 (260)	12 (480)	16.5 (660)	17.8 (710)	18.8 (750)	17.8 (710)	16.5 (660)	12 (480)	6.5 (260)	2.5 (100)	0 0
3. Linear Roller Bearing	1 (40)	←										→	1 (40)
4. Horizontal Lead Screw 122 cm Long (48 in.)	7.5 (300)	←										→	7.5 (300)
5. Heading Control Bearing	5 (200)	←										→	5 (200)
RANDOM ERROR SOURCE													
6. Linear Roller Bearing	0.25 (10)	←										→	0.25 (10)
7. Horizontal Lead Screw	0.75 (30)	←										→	0.75 (30)
8. Heading Control Bearing	0.7 (28)	←										→	0.7 (28)

* Top number is expressed in microns. Bracketed number ( ) in micro inches.

Approved for Public Release

Contrails

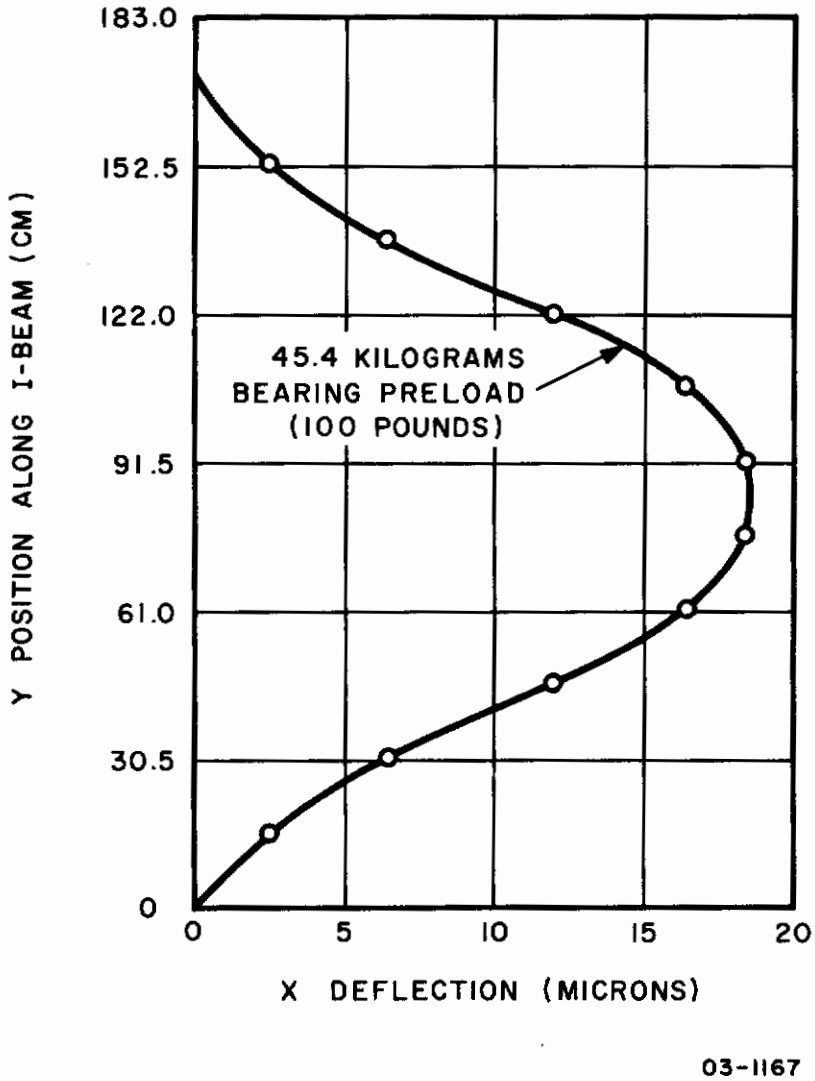

Figure 16 DYNAMIC DEFLECTION PLOT OF THE VERTICAL GUIDEWAY IN THE X DIRECTION

Approved for Public Release

Contrails

and exhibit a random variation of ± 0.13 (± 5 microinches) due to roller variations in size. Due to the number of rollers in contact with the guide way the random effect is averaged out. The lead screw, in turn, exhibits a total cumulative error over 122 cm (48 inches) of 7.5 microns (300 microinches). It has a cyclic error of 0.75 microns (30 microinches) which appears at a frequency of once per revolution. Lead screw sag is eliminated by kinematically supporting the screw at points along its length. This method of support also eliminates transverse errors. The lead screw is immersed in oil and has a number of threads in simultaneous contact with the nut. This condition effectively smooths out many cyclic errors.

The scanning disc with its objective lenses is supported on a gas bearing. This bearing contributes 0.4 micron (15 microinches) deviation from true position due to radial runout. The Heading Control Assembly is, in turn, supported by precision machined antifriction bearings. These bearings are installed in a phased relationship to provide the least radial runout. They contribute 5 microns (200 microinches) radial runout and have a ball cyclic variation of 0.635 microns (25 microinches). The ball variation will not create jitter during operation, since the heading will be fixed for each simulated flight across the transparency. Reflecting on the worst case of tolerance buildup pyramiding in one direction, the total horizontal drive system error could add up to 34 microns (1370 microinches), as shown in Table VI. The probability of this happening, is small, since the error is distributed and would have a very low possibility of accumulating to its maximum value.

POSITION ACCURACY IN THE Y DIRECTION

In the horizontal drive system the scanner is positioned by a motor driven lead screw nut attached to a scanner carriage. Position accuracy is affected by structural deflection of the guide way and its support beam, as well as guide way linear bearing runout, lead screw error, scanner gas bearing runout, and heading control bearing runout. Structural deflections cause an error of approximately 2.3 microns (92 microinches) from true position. Table VII and Figure 17 present a complete picture of y direction error as a function of distance along horizontal guide way. Linear roller bearings, as shown in Figure 8, are used to support the film transparency from motion perpendicular to its plane of travel. These bearings are accurate within ± 0.5 microns (± 20 microinches) and exhibit a random error of ± 0.13 microns (± 5 microinches) due to diametral variations. This jitter component is not seen due to the averaging effect of all the rollers used. The lead screw has a total cumulative error of 7.5 microns over 122 cm (300 microinches in 48 inches). It has a cyclic error component of 0.75 micron (30 microinches) but is damped out due to the hydrostatic load capability of the lubricant and the averaging effect of a number of lead screw threads. The scanner gas bearing has a 0.4 micron radial runout (15 microinches). The antifriction ball bearings, which support this disc, and in addition, support the heading control, contribute 5 microns (200 microinches) radial runout and have a cyclic variation of 0.635 micron (25 microinches) which is not seen during traversal of the transparency because the bearing is stationary. Again, if the worst possible combination of tolerance

Approved for Public Release

Contrails

Table VII

VERTICAL DRIVE SYSTEM ERRORS

MAXIMUM VALUES OF ERRORS ALONG HORIZONTAL AXIS FROM OPTICAL CENTER

SYSTEMATIC ERROR SOURCE	48	42	36	30	24	18	12	6	0	6	12	18	24	30	36	42	48
1. Horizontal Guideway Deflection	0	*1.15 *(46)	0	1.15 (46)	0	1.15 (46)	0	1.15 (46)	0	1.15 (46)	0	1.15 (46)	0	1.15 (46)	0	1.15 (46)	0
2. I-Beam Deflection	0	0.68 (27)	1.13 (45)	1.15 (46)	1.07 (43)	0.75 (30)	0.4 (16)	0.12 (5)	0	0.12 (5)	0.4 (16)	0.75 (30)	1.07 (43)	1.15 (46)	1.13 (45)	0.68 (27)	0
3. Linear Roller Bearing Runout	1 (40)	←														→	1 (40)
4. Vertical Lead Screw 122 cm Long (48 in.)	7.5 (300)	←														→	7.5 (300)
5. Heading Control Bearing	5 (200)	←														→	5 (200)
RANDOM ERROR SOURCE																	
6. Linear Roller Bearing Runout	0.25 (10)	←														→	0.25 (10)
7. Vertical Lead Screw	0.75 (30)	←														→	0.75 (30)
8. Heading Control Bearing	0.7 (28)	←														→	0.7 (28)

* Top number is expressed in microns. Bracketed number ( ) in microinches.

Approved for Public Release

Contrails

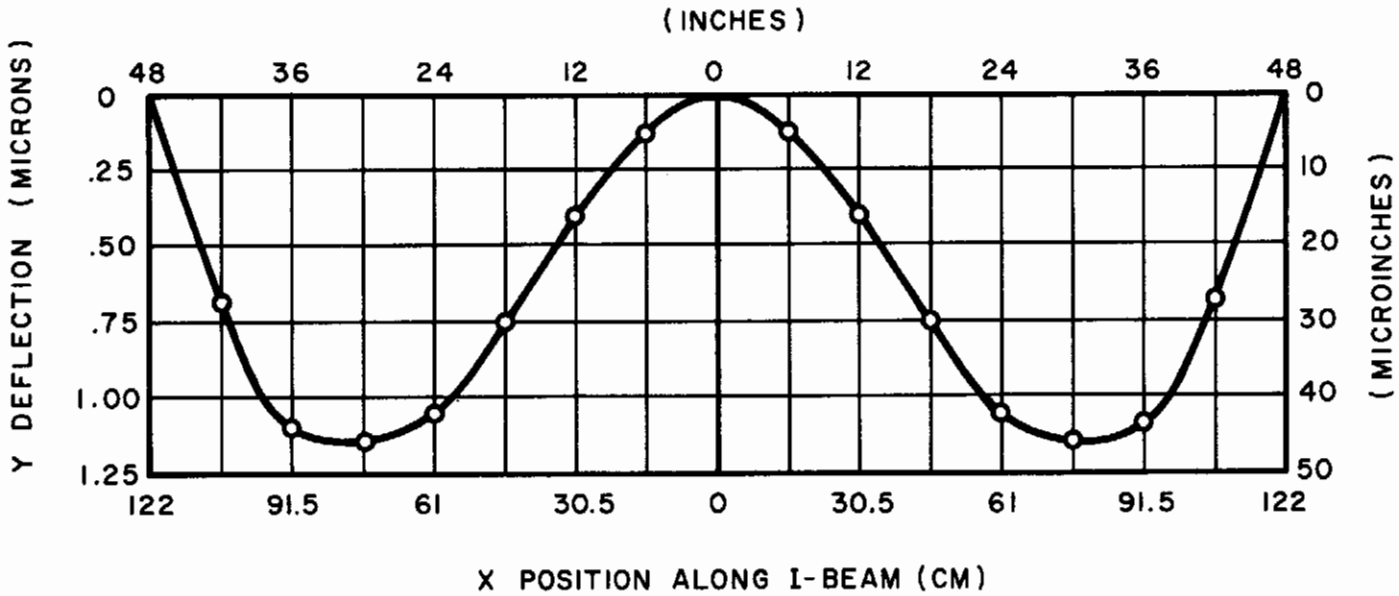

03-1167

Figure 17 DYNAMIC DEFLECTION PLOT OF THE HORIZONTAL GUIDEWAY IN THE Y DIRECTION

Approved for Public Release

Contrails

buildup were to occur simultaneously, the maximum error would be 18 micron (712 microinches). Since this error accumulation is compounded by errors already accounted for in the x-drive system, the net y-direction error is 12 micron (472 microinches).

FILM HANDLING

The system is Human Engineered for ease and simplicity of film transparency loading and unloading.

Film loading can be accomplished by one operator as follows: The transparency mount (support frame and glass window) is moved automatically to one side when the operator puts the system controls on load sequence. The mount is stopped automatically when it reaches the appropriate loading position (by microswitch). At this position the operator releases the transparency release latches. This allows one half of the glass frame to pivot down from the vertically locked position. The window is spring loaded in order to counter balance the weight of the window, thus avoiding physical injury to the operator. A positive stop keeps the window from falling to the floor. The operator then pulls the window down so that it lies in a horizontal position, as illustrated in Figure 18. If a transparency is already positioned on the window, the spring finger clips at the periphery of the film are released and the film is removed. The knee high position of the window during loading permits the operator to gently float a film transparency onto the window without wrinkling or mutilating the film. Then the operator aligns the x and y coordinate markings on the film with fiducial markings etched on the window. Once the film is smoothed out and clipped in place (the operator uses cotton gloves to avoid damaging the film), the window is repositioned in reverse order for operation. The next step is recalibrating the film so that exact position coordinates are established with respect to computer information. Calibration is further discussed in Section 5.

TEMPERATURE AND HUMIDITY EFFECTS

System errors are not only attributed to mechanical tolerance build-up, machining and deflection errors, but also to those errors caused by temperature and humidity changes. A difference in room temperature of $\pm$ 0.55°C ($\pm$ 1°F) will cause expansion or contraction of lead screws and frame work, in addition to its effect on the film. As an example, consider the increase in length of the lead screw over 122 centimeters (48 inches).

$$\alpha st = 10.8 \times 10^{-6} \text{ cm/cm °c}$$

$$\ell = 122 \text{ cm}$$

$$\Delta T = \pm 0.55°C$$

$$L_{lead} = (10.8 \times 10^{-6})(122)(0.55)$$

$$= \pm 7.25 \text{ microns } (\pm 285 \text{ microinches}).$$

Approved for Public Release

Contrails

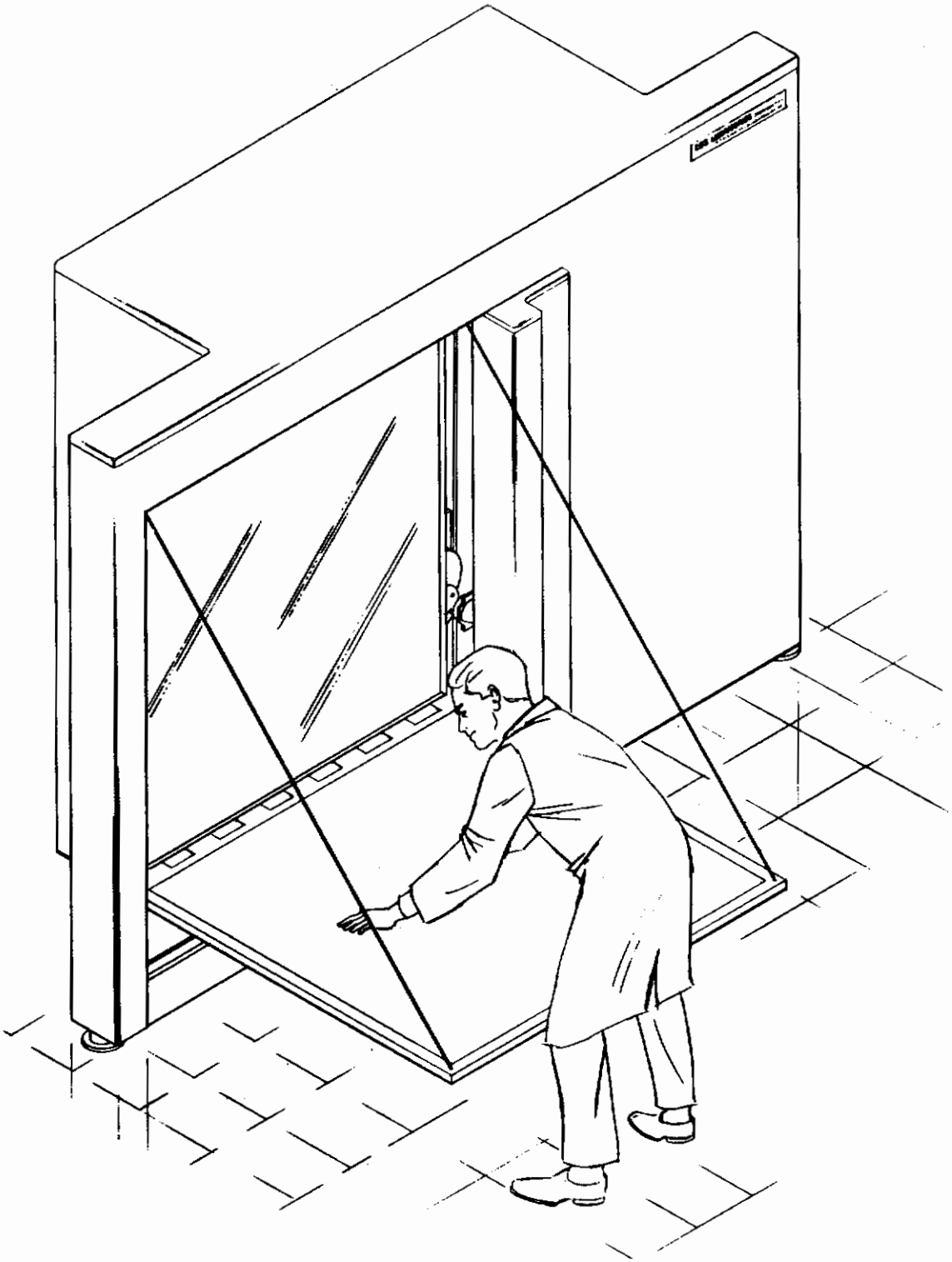

03-1167

Figure 18 SIMULATOR WITH WINDOW LOWERED FOR CHANGE OF FILM TRANSPARENCIES

Approved for Public Release

Contrails

This would affect position accuracy and it is therefore important to provide air circulation, especially if larger temperature excursions are anticipated. The film itself is very susceptible to dimensional variation with temperature; for Kodak high definition aerial film number 3404

$$\alpha_{film} = 27 \times 10^{-6} \text{ cm/cm °C}$$

$$\ell = 122 \text{ cm}$$

$$\Delta T = 0.55°C$$

$$L_{film} = (27 \times 10^{-6})(122)(.55) = \underline{\pm 18 \text{ micron}} \ (\pm 725 \text{ microinches})$$

This amount of thermal variation appears severe at first glance. The glass support, however, acts as a sizeable heat sink opposing thermal variants and changes of this amplitude would not be expected. Humidity control should be maintained within ± 2%. Humidity will not affect the equipment since hygroscopic materials are not used. The film itself is affected by humidity, as follows.

$$\beta_{film} = 35 \times 10^{-6} \text{ cm/cm/\% RH linear Humidity coeff.}$$

$$\ell = 122 \text{ cm}$$

$$\Delta RH = \pm 2\% \text{ Relative Humidity}$$

$$L_{film} = (35 \times 10^{-6})(122)(2) = \pm 85.4 \text{ micron } (\pm 3410 \text{ microinches})$$

This increase appears substantial, but since the film is sandwiched between glass plates, only a very minute amount of moisture will be absorbed and even then, only at the exposed edges.

PMT DRIVE SYSTEM

The photomultiplier tube, light pipe and its electronics are supported on a box frame and sidemounted to provide adequate room for film transparency loading and unloading. The PMT black box assembly translates vertically (y-direction) with the scanner assembly. The PMT is slaved to the scanner mechanically via a pulley system which functions both to control the position of the PMT relative to the scanner and also to counter-weight the load of the scanner assembly on the vertically mounted lead screw. The pulley system uses a flat steel belt to achieve high positioning accuracy. All the pulleys are carefully mounted on precision antifriction ball bearings to provide smoothness of motion. To assure positive steel belt tensioning, the PMT assembly is spring loaded by a constant force spring. Positioning accuracy of such a drive system is a function of pulley runout and temperature. Position inaccuracy, caused by

Approved for Public Release

Contrails

the pulleys, would be less than $\pm$ 7.5 microns ($\pm$ 300 microinches). This error consists of the pulley machining error and the supporting bearing runout. Air stratification, or layering of air, from floor to ceiling can cause thermal gradients up to 0.55°C ($\pm$ 1°F) over the length of the steel belt. The error introduced is illustrated by the following example.

$$\delta = \alpha \ell \Delta T$$

where

δ = expansion or contraction of steel belting

α = coefficient of expansion for steel = $10.8 \times 10^{-6} \frac{cm}{cm°C}$

$\alpha T = \pm 0.55°C$

ℓ = length of steel belting 122 cm

$\delta = (10.8 \times 10^{-6})\ (122)\ (0.55) = \pm 7.25$ micron

$= (\pm 285$ microinches)

It is therefore possible that the PMT assembly could have an error of $\pm$ 15 micron ($\pm$ 585 microinches) relative to the scanner. This, however, does not affect the registration of the information being read off the film transparency.

Conclusion On Position Accuracy

It can be seen from the previous paragraphs that the systematic errors are small, less than 25 microns (0.001 in.) for x and y positioning systems. It was also seen that temperature can affect the lead screw and film transparency. Proper air circulation would significantly reduce this error component, and the random error on the film would be held within 25 micron (0.001 in.) anywhere on the transparency. Humidity was not a problem to either the equipment accuracy or the film, but room relative humidity should be maintained within $\pm$ 2% to reduce dimensional changes in the stored transparencies.

Approved for Public Release

Contrails

SECTION V

SYSTEM MAINTAINABILITY

SELECTION OF BEARINGS, COMPONENTS, AND MECHANISMS

A large transparency readout system presents some critical component design problems. It is important to make the unit easy to fabricate, assemble, install, align, repair and operate. This is accomplished by utilizing precision components, readily available on the machinery market today. Very accurate linear bearings and guide ways are stock items with machinery manufacturers, thereby simplifying the mechanical design. Higher precision may be achieved with custom fabricated guide ways and rollers. These components would be necessary if higher accuracy was desired. Castings would be employed and precision Vee-guideways machined into the casting. This is an economical approach, and is not necessary in order to meet the present objectives. Readily available structural parts such as channels, I-Beams and plates are employed to advantage and provide ease in alignment and calibration. Acme lead screws, due to their accuracy, are employed on both drive systems. Every dynamic component and structural member will be made from steel or equivalent materials to avoid differential expansion or contraction of components due to temperature variations.

Component Service Life

The structures and associated static components will have an infinite life capability. Dynamic components such as bearings and gears will exhibit life in excess of 1000 hours.

Periodic Maintenance

Maintenance will be very low on this unit. Bearing lubrication will be for the life of the bearings. Lubrication of other components such as lead screws will be on an extended basis, perhaps in excess of 1000 hours. The equipment should be installed in a dust free environment thus reducing maintenance and cleaning of the equipment. Some minor maintenance of wiping mirrors, lenses, and the transparency mounting windows should be performed periodically to ensure optical spot quality.

Alignment And Adjustment

Alignment of the transparency in its supporting frame is discussed in Section 4. Alignment checks of the transparency support and scanner support guideways should be necessary only if the equipment is moved, to assure integrity of display. This is accomplished by auto collimating each guideway support structure. In addition, each lead screw can be calibrated against Bureau of Standard gage blocks to assure lead screw trueness. Mirrors and lenses can be optically realigned if necessary to maintain optical spot resolution and position accuracy.

Approved for Public Release

Contrails

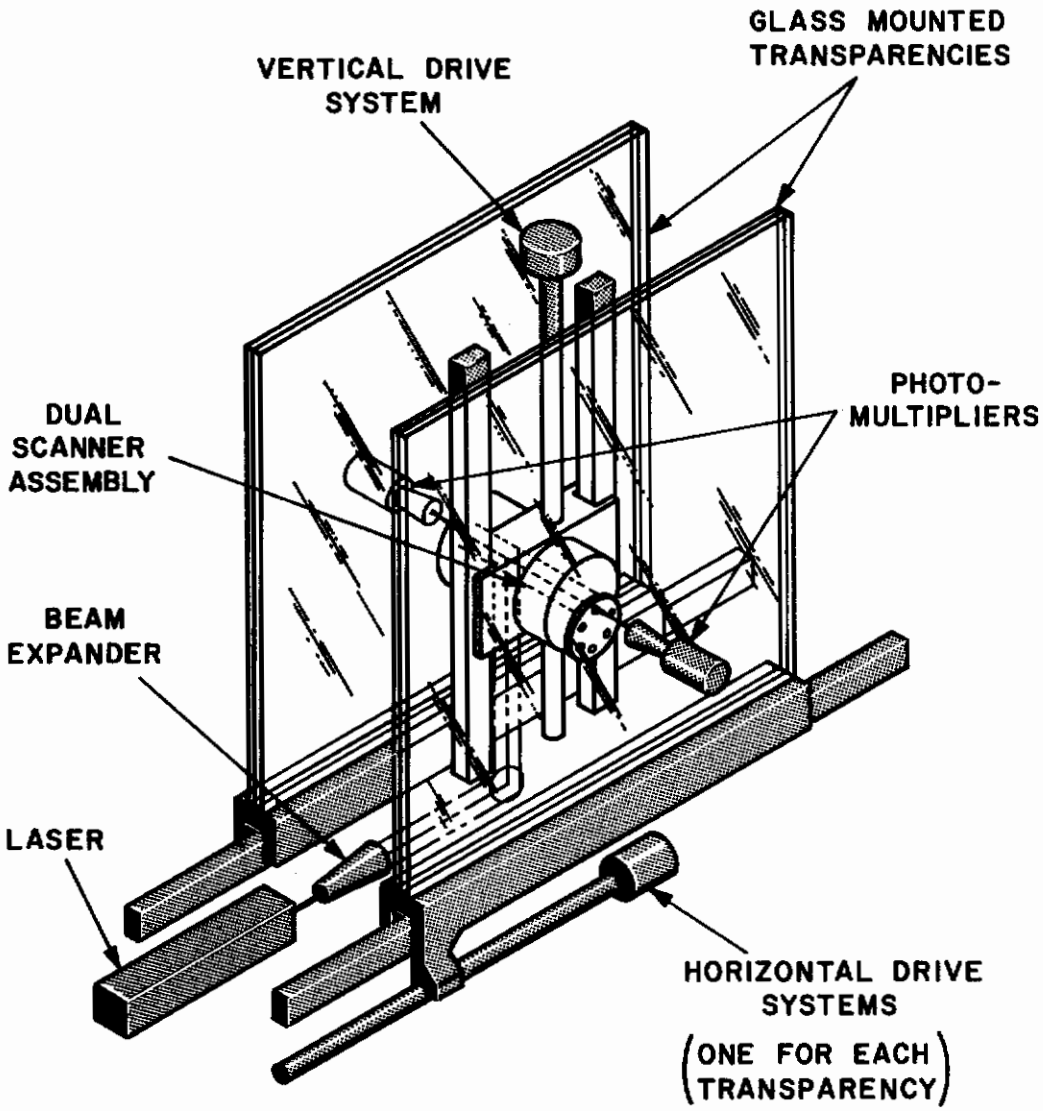

03-1167

Figure 19 DUAL TRANSPARENCY READOUT SYSTEM

Approved for Public Release

Contrails

Conclusions

The selection of reliable components and self lubricating wear points provides for ease of maintenance, high mean time between component failure, and a long service life for the whole unit. The system will be structurally sound, but, at the same time, it will easily facilitate any adjustments or alignment which might be required during the life of the equipment.

SECTION VI

DUAL TRANSPARENCY READOUT SYSTEM

The single transparency readout system discussed in this study will perform the task of reading a single transparency for terrain reflectance. It is realized, however, that some systems will require both elevation and reflectance readout. It is intended here to point out that the system presented in this study has the additional merit of being adaptable for dual transparency readout. This is achievable by adding a second transparency and track directly behind the scanning mechanism and in line with the first transparency. This adds approximately 25 centimeters to the width of the unit and does not change the height or length of the structure. A second optical scanner and a beam splitter is added to the present scanner carriage. Position accuracy is not significantly affected in the y-direction. A slight decrease in x-direction accuracy is expected due to dual drive loops. The advantages gained in this type of system far outweighs the necessity of having two separate readout systems. A schematic presentation of a dual transparency readout system is shown on Figure 19.

Approved for Public Release

Contrails

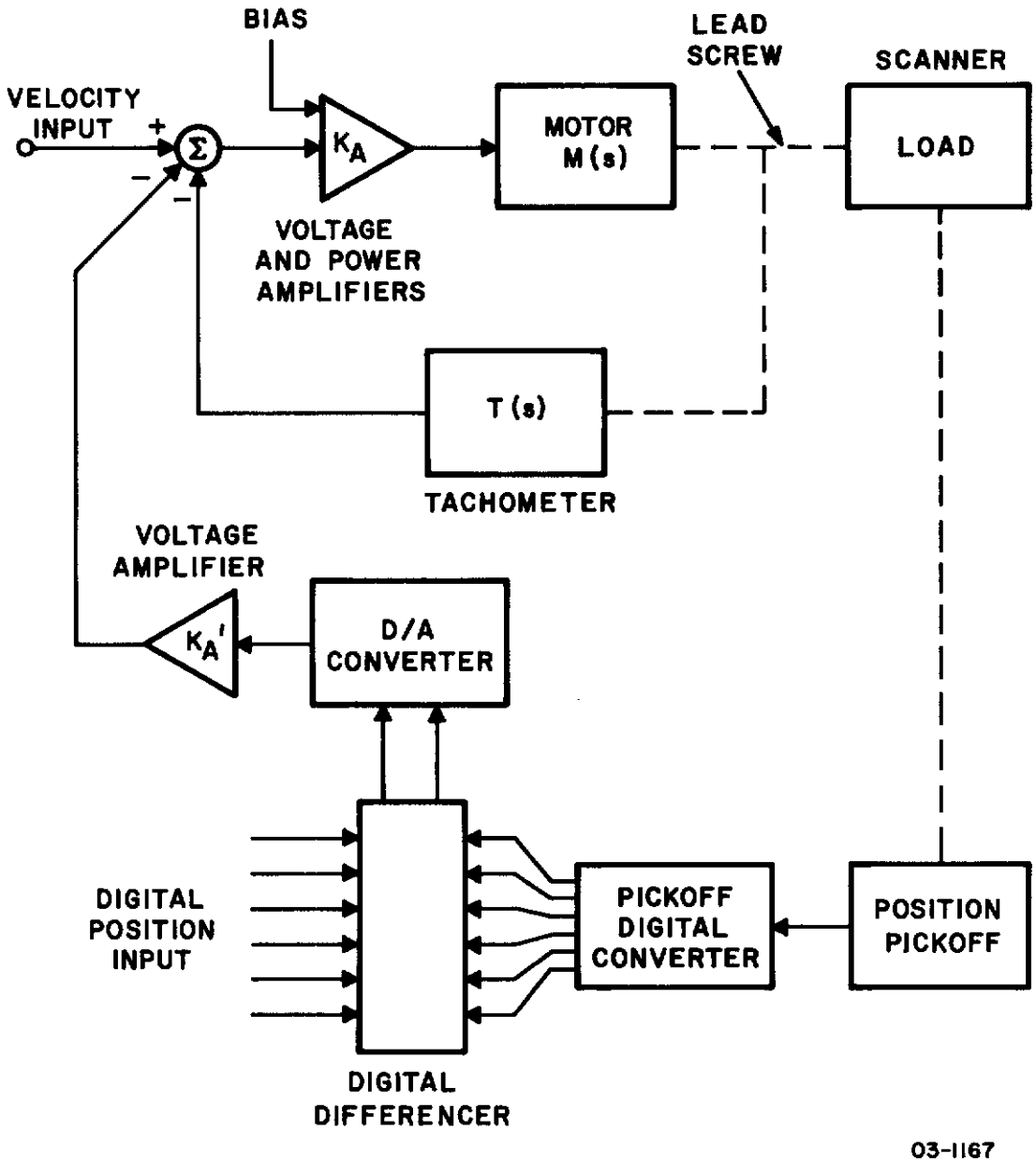

Figure 20 CONSTANT SPEED FEEDBACK CONTROL SYSTEM

Approved for Public Release

Contrails

SECTION VII

CONTROL SYSTEM DESIGN

CONTROL REQUIREMENTS

The scanner position control system is designed to meet the following requirements:

a) Constant velocity mode.
b) 10% maximum variation in scan line separation.
c) $\pm$ 0.0005 inch position accuracy over 48 inches, with respect to input.
d) 100:1 speed range from 0.1 in./sec to 0.001 in./sec.

SYSTEM DESIGN

The control system offering the best solution to the requirements presented by the desired scanning modes is a constant speed servo with tachometric feedback enclosed by a position correction loop accurate to 0.00254 cm (0.001 in.) over the entire 122 cm x 122 cm (48 in. x 48 in.) transparency. Such a control system is illustrated in Figure 20.

The scanner moves at a constant velocity for a given command (a constant voltage). Tachometric feedback is provided in order to reduce system torque disturbance sensitivity. Position feedback is employed to increase accuracy over long distances of travel. The position feedback enables the system to sense "where it is" not just "how fast it is moving". Note that this system is quite different from a position servo employing a tachometer feedback loop to dampen the loop response and increase the accuracy.

Under the headings VELOCITY SENSITIVE SYSTEM DESIGN and POSITION SENSITIVE SYSTEM DESIGN, a description and theory of operation is presented for the constant speed feedback control system, as illustrated in Figure 20. This control system has two parts: a velocity loop and a position loop.

Various figures illustrate the system's torque rejection characteristics, displacement errors due to torque disturbances and frequency response.

The design is such as to encompass both x and y scan controls using worst case values to arrive at design constants. The two scanning modes act independently according to input commands (voltage as a function of Ψ , the angle of scan off of the x direction), and thus, one design will be used for both.

Speed regulation will be held to less than $\pm$ 0.25%* from nominal value when all parameter variations are at worst case limits. The 10% maximum varia-

---

* NOTE: $\pm$ 0.25% has been chosen as a design value because it represents a smooth constant velocity system whatever the torque variation may be, and it is a realistic value. A torque rejection of say R db could be used instead as a design value, but this does not directly relate to the smoothness of motion. This value of regulation is important in the determination of the amplifier gain K_A determined in another section.

Approved for Public Release

Contrails

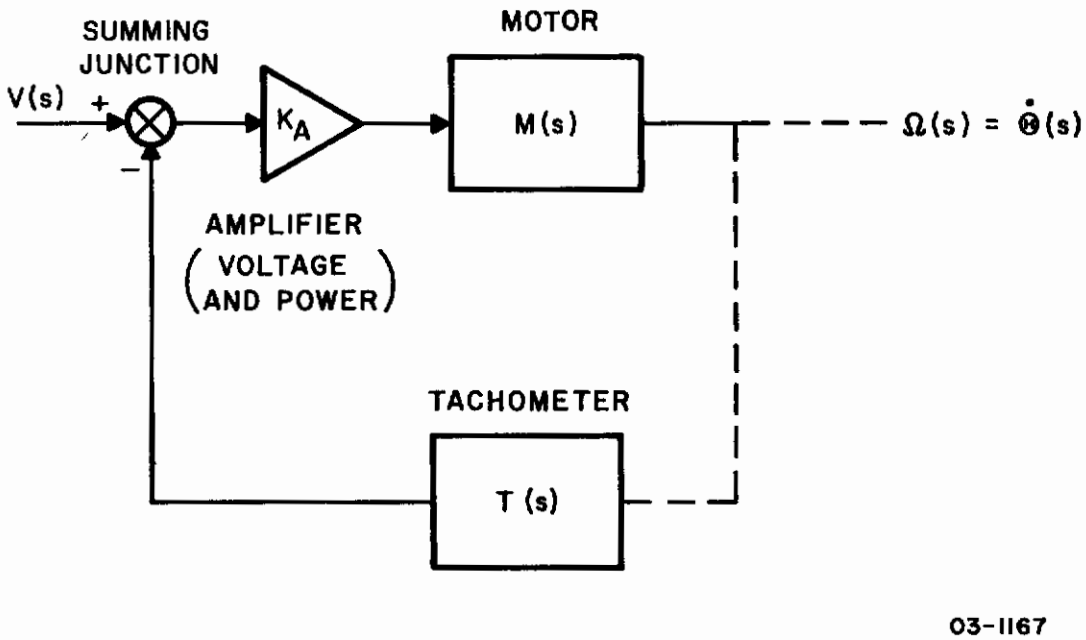

Figure 21 BASIC VELOCITY SERVO

Approved for Public Release

Contrails

tion in scan line separation can be translated directly to a 10% speed variation. If such a speed tolerance is allowed, however, a position loop correction would be necessary after a few scan lines. The advantage, then, to improved speed regulation to a much more stringent value, such as that chosen, is much smaller line to line deviations, i.e., smooth (constant) linear velocity and relaxed position loop requirements.

Constants and Variables

Table VIII presents a list of those constants and variables used in the mathematical formulas for Section VII.

VELOCITY SENSITIVE SYSTEM DESIGN

The inner loop of Figure 20, reproduced in Figure 21, corrects for variations in velocity which occur at the load. The design of this loop encompasses the following:

a. Uncompensated closed loop
b. Motor transfer function
c. Tachometer transfer function
d. Motor amplifier gain
e. Compensation networks
f. Torque rejection characteristics
g. Step torque response.

Uncompensated Closed Loop

The closed loop transfer function for the tachometric servo shown in Figure 21 is

$$\frac{\Omega(s)}{V(s)} = \frac{\text{Forward Path Transfer Function}}{1 + \text{Open Loop Transfer Function}} \qquad (1)$$

Substitution of the various transfer functions results in

$$\frac{\Omega(s)}{V(s)} = \frac{K_A M(s)}{1 + K_A M(s)\ T(s)} \qquad (2)$$

It is the purpose of the following sections to determine M(s) and T(s) according to manufacturer's data, and K_A to achieve a desired speed regulation of at least $\pm$ 0.25%. A Bode plot of the open loop transfer function will reveal the type of compensation necessary to achieve closed loop stability. The torque rejection characteristic will be given and the system's response to a step torque disturbance will be shown.

Approved for Public Release

Contrails

TABLE VIII (1 of 3)

LIST OF CONSTANTS USED

Symbol	Description	Units
$V(s)$	Velocity System Input Voltage	Volts
$\Omega(s)$, $\Theta(s)$	Time Derivative of Output Shaft Angle	Radians/sec
K_A	Velocity Loop Amplifier Gain	Volts/volt
$M(s)$	Motor Transfer Function	$\frac{\text{radians/sec}}{\text{volt}}$
$T(s)$	Tachometer Transfer Function	$\frac{\text{volts}}{\text{radians/sec}}$
J_M	Motor Inertia	gm-cm-sec^2 (oz-in.-sec^2)
K_T	Motor Torque Constant	gm-cm/amp (oz-in./amp)
K_B	Motor Back EMF Constant	$\frac{\text{volts}}{\text{radians/sec}}$
R_a	Motor Input Winding Resistance	ohms
L_a	Motor Input Winding Inductance	henries
J_T	Tachometer Inertia	gm-cm-sec^2
J_L	Load Inertia	gm-cm-sec^2
J	Total System Inertia Without Wheel	gm-cm-sec^2
J_X	Total Inertia of System and Flywheel	gm-cm-sec^2

Approved for Public Release

Contrails

TABLE VIII (2 of 3)

Symbol	Description	Units
J_A	Flywheel Inertia	gm-cm-sec^2
R	Total Input Circuit Resistance	ohms
τ_E	Motor Electrical Time Constant	sec.
τ_M	Motor Mechanical Time Constant	sec.
τ_X	Modified Mechanical Time Constant	sec.
V_M	Motor Input Voltage	volts
V_B	Motor Back-EMF Voltage	volts
V_T	Motor Friction Torque Voltage	volts
T_F	Motor Friction Torque	gm-cm
T_R	Motor Ripple Torque	gm-cm
T_G	Tachometer Torque	gm-cm
$(T_L)_{ver}$	Vertical System Torque	gm-cm
$(T_L)_{hor}$	Horizontal System Torque	gm-cm
T_O	Total Lead Screw Torque	gm-cm
r	Velocity Loop Speed Regulation	%
T	Load Torque Variation	gm-cm
T_1	Returned Torque due to Variation	gm-cm

Approved for Public Release

Contrails

TABLE VIII (3 of 3)

Symbol	Description	Units
V_0	Motor Voltage Required Under Running Conditions to Produce Torque T_0	volts
V_1	Motor Voltage Required Under Running conditions to Produce Torque T_1	volts
ω	Motor Rotational Velocity	radians/sec
$\varepsilon(s)$	Amplifier Input Voltage	volts
$\varepsilon_o(s)$	Loop Return Voltage	volts
ϕ_M	Loop Phase Margin	degrees
$D_T(s)$	Torque Disturbance	gm-cm
K_{PC}	Pickoff to D/A Ouput Constant	$\frac{\text{volts}}{\text{cm}}$

Approved for Public Release

Contrails

Motor Transfer Function

The motor transfer function is determined from the data supplied by the manufacturer. The motor chosen for this analysis exhibits good low speed characteristics, a high value of maximum available torque, small size, and a low value of friction torque.

The following constants are supplied by Inland Motor Corporation for their Model #T-2171 winding D:

$$J_M = 1.59 \text{ gm-cm-sec}^2 \ (22 \times 10^{-3} \text{oz-in-sec}^2)$$

$$K_T = 4125 \text{ gm-cm/amp } (57.2 \text{ oz-in/amp})$$

$$K_B = 0.40 \text{ volt-sec/radian}$$

$$R_a = 10.9 \text{ ohms}$$

$$L_a = 17 \times 10^{-3} \text{ henries}$$

Other constants which alter the inherent time constants of the motor are the tachometer and load inertias (See Appendix III),

$$J_T = 0.505 \text{ gm-cm-sec}^2 \ (7 \times 10^{-3} \text{oz-in-sec}^2)$$

$$J_L = 13.1 \text{ gm-cm-sec}^2 \ (181.7 \times 10^{-3} \text{oz-in-sec}^2)$$

and the motor amplifier output resistance chosen as $R_S = 0.2\ \Omega$. Thus, the total drive shaft inertia and the total input circuit resistance become

$$J = J_M + J_T + J_L \tag{3}$$

$$= 0.022 + 0.007 + 0.182$$

$$= 15.2 \text{ gm-cm-sec}^2 \ (0.211 \text{ oz-in-sec}^2)$$

$$R = R_a + R_s \tag{4}$$

Approved for Public Release

Contrails

$$= 10.9 + 0.2$$

$$= 11.1 \text{ ohms}$$

An accurate approximation for M(s) is given by

$$M(s) = \frac{\frac{1}{K_B}}{(1 + \tau_M S)\ (1 + \tau_E S)} \tag{5}$$

where

$$\tau_E = L_a/R, \quad \text{electrical time constant} \tag{6}$$

$$\tau_M = \frac{J}{\frac{K_B K_T}{R}}, \quad \text{mechanical time constant}$$

The validity of this expression is subject to the condition

$$\frac{R}{2L_a} >> \frac{2K_T K_B}{J\ R} \tag{7}$$

$$\frac{11.1}{3.4 \times 10^{-2}} >> \frac{2\ (57.2)\ (0.40)}{(0.211)\ (11.1)}$$

$$330 >> 19.4$$

which, for this case, is certainly true. Then the actual time constants are

$$\tau_E = \frac{17 \times 10^{-3}}{11.1}$$

$$\tau_E = 1.53 \times 10^{-3}$$

Approved for Public Release

Contrails

$$\tau_M = \frac{0.211}{\frac{(0.40)\ (57.2)}{11.1}}$$

$$\tau_M = 0.103 \text{ sec}$$

The motor transfer function is then written as:

$$M(s) = \frac{2.5}{(1 + 0.103S)\ (1 + .00153S)} \tag{8}$$

Tachometer Transfer Function

The general expression for the tachometer transfer function T(s) exhibits an electrical pole due to the inductance and resistance in the output circuit. In this case, as in general, however, the pole is quite far out in frequency and thus can be neglected.

The inland Tachometer generator, #TG2139, was chosen for its moderate output, low friction torque, low ripple percentage, and high frequency of ripple. The parameters, as given, are

R_G = 1130 ohms

L_G = 0.60 henries

K_G = 1.2 volt-sec/radian

R_L = 10^5 ohms

T_G = 86.5 gm-cm (1.2 oz-in.)

Ripple Voltage = 2%

Ripple Frequency = 33 cycles/revolution

The general expression for the transfer function is

$$T(s) = \frac{V(s)}{\theta(s)} = \left[\frac{\frac{R_L}{R_G + R_L}}{1 + \frac{L_G}{R_G + R_L} S} \right] K_G \tag{9}$$

Approved for Public Release

Contrails

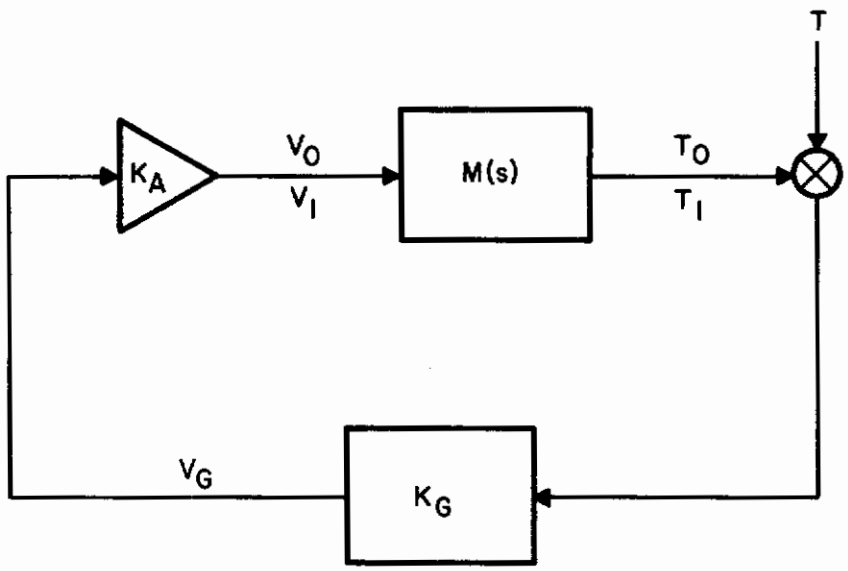

03-1167

Figure 22 DETERMINATION OF AMPLIFIER GAIN K_A

Approved for Public Release

Contrails

$$= \left[\frac{1}{1 + 0.592 \times 10^{-5}\, s} \right] 1.2$$

or

$$T(s) \approx \qquad \text{when} \quad \omega = \frac{s}{j} < 10^4 \ \frac{\text{radian}}{\text{sec}}$$

Amplifier Gain Constant K_A

The gain K_A, which will reduce the load variations to the desired level, will be determined with the aid of Figure 22. It is dependent upon load torques as well as load torque variations, the back emf of the motor, and the tachometer gain constant, K_G.

With reference to the footnote at the beginning of Section VII, the amplifier gain K_A will be determined from a prespecified value of speed regulation. This gives an exact indication of the smoothness of motion of the system under all expected conditions. If instead a torque rejection value were specified and the amplifier gain determined from it, the smoothness of motion would not be obvious until all constants were determined.

The voltage which runs the motor at the desired speed must overcome the back emf produced as well as the load torques present. This is made evident by the equation for running voltage,

$$V_M = V_T + V_B$$

$$= \frac{K_T R_a}{T} + K_W L \qquad (10)$$

The stall torque, represented by T, is the sum of three components, the motor resistance torque, the tachometer resistance torque, and the load torques. Variations in these values are expected and thus must be considered. The constants given by the manufacturer are

T_F = 216.3 gm-cm (3.0 oz-in.)

T_R = $\pm$ 6% of command torque

T_G = 86.5 gm-cm (1.2 oz-in.)

Previously calculated values for the two lead-screw-with-scanner assemblies are,

Approved for Public Release

Contrails

(T_L)ver = 420 gm-cm $\pm$ 1.18% short term (5.82 oz-in. $\pm$ 1.18% short term)

(T_L)hor = 485 gm-cm $\pm$ 0.64% short term (6.72 oz-in. $\pm$ 0.64% short term)

The sum of the load torques, irrespective of variations, is found as follows, (see Appendix I)

$$T_o = T_F + T_L + T_G$$

$$T_o = 809 \text{ gm-cm } (11.2 \text{ oz-in.}) \qquad (11)$$

The $\pm$ 6% ripple torque variation represents $\pm$ 6% of the command torque T_o or 48.5 gm-cm (0.672 oz-in.). This appears as an injected load variation in torque at a fundamental frequency of 33 cp rev. The system must be capable of reducing this to the acceptable level of $\pm$ .25% or less. In addition, there is the load variation which will be assumed to be $\pm$ 5% of 505 gm-cm ($\pm$ 5% of 7.00 oz-in.)(over long terms). This disturbance will occur with a dominant frequency equal to or less than the speed of rotation of the motor.

Before an intelligent determination of amplifier constant K_A can be made, one must keep in mind a crucial point in an all dc servo: The tachometer output will consist of a dc term with a ripple riding on it. After all efforts have been made mechanically to reduce this ripple to a minimum, resort must be to electrical filtering for further reduction. Inasmuch as this ripple appears as part of the command signal at the tachometer output, it cannot be distinguished from variations in load speed. Since, however, load torque variations must be detected if too large, the loop must be capable of passing their frequency of occurrence. Unfortunately, it is generally true that motor ripple frequency and tachometer ripple frequency are not far enough apart to profitably apply electrical filtering in a broad speed range servo. This is the case here.

Fortunately, one of the requirements in this system is constant speed. The servo will not be required to follow fast changes in input command levels. Instead, command levels will remain constant over entire scans. In addition, the acceleration time constant has been set in the 10 sec range.

When all of the above aspects have been considered, only one solution is practical: reduce the effects of motor ripple torque through the addition of inertia to the load. This will serve to reduce motor torque variations from $\pm$ 6% to less than $\pm$ 0.25%. Amplifier gain constant K_A can then be determined solely from load torque variations.

The lowest speed of rotation will be 0.0628 radian/sec. If the mechanical time constant is made equal to inverse of this value, then, at 33 times this value motor ripple response will be down approximately 30 db from 6% to 0.2%.

Approved for Public Release

Contrails

Harmonics of the wave form will also be reduced below this figure. The required inertia is calculated as follows. The modified mechanical time constant, τ_X, is determined from the new break point as:

$$\tau_X = \frac{1}{0.0628} \approx 15.9 \text{ sec}$$

$$F = \frac{K_T K_B}{R} = (149 \text{ gm-cm-sec})\ 2.06 \text{ oz-in-sec}$$

$$J_X = \tau_X F = (15.9)(2.06) \approx (2380 \text{ gm-cm-sec}^2)\ 33 \text{ oz-in-sec}^2$$

$$J_X = J_A + J$$

$$\therefore J_A = J_X - J$$

$$J_A = 33 - 0.211$$

$$J_A \approx (2380 \text{ gm-cm-sec}^2)\ 33 \text{ oz-in-sec}^2 \qquad (13)$$

Figure 23 presents a curve of wheel diameter (d) vs. thickness (ℓ). The values along this curve will produce an inertia of 2380 gm-cm-sec^2 (33.0 oz-in.-sec^2) when they are applied to a steel wheel. The boxed-in area represents the most desirable one in which to work. The final choice has been set at ℓ = 0.635 cm (0.25 in.) and d = 10.54 cm (4.15 in.) as these values are quite compatible with the motor diameter of 7.11 cm (2.8 in.), and wheel weight is kept to a minimum.

The gain constant K_A may now be determined from the load torque, load torque variation, desired regulation and tachometer gain constant, K_G.

Refer to Figure 22 for the identification of the constants used in the following calculations. The variation in load torque T_0 will be designated T. The returned torque produced by the presence of disturbance torque T is T_1. The regulation, herein assumed to be reduced to $\pm$ 0.1%, to allow a margin for component variations, is labled r. The equation for the voltage V_M required to overcome the torque T_0 and to run the motor at ω radian/sec. is given as

$$V_M = \frac{T_0 R_a}{K_T} + \omega K_B$$

Approved for Public Release

Contrails

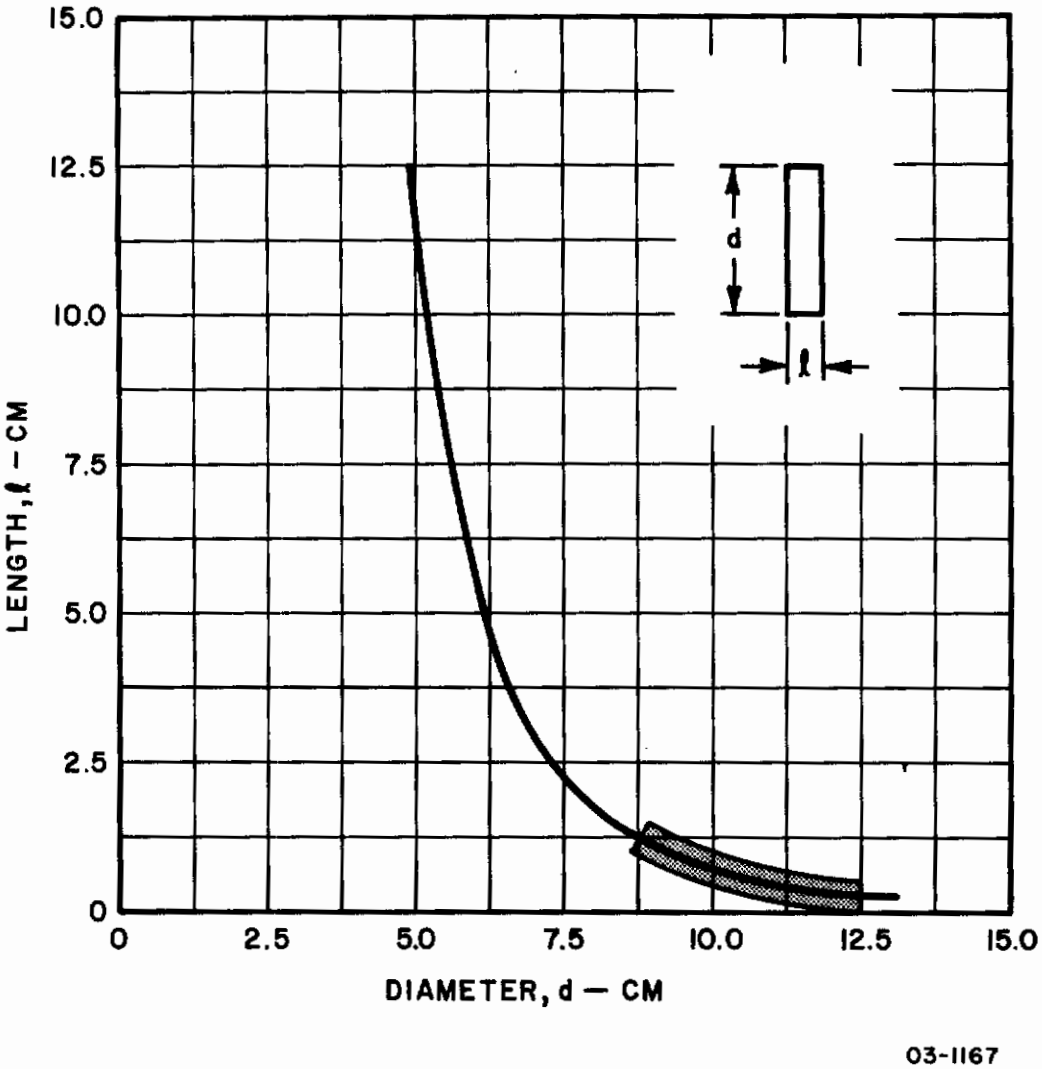

Figure 23 INERTIA WHEEL DIAMETER vs LENGTH FOR CONSTANT INERTIA OF 2365 GM-CM-SEC^2 (33 OZ-IN.-SEC^2)

Approved for Public Release

Contrails

Where, for any constant speed we may write

$$\frac{T_0 R_a}{K_T} = V_M - V_B$$

$$= V_0$$

or

$$T_0 = \frac{V_0 K_T}{R_a} \tag{14}$$

which states that for any constant speed the applied voltage and resultant torque are related through a constant, K_T/R_a. Therefore, to produce returned torque T_1, the voltage V_1 is required,

$$V_1 = \frac{T_1 R_a}{K_T} \tag{15}$$

Or, upon substitution of equation 14 into 15,

$$V_1 = \left(\frac{T_1}{T_0}\right) V_0 \tag{16}$$

The difference between T_1 and T is proportional to the regulation, r.

$$T_1 = T - rT = (1 - r)T \; [\approx T \; (r << 1)] \tag{17}$$

The change in speed that will occur after T_1 is returned is $r\omega$ radian/sec. Thus, the output of the tachometer will change by

$$rV_G = r\omega K_G \text{ volts}$$

This error signal is fed to the amplifier. The motor input V_1 is equal then to the amplifier output, or,

$$\left(\frac{T_1}{T_0}\right) V_0 = r\omega K_G K_A \tag{18}$$

Approved for Public Release

Contrails

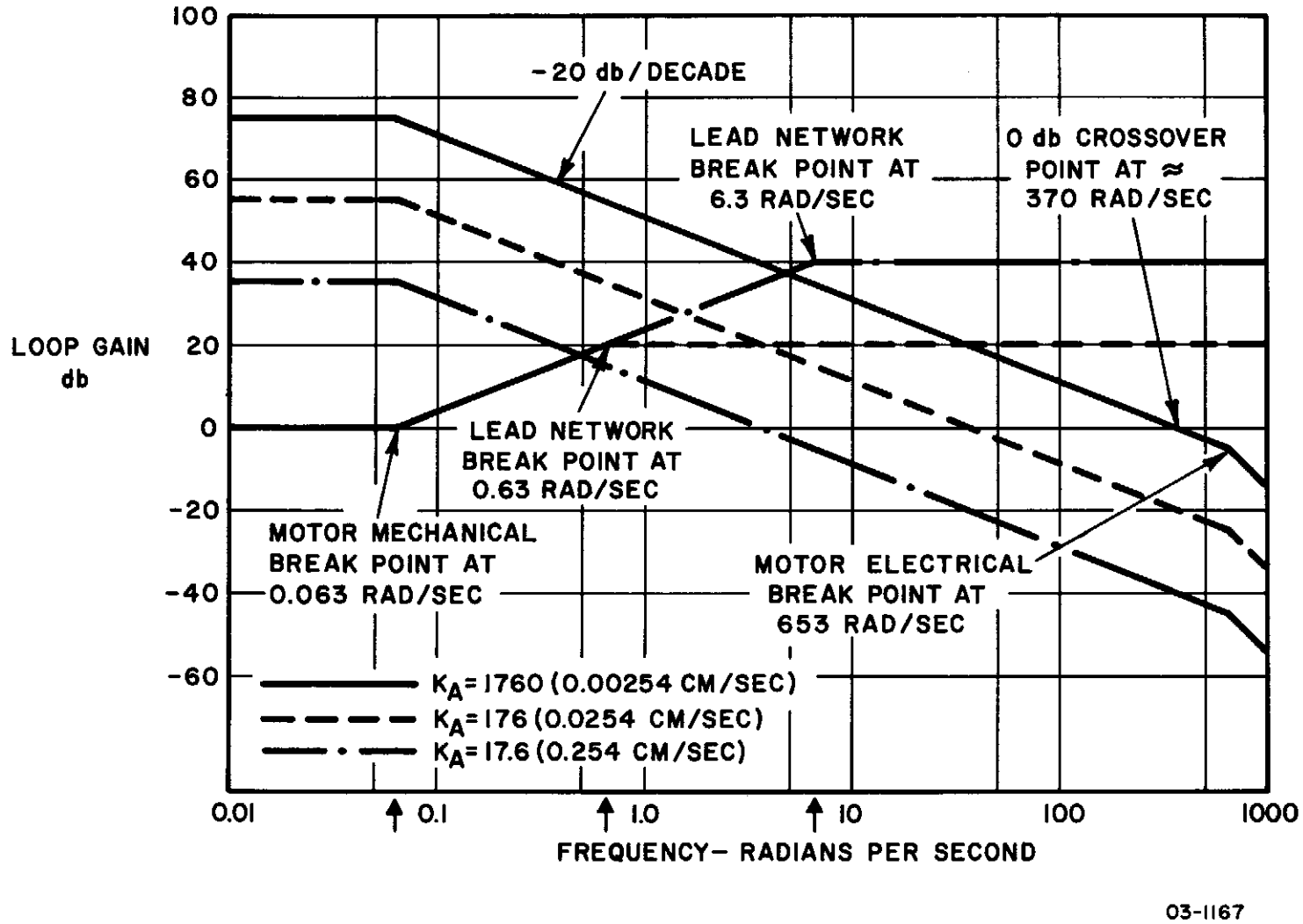

Figure 24 BODE PLOTS OF LOOP RESPONSE AND CORRECTIVE NETWORK RESPONSE

Approved for Public Release

Contrails

Thus, amplifier gain is determined from

$$K_A = \frac{\frac{T_1}{T_0} V_0}{r\omega K_G} \tag{19}$$

Substitution of equation 17 into the previous equation (19) yields,

$$K_A = \frac{\left(\frac{(1 - r)T}{T_0}\right) V_0}{r\omega K_G} \tag{20}$$

The values of K_A at ω = 0.063 radian/sec, 0.63 radian/sec and 6.3 radian/sec are given below, where V_0 = 2.14 v, T_0 = 809 gm-cm and T = 50 gm-cm.

ω	ωK_G	K_A
0.063	0.076	1760
0.630	0.76	176
6.30	7.6	17.6

Compensation Networks

In order that the closed loop be stable with the above amplifier gains, it is mandatory that the phase margin (loop response phase shift at 0 db gain) be considerably less than 180°. In most cases this means that some kind of correction network will be necessary. In addition to these requirements, the tachometer ripple must be suppressed sufficiently so that it is not taken as a command signal. A suppression of 26 db will be considered adequate as this will reduce the tachometer ripple to ± 0.1% at the amplifier output.

To determine what types of networks, if any, are necessary, a plot of the open loop gain is made. If the loop response is plotted for each of the three amplifier gains determined in the previous section, the result is seen in Figure 24. Note the arrows along the horizontal axis. These indicate the running speed at which the amplifier gain was calculated. Because of the location of the mechanical break point, the actual loop gain has fallen off considerably. One way to bring the loop gains back up is shown in the same figure. Correction networks,

$$\frac{A(s)}{B(s)}$$

Approved for Public Release

Contrails

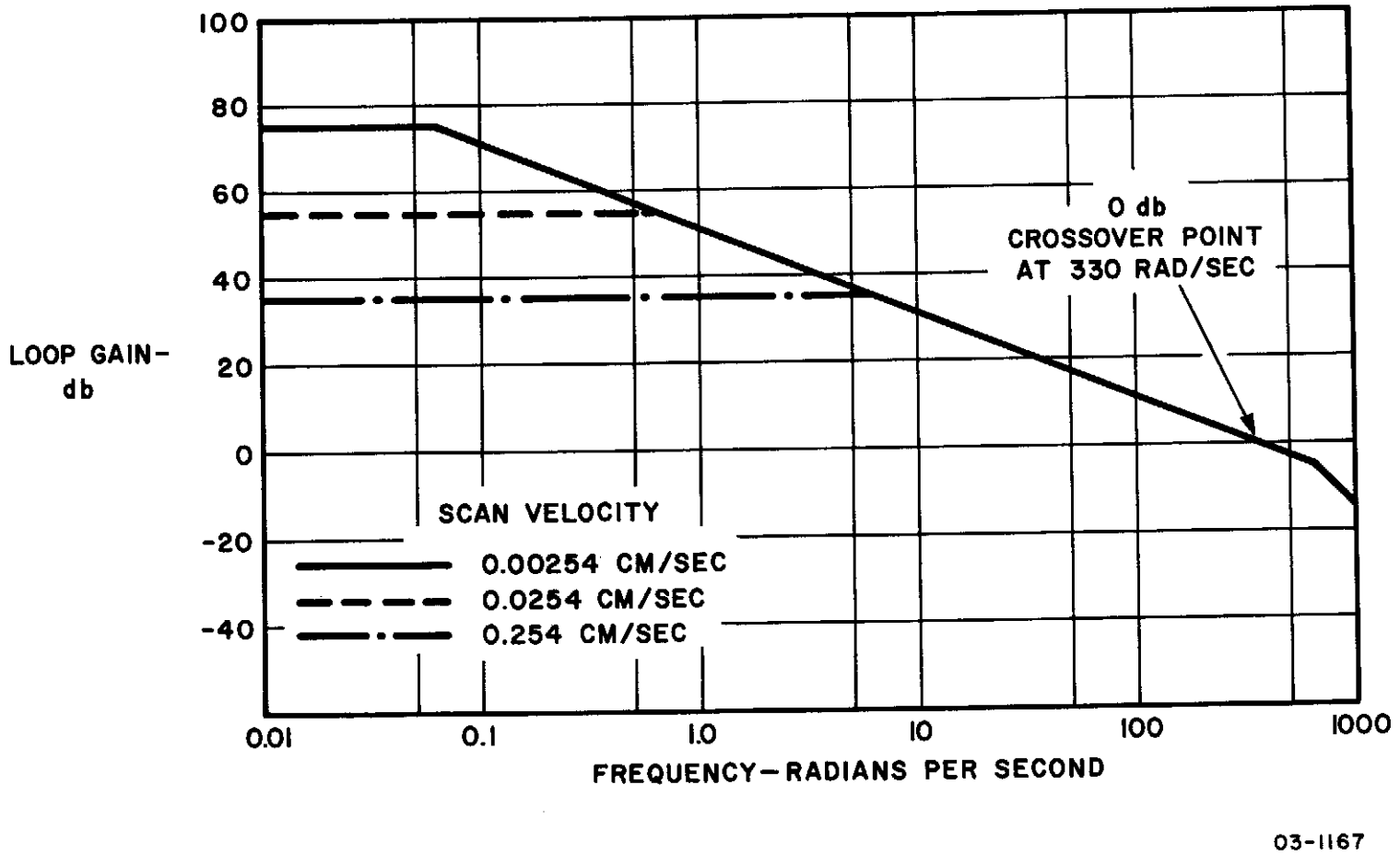

Figure 25 BODE PLOT OF LOOP RESPONSE WITH CORRECTIVE NETWORKS ADDED TO LOOP

Approved for Public Release

Contrails

as approximated by the Bode plots, could be added. The resultant loop responses would be those of Figure 25.

Another method is to use the amplifier gain determined for the lowest scanner velocity (K_A = 1760 v/v) and allow the natural loop falloff determine loop gain at any particular speed. This yields the curve in Figure 26. This is the final solution chosen, eliminating $\frac{A(s)}{B(s)}$ from the velocity loop.

The phase margin is quite easily determined from the expression for the loop response,

$$\frac{\varepsilon_o(s)}{\varepsilon(s)} = K_A M(s) K_G$$

$$= \frac{K_A K_G}{K_B} \left[\frac{1}{(1 + \tau_M S)\ (1 + \tau_E S)} \right] \tag{21}$$

which is obtained from Figure 27. At ω = 330 radian/sec, the approximate 0 db point in the previous figure,

$$\frac{\varepsilon_o(330)}{\varepsilon\ (330)} = \frac{(1760)\ (1.2)}{(0.40)} \left[\frac{1}{(1 + j(15.9)\ (330))\ (1 + j\ (0.00153)(330)} \right]$$

$$\approx 5600 \left[\frac{1}{(5250\ \angle 90°)\ (1.12\ \angle 26.5)} \right] \tag{22}$$

$$\approx 1\ \angle -116.5$$

The phase margin is then

$$\phi_M = 180° - 116.5$$

$$= 63.5° \tag{23}$$

which is quite adequate for stability.

The large phase margin is indicative of the large inertia at the load and shows the system is acceptable without compensation.

Torque Rejection Characteristic

The response of the closed loop system to torque disturbances at the load

Approved for Public Release

Contrails

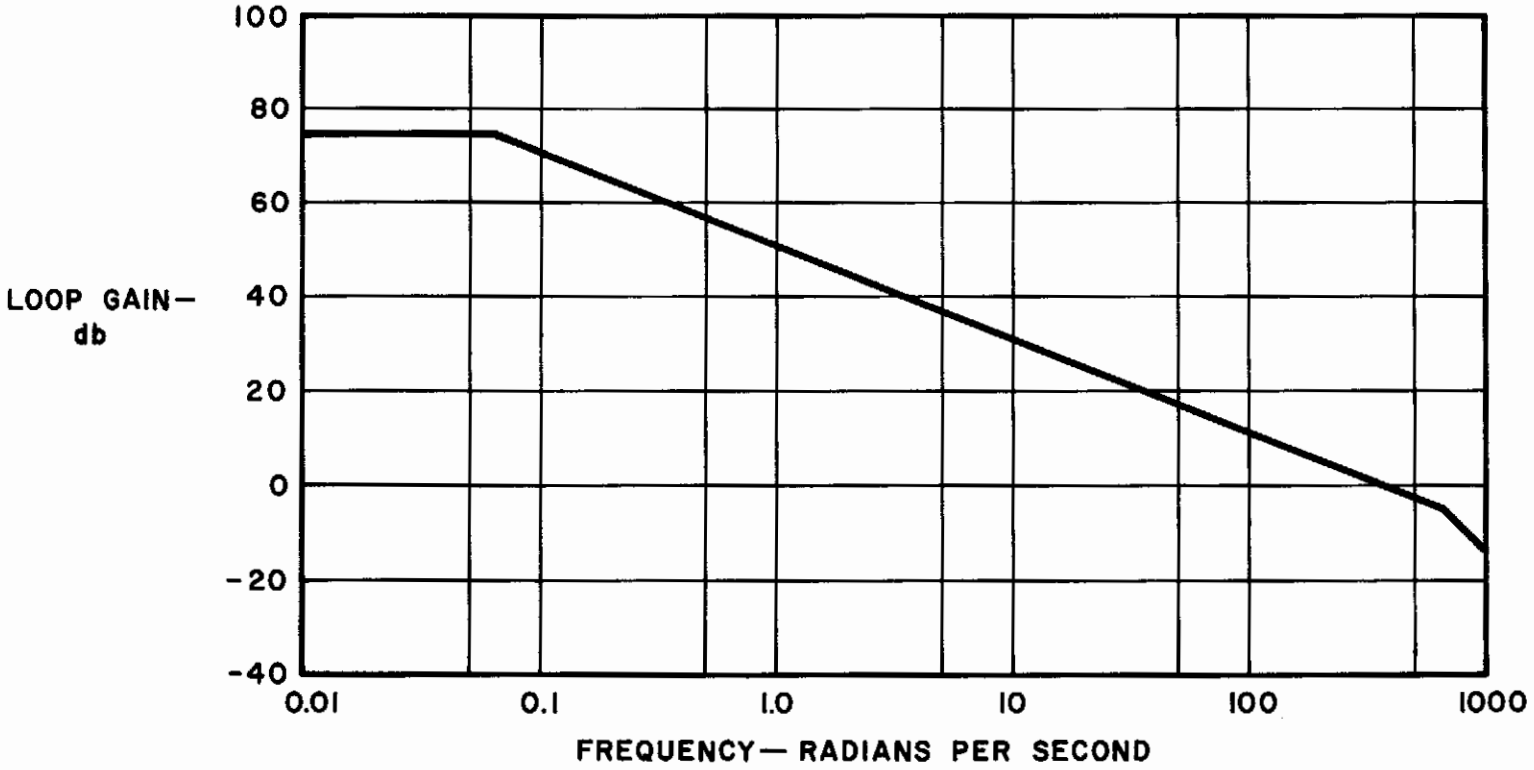

03-1167

Figure 26 BODE PLOT OF OPEN LOOP RESPONSE WITHOUT CORRECTIVE NETWORKS AND A SINGLE AMPLIFIER GAIN OF 1760 VOLTS/VOLT FOR ALL SPEEDS

Approved for Public Release

Contrails

can be easily found from Figure 28. In essence, a torque disturbance T_Q is modified by $D_T(S)$ and this function divided by (1 + Open Loop Transfer Function). That is

$$\frac{\Omega(s)}{T_D(S)} = \frac{-D_T(S)}{1 + K_A K_G M(S)} \tag{24}$$

where

$$D_T(S) = \frac{R}{K_T\ K_B} \quad \frac{1}{1 + \tau_X S} = \frac{0.485}{1 + 15.9S}$$

$$M(S) = \left[\frac{\frac{1}{K_B}}{(1 + \tau_X S)\ (1 + \tau_E S)} \right] = \frac{2.5}{(1 + 15.9S)\ (1 + 0.00153S)}$$

Substitution of all pertinent functions yields,

$$\frac{\Omega(s)}{T_D(S)} = \frac{-\frac{0.485}{1 + 15.9S}}{1 + \frac{K_A K_G\ (2.5)}{(1 + 15.9S)(1 + 0.00153S)}} \tag{25}$$

which simplifies to,

$$\frac{\Omega(s)}{T_D(S)} = \frac{-1}{9180} \left[\frac{1 + 0.00153S}{1 + 0.00301S + 4.6 \times 10^{-6} S^2} \right] \tag{25}$$

The denominator is compared to

$$1 + 2\ \xi \frac{S}{\omega} + \left(\frac{S}{\omega}\right)^2 \tag{26}$$

where ξ, the damping factor, is the overshoot in the frequency domain as shown in Figure 29. With this knowledge and the actual values for ξ and ω, a Bode plot may be made of the above equation 25.

$$\omega = \frac{1}{\sqrt{4.6 \times 10^{-6}}} = \frac{1}{2.14 \times 10^{-3}} = 467 \text{ radian/sec}$$

Approved for Public Release

Contrails

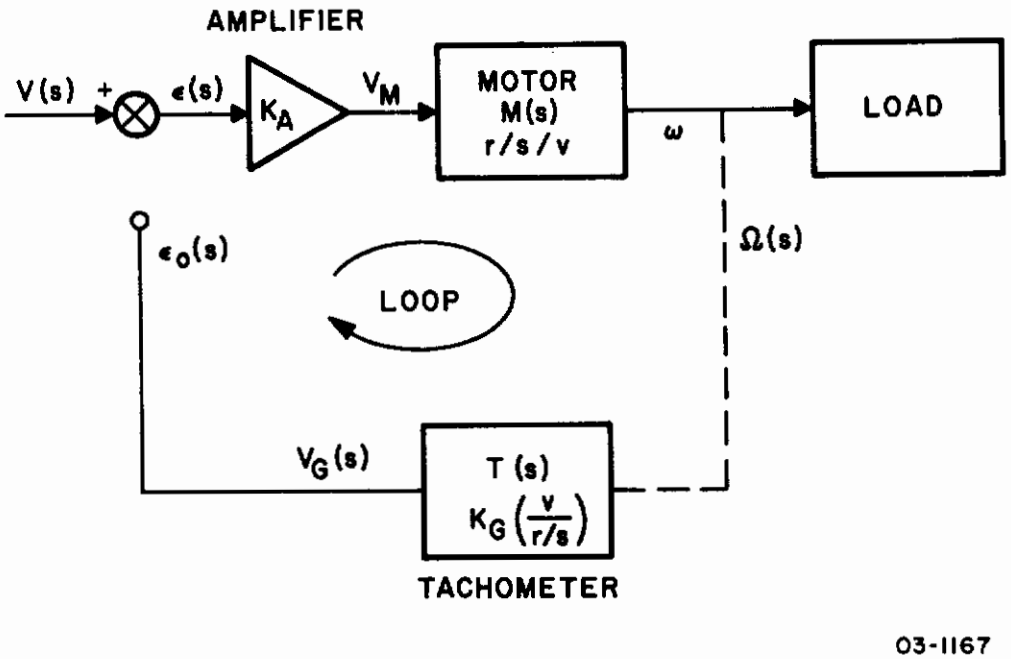

Figure 27 COMPLETED VELOCITY SENSITIVE SERVO LOOP FOR CALCULATION OF PHASE MARGIN

Approved for Public Release

Contrails

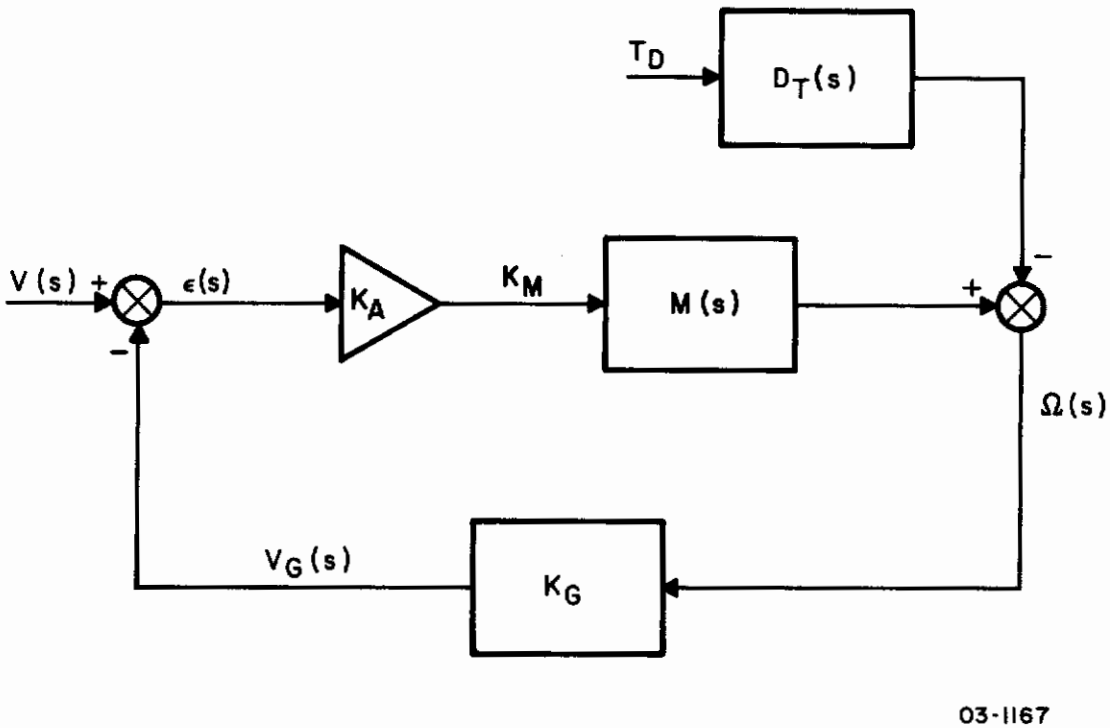

Figure 28 VELOCITY SENSITIVE SERVO WITH LOAD TORQUE DISTURBANCE

Approved for Public Release

Contrails

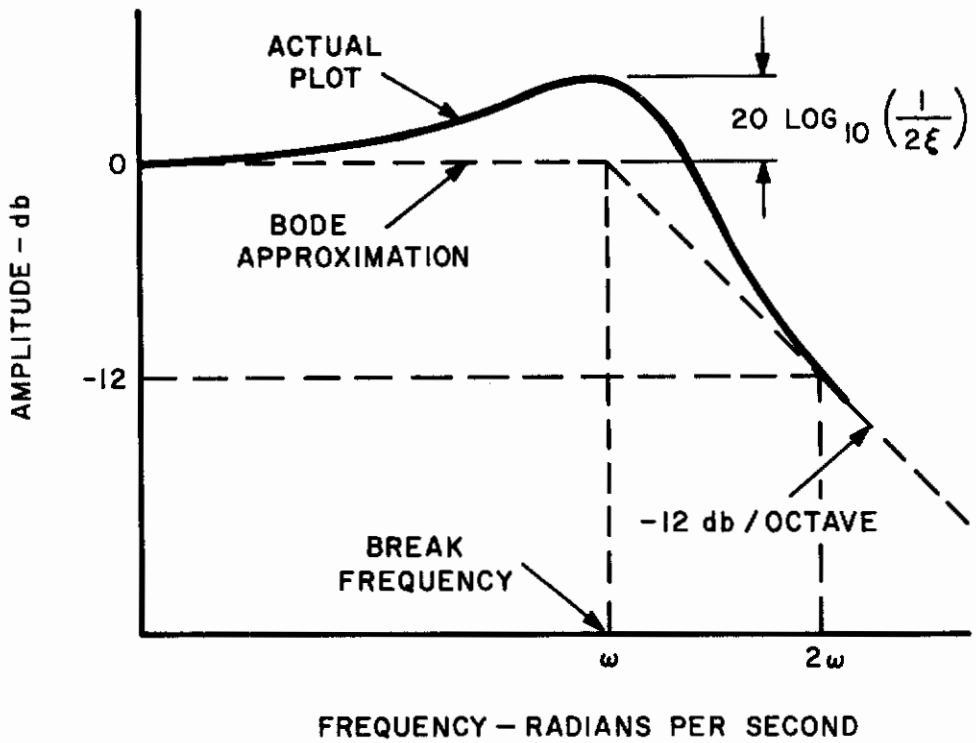

03-1167

Figure 29 BODE PLOT OF $1 + 2\xi \frac{s}{\omega} + \left(\frac{s}{\omega}\right)^2$

Approved for Public Release

Contrails

$$\xi = \frac{3.01 \times 10^{-3}}{4.28 \times 10^{-3}} = 0.703$$

$$\text{Overshoot} = 20 \log_{10} \left(\frac{1}{2\xi}\right) = 1.7 \text{ db}$$

The Bode plot is shown in Figure 30. It is quite obvious from the Figure that the torque disturbance rejection is excellent. This is further realized when the system response to a step torque of 72.1 gm-cm (1 oz-in.) is found.

Step Torque Response

The system response to a step torque disturbance is

$$\Omega(S) = K_0 \left[\frac{1 + 0.00153S}{S(1 + 3.01 \times 10^{-3}S + 4.6 \times 10^{-6}S^2)} \right] \tag{27}$$

The time domain response is the inverse Laplace Transform

$$\omega(t) = K_0 \{ 1 - 1.07 \, \varepsilon^{-328t} \cos (332t + 1°) \} \tag{28}$$

$$K_0 = \frac{1}{9180} \approx -79.2 \text{ db}$$

This function is depected in Figure 31. The ordinate units of change in velocity represent units of K_0, which is a change of 0.0109% of normal speed per unit. The insignificant overshoot (6%) is indicative of the large inertia added to the system.

In Figures 32 and 33, displacement in micro-inches is shown over a short time period (short distance of travel) and a long distance. Note that the error after 2.5 cm (1 in.) of travel on the transparency the error in position is only 1 spot, or 100 micro-inches. If this condition were allowed to prevail, however, 12.2 thousandths of a centimeter error will have accumulated over a linear 122 cm scan.

The abscissa scale of Figure 33 shows two time scales. The displacement in microns is converted into time displacement at 0.00254 cm/sec (0.001 in./sec) and 0.254 cm/sec (0.1 in./sec), in that order, for the two scales.

The accumulation of error due to a speed change must be detected and dealt with by a position loop. The design criteria for this loop are given in the next section.

Approved for Public Release

Contrails

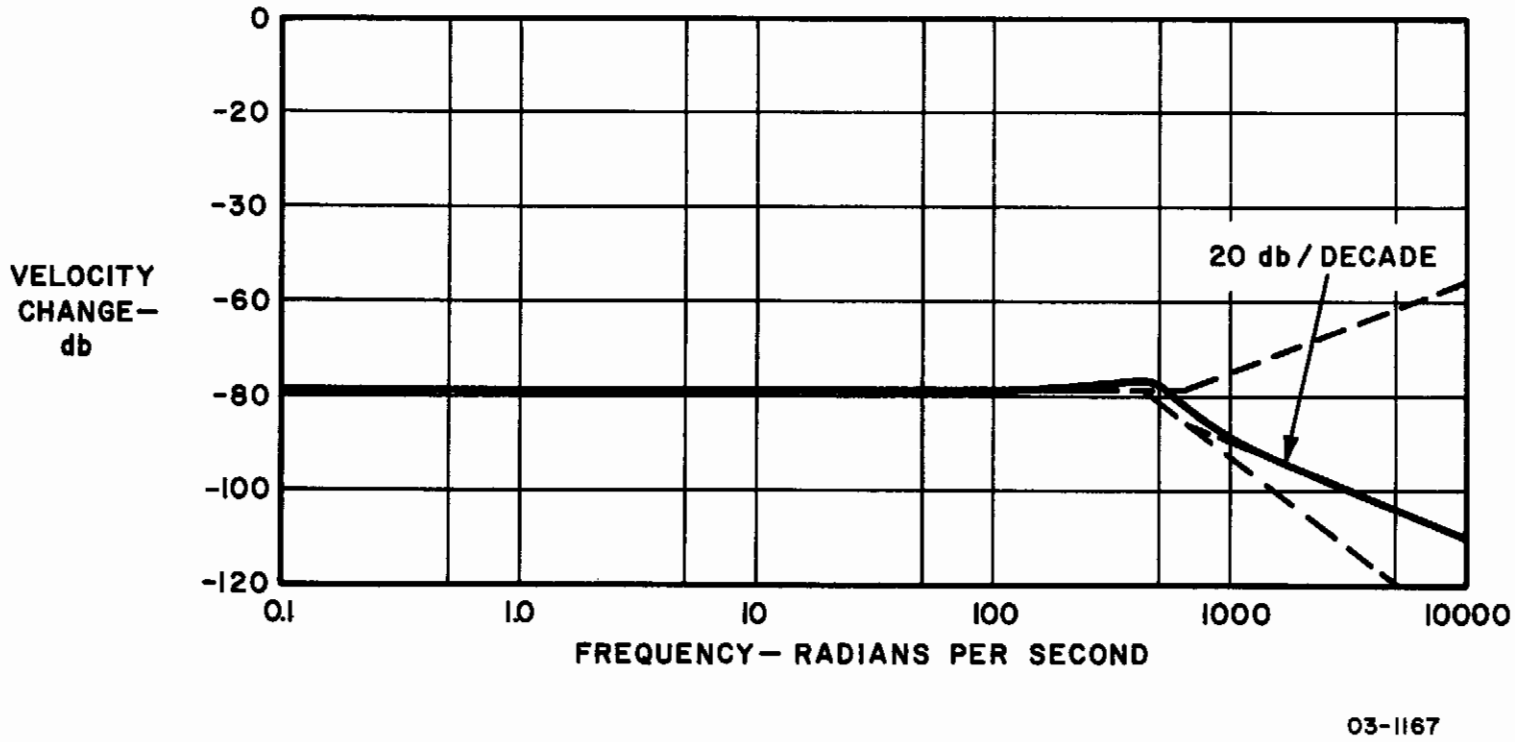

Figure 30 TORQUE REJECTION CHARACTERISTIC

Approved for Public Release

Contrails

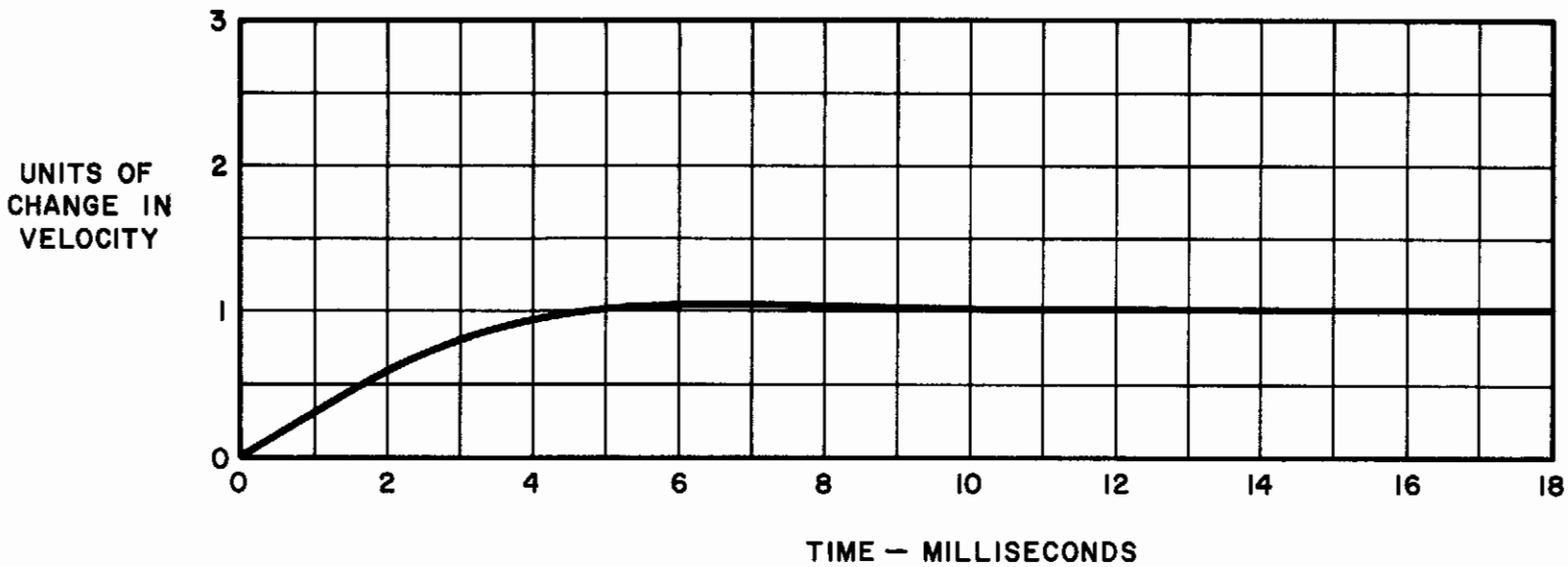

03-1167

Figure 31 VELOCITY SYSTEM RESPONSE TO UNIT STEP TORQUE DISTURBANCE OF 72.1 GM-CM (1 OZ-IN.)

Approved for Public Release

Contrails

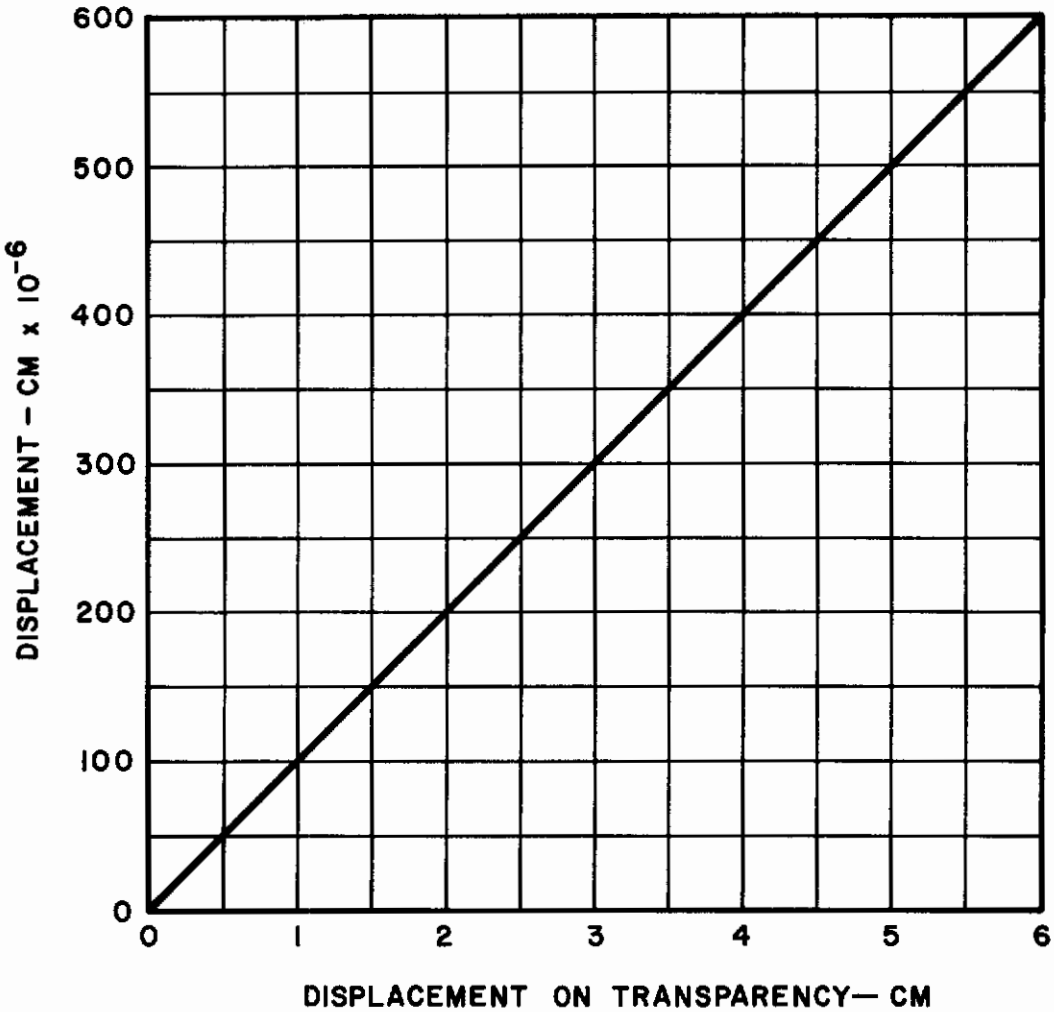

03-1167

Figure 32 DISPLACEMENT OF SPOT DUE TO 72.1 GM-CM (1 OZ-IN.) STEP TORQUE DISTURBANCE

Approved for Public Release

Contrails

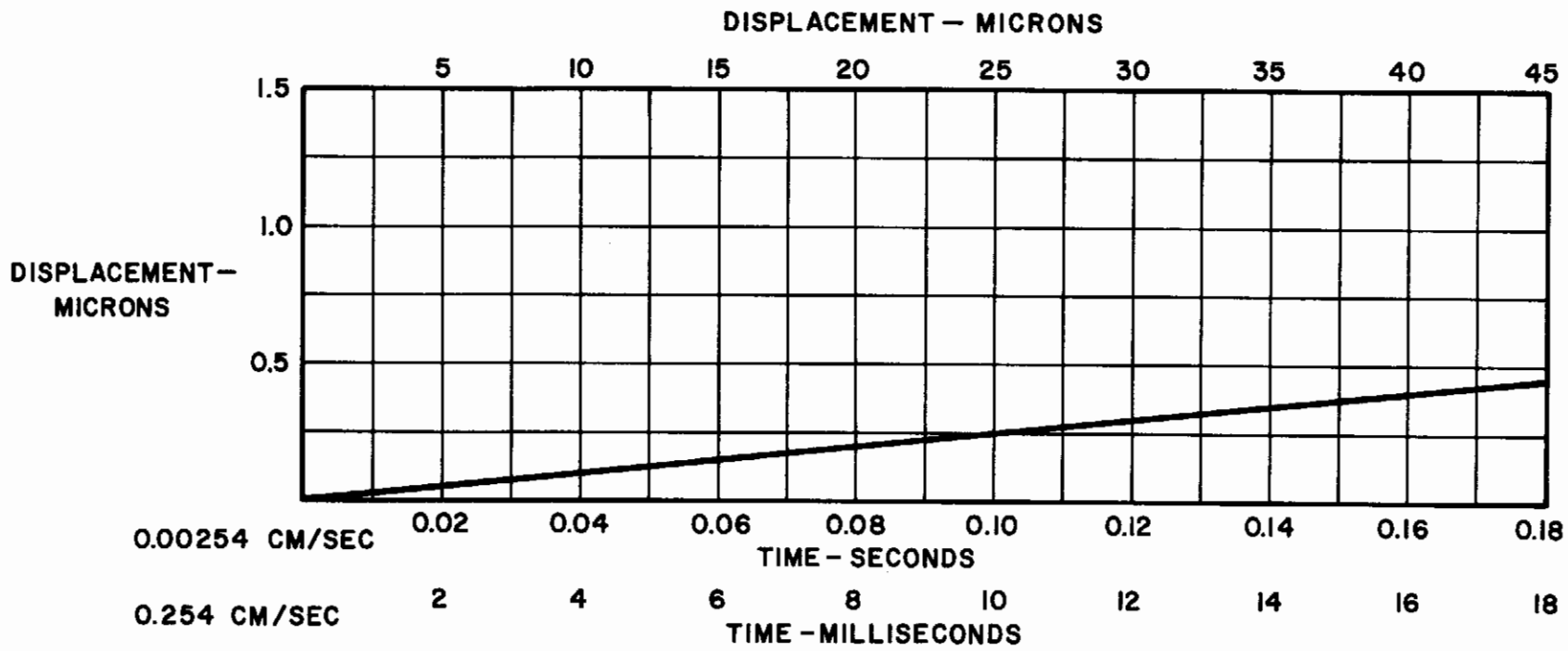

03-1167

Figure 33 DISPLACEMENT DUE TO 72.1 GM-CM (1 OZ-IN.) STEP TORQUE OF VELOCITY SERVO LOOP

Approved for Public Release

Contrails

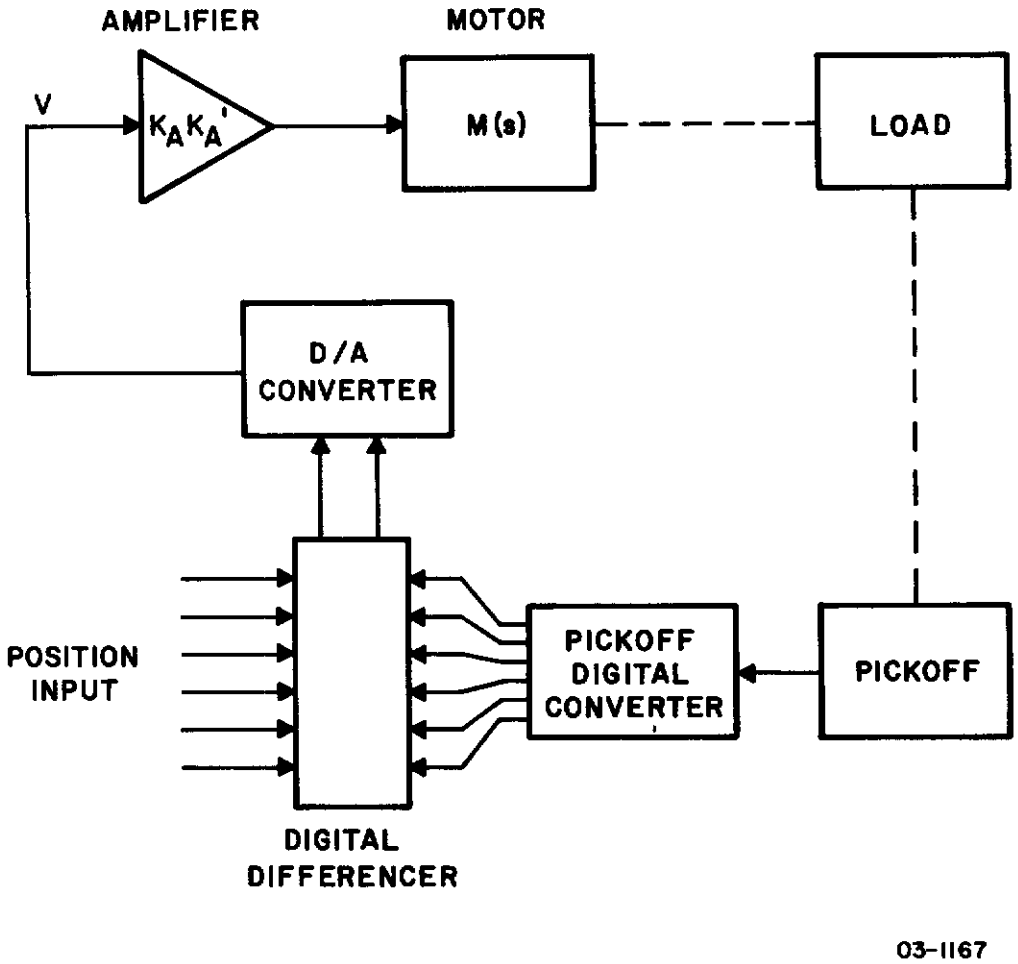

Figure 34 POSITION CORRECTION LOOP

Approved for Public Release

Contrails

POSITION SENSITIVE SYSTEM DESIGN

The position loop is shown in Figure 34. This section covers the position loop design. It will be assumed that position is determined by a linear inductosyn position pickoff. This device produces an output proportional to the (mutual) inductance between two circuits. The two circuits are called grids. One grid, the rotor, moves over the other, the stator, as the scanner moves over the film. With this method the actual spot position is identified directly rather than indirectly through coupling to the lead screw where a rotating disc would be used for position identification.

The absolute accuracy of the linear inductosyn is $\pm$ 0.000152 cm ($\pm$ 0.00006 in.) over a 30.5 cm (12 in.) section. This is extended to longer distances by placing two or more units end to end.

An electronic transducer converts the output into a binary code. The converter has a slope of 39.4 volts/cm (100 volts/in.). The resultant output ramp converts any 0.508 cm (0.2 in.) interval into 1000 steps of 0.02 volts each.

Thus, accuracy is reduced to 0.000508 cm (0.0002 in.) as can be seen in Figure 35. Since the system is a constant speed system, deviations in position will be small. This will keep operation of the position feedback system close to the center of the 0.508 cm interval.

Loop Gain Calculations

Loop gain calculations are based upon the dynamic motor characteristics and the static friction properties. Under normal running condition the voltage across the motor input terminals is given by

$$V_M = \frac{TR_a}{K_T} + K_B\omega \qquad (10)$$

where the term

$$\frac{TR_a}{K_T}$$

is friction torque voltage and $K_B\omega$ is the back emf produced at running speed ω. This function is illustrated in Figure 36. At low rotational speeds a small voltage change results in a large speed change. This reduces loop gain requirements at lower speeds.

At motor rotational speeds much lower than that which corresponds to the lowest linear scan velocity of 0.00254 cm/sec, i.e., the x-direction motor rotational speed, when traveling at an angle of 5° to the y-direction, the

Approved for Public Release

Contrails

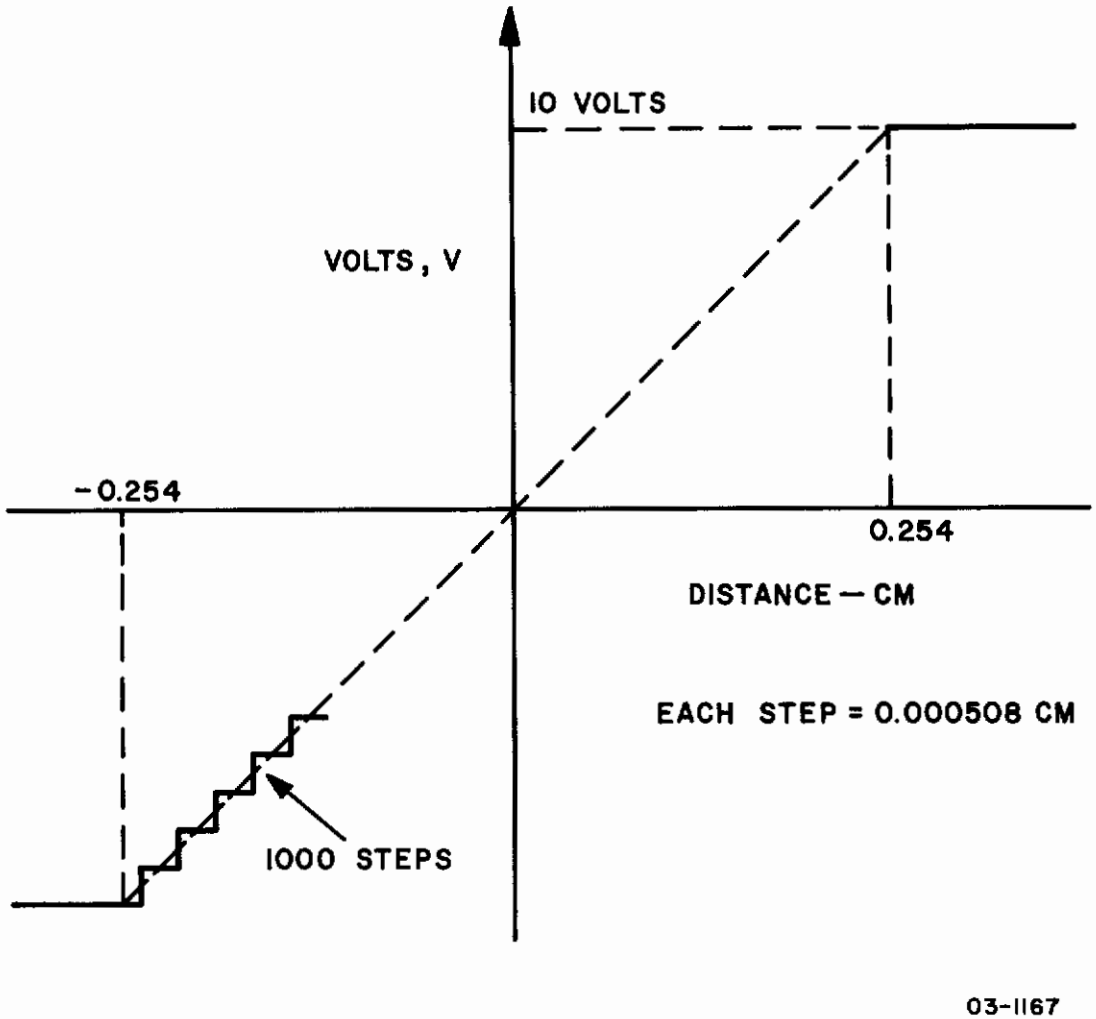

Figure 35 DIGITAL TO ANALOG CONVERTER OUTPUT

Approved for Public Release

Contrails

tachometer ripple is $\pm 2\%$ at 49 times the rotational frequency. This is a cyclic error and thus it falls within the $\pm 5\%$ line to line error allowable. The $\pm 6\%$ command torque variation is reduced by the high loop gain to an insignificant level. The only errors the position loop will have to correct for then, are long term velocity errors due to torque disturbances or errors in command voltage at the motor input.

The first term in equation (10) is the friction torque voltage V_{FT}, and for the calculations has a value,

$$V_{FT} = \frac{TR_a}{K_T}$$

$$= \frac{(809)\ (10.9)}{4125}$$

$$= 2.14 \text{ V}$$

The ideal characteristic of Figure 36 is used as a basis for loop gain calculations. It is assumed that the friction torque voltage which is supplied as a bias voltage is accurate to 1%. Based on previous calculations the maximum expected velocity error is $\pm$ 0.25% over long terms. For the two extremes in velocity, the voltages required to overcome the 1% error in bias and the 0.25% error in velocity are

$$@\ V_o = 0.00254 \text{ cm/sec}$$

$$V = (0.01)(2.14) + 0.0025\ (0.40 \times 0.0628)$$

$$= 0.0214 \text{ v}$$

$$@\ V_o = 0.254 \text{ cm/sec}$$

$$V = (0.01)(2.14) + 0.0025\ (0.40 \times 6.28)$$

$$= 0.0277 \text{ v}$$

When a position error is sensed the resultant correction voltage will be in the form of a step. Since the system is loaded down with inertia, it

Approved for Public Release

Contrails

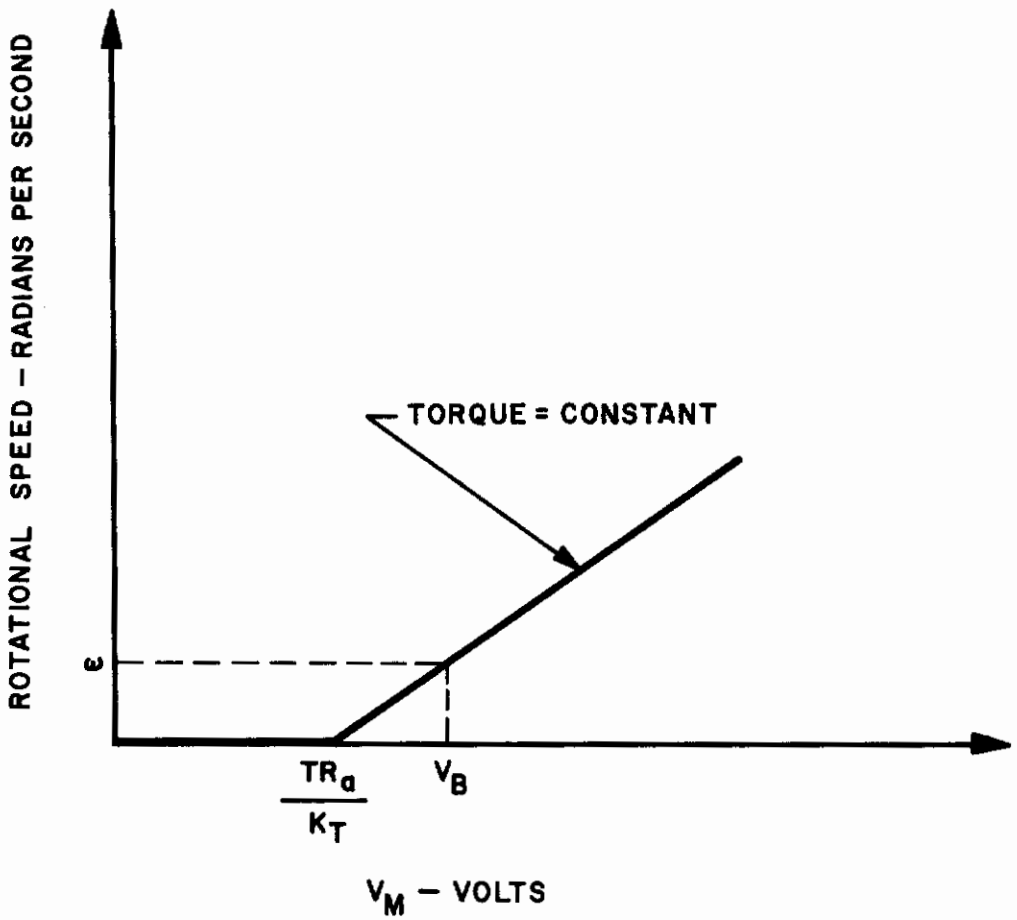

03-1167

Figure 36 FRICTION TORQUE BACK EMF MOTOR CHARACTERISTIC

Approved for Public Release

Contrails

is desirable to apply a larger than necessary voltage to accelerate the system more quickly toward correction. An increase to five times the normal running voltage computed in (29) results in

$$V = 0.0217 \text{ v.} \quad @ \; V_o = 0.00254 \text{ cm/sec}$$

$$V = 0.0528 \text{ v.} \quad @ \; V_o = 0.254 \text{ cm/sec}$$

In fact, correction voltages could be increased even further for better correction chatacteristics as long as a stable system results.

The overall loop gain and amplifier constant are determined from each of these values. An error of 0.000508 cm (0.002 in.) is detected by the position pickoff and digital differencer. An output of 20 millivolts is produced as indicated by Figure 35. This 20 millivolt signal must be amplified and applied to the motor to correct the error. The amplifier gains are then,

$$V_{PC} K_A K'_A = V$$

$$K_A K'_A = 1.09 \text{ V/V} \; @ \; 0.00254 \text{ cm/sec}$$

$$K_A K'_A = 2.64 \text{ v/v} \quad @ \; 0.254 \text{ cm/sec}$$

A value of 3.00 is chosen to cover the entire speed range of 100:1.

The Bode plot, shown in Figure 38, is determined from the open loop transfer function obtained from Figure 37.

$$\frac{\varepsilon_o(s)}{\varepsilon(s)} = K_A K'_A \, M(s) \, K_{PC}$$

$$= \frac{K_A K'_A \, K_{PC}}{K_B} \left[\frac{1}{A \, (1 + \tau_M S) \quad (1 + \tau_E S)} \right]$$

$$K_A K'_A = 3.00$$

$$K_{PC} = 39.4 \, \frac{\text{volts}}{\text{cm}} \times \frac{1 \text{ cm}}{24.7 \text{ radians}} = 1.59 \, \frac{\text{volts}}{\text{radians}}$$

Approved for Public Release

Contrails

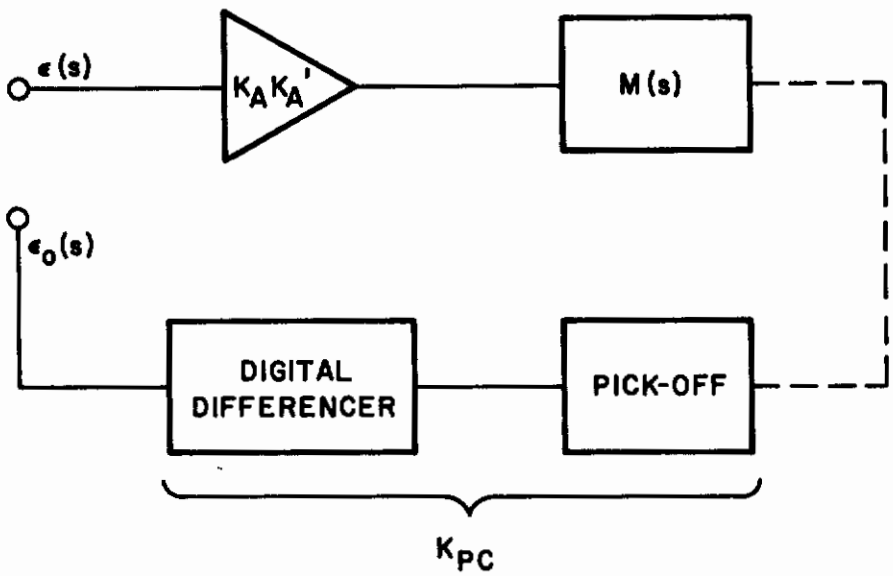

03-1167

Figure 37 LOOP FOR DETERMINATION OF AMPLIFIER CONSTANT $K_A K_A'$

Approved for Public Release

Contrails

$$K_B = 0.40 \frac{\text{volts-sec}}{\text{radian}}$$

$$\frac{\varepsilon_o(s)}{\varepsilon\ (s)} = \frac{11.92}{S\ (1 + 15.9s)\ (1 + 0.00153s)}$$

$$\approx \frac{11.92}{s\ (1 + 15.9s)} \qquad s = j\omega < j10$$

The 0 db axis crossing is determined from

$$\left| \frac{11.92}{s(1 + 15.9s)} \right| = 1$$

or,

$$(15.9\omega^2)^2 + \omega^2 - (11.92)^2 = 0$$

from which

$$\omega = 0.87$$

Obviously, the closed loop system would be unstable. The -40 db/decade slope crossing the 0 db axis must be reduced to a 20 db/decade slope by a network with breakpoints such as those shown in Figure 38. The overall loop response also shown in Figure 38 has a phase margin of

$$\phi_M = \angle \frac{11.92\ (1 + 3.33s)}{s(1 + 15.9s)(1 + 0.02s)} \Big|_{s = 2.5} + 180°$$

$$= \angle \frac{11.92\ (\ 1 + j8.32\ )}{(j2.5)\ (1 + 39.8)\ (1 + j0.05)} + 180°$$

$$= 180° + (81.5 - 180)$$

$$\phi_M = 81.5°$$

which is very adequate for stability.

Approved for Public Release

Contrails

The feedback control system discussed offers constant velocity motion with position correction. Because of the large inertia present, motion will be very smooth over the entire 100:1 speed range. The design values arrived at will produce spot motion which is well within the requirements set forth at the beginning of this section.

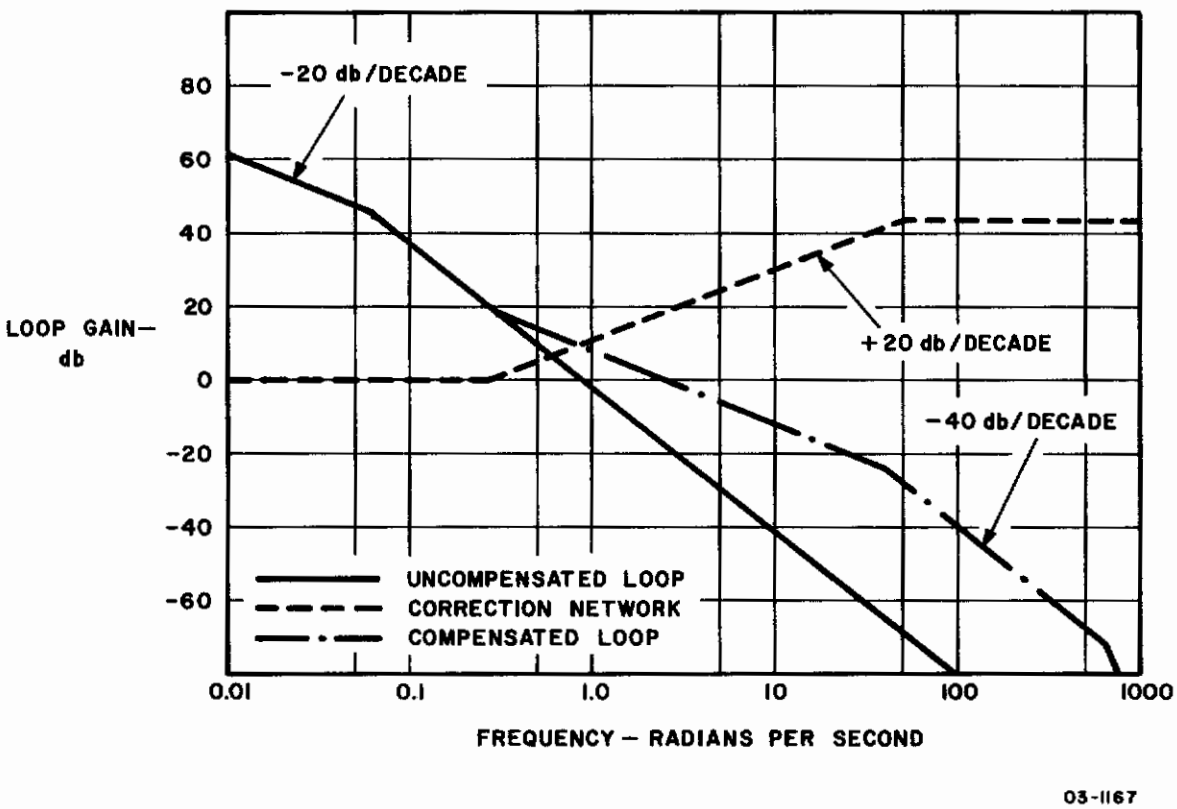

Figure 38 BODE PLOTS FOR POSITION LOOP

Approved for Public Release

Contrails

APPENDIX I

LOAD TORQUE ANALYSIS OF X-Y MOTION SYSTEMS

GENERAL

The following torque analyses were performed to establish design criteria required in the selection of servo motors and provide inputs to the control system analyses. The horizontal x-drive system, the vertical y-drive system, and heading control coulomb friction, were analyzed with emphasis on torque perturbations in the x and y drive systems. These torque perturbations are very low due to quality of materials utilized. The torque effect on the lead screws due to offset center of gravity is also analyzed and discussed further in that paragraph. Windage torques on lead screws and their drive motors are very low since windage torque is directly proportional to the product of speed and radius squared. An example of this is seen in the windage torque on the scanner disc shown on the following page.

A comparison of the horizontal (x) and vertical (y) drive system torques is shown on Figure 39. This plot readily shows how equal the load torques are in the two drive systems.

TORQUE ANALYSIS - HORIZONTAL MOTION SYSTEM

The horizontal drive system torque is reflected directly to the motor/lead screw shaft. The following torque equation is valid for Acme lead screws:

$$T_H = W_H \quad r_{mh} \quad \left(\frac{\text{Tan } \alpha + f/\cos \theta_n}{1 - f \text{ Tan } \alpha/\cos \theta_n} \right) + f_e r_{c_w}$$

where:

T_H = Torque applied to turn screw (gm-cm)

W_H = Load Parallel to Screw Axis (gms)

r_{mh} = Mean Thread Radius (cm)

α = Helix angle of thread at mean radius (degrees)

f = Coefficient of friction between screw and nut threads

f_c = Coefficient of friction at collar

θ_n = Angle between tangent to tooth profile and a radial line measured in a plane normal to thread Helix at mean radius (degrees)

Approved for Public Release

Contrails

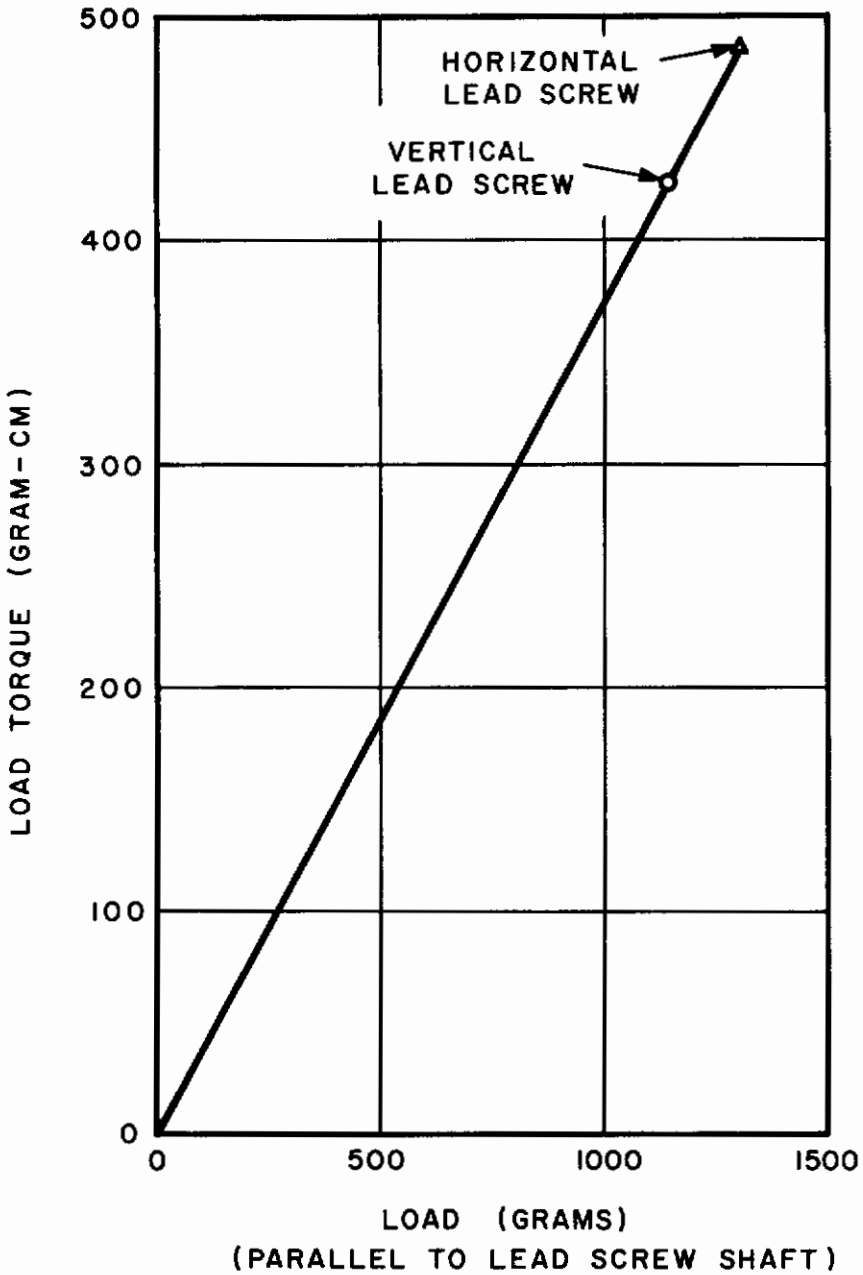

03-1167

Figure 39 LEAD SCREW TORQUE vs LOAD

Approved for Public Release

Contrails

r_{c_h} = Effective radius of rubbing surface against which load bears, called collar radius. (cm)

The Load Parallel to the Screw Axis Must First be Determined. (W_H)

This load is made up of optical window dead weight which is $W_w = 1.59 \times 10^5$ gms (350 lbs) as calculated on the other page, and four sets of spring loaded linear roller bearings at $W_s = 9.08 \times 10^4$ gms (200 lbs) preload each. The linear bearings have a coefficient of friction of 0.0025 gm/gm.

Therefore,

$$W_H = [W_w + 4W_s] \quad (0.0025) =$$

$$= (10^4) \quad [15.9 + (4)\ 9.08] \quad (0.0025) = 1310 \text{ gms}$$
$$(2.88 \text{ lbs})$$

There is a very small variation on this value due to dimensional variation of the rectangular guideway amounting to 5 microns (200 microinch) (it could also be a dust particle of this size).

Since the spring rate of the linear bearings is 1.79×10^6 gm-cm (14000 lb/in.)

$$W_H = (1.79 \times 10^6)(0.0005)(4)(0.0025) = \underline{8.95 \text{ gms}}$$

The mean thread radius $\underline{r_{mh} = 1.59 \text{ cm } (0.625 \text{ in.})}$

This is a theoretical dimension and has no tolerance.

The Helix Angle α is related to the lead and the mean radius r_{mh} by

$$\text{lead} = 0.254 \begin{array}{l} + 1.25\ \mu \\ - 0 \end{array}$$

$$\text{Tan } \alpha = \frac{\text{Lead}}{2\pi r_{mh}}$$

$$= \frac{(0.254)}{(2\pi)(1.59)} = 0.0254$$

$$\underline{\alpha = 1.4° = 5050 \text{ seconds}}$$

Approved for Public Release

Contrails

with 1.25 μ tolerance -

$$\text{Tan } \alpha' = \frac{0.000125}{(2\pi)(1.59)} = 0.0000125$$

$$\underline{\alpha' = 2.6 \text{ seconds}}$$

The coefficient of friction f is considered constant due to excellent lubrication of lead screw and nut. f = 0.2

θ_n is a function of pressure angle θ and the helix angle α and is expressed by (θ_n = 14.5°),

$$\text{Tan } \theta_n = \text{Tan } \theta \cos \alpha$$

$$= (0.2586)(0.9997) = 0.25859$$

$$\underline{\theta_n = 14.5°}$$

For all practical purposes

$$\underline{\theta_n = \theta} \text{ and remains constant}$$

The term $f_c r_c$ is not applicable to this lead screw since it is supported on an antifriction bearing which has a torque equation as shown

$$T_B = W_H r_{ch} (0.0015) =$$

$$T_B = (1310)(1.59)(0.0015) = \underline{3.13 \text{ gm-cm}}$$

where

This is negligible.

r_{ch} = 1.59 cm (0.625) in.)
Bearing Bore

W_H = 1310 gms

0.0015 is friction coefficient for an antifriction bearing.

The normal torque can now be calculated:

$$T_H = W_H \; r_{mh} \left[\left(\frac{\text{Tan } \alpha + f/\cos \theta_n}{1 - f \text{ Tan } \alpha/\cos \theta_n} \right) \right] + T_B$$

Approved for Public Release

Contrails

$$= (1310)(1.59) \left[\frac{\text{Tan } 1.4° + (0.2)/\cos 14.5}{1 - (0.2)(\text{Tan } 1.4)/\cos 14.5}\right]$$

$$= (1310)(1.59) \left[\frac{0.0255 + (0.2)/(0.968)}{1 - (0.2)(0.0255)/0.968}\right]$$

$$= (1310)(1.59)(0.233) = \underline{485 \text{ gm-cm}} \quad (0.42 \text{ lb-in.})$$

See Figure 38 for a plot of torque vs load.

The maximum torque variation is calculated

$$\Delta T'_H = (8.95)(1.59) \left[\frac{0.0255125 + (0.2)/(0.9681)}{1 - (0.2)(0.0255125)/(0.9681)}\right]$$

$$= (8.95)(1.59)(0.2331) = \underline{3.31 \text{ gm-cm}} \quad (0.00287 \text{ lb-in.})$$

Horizontal Drive System Torque Perturbation

$$T_H = x \ 100 = \frac{3.31}{485} \times 100 = \underline{0.68\%}$$

TORQUE ANALYSIS - VERTICAL MOTION SYSTEM

The vertical drive system torque is reflected directly to the motor/lead screw shaft similar to the horizontal drive system.

The following torque equation is valid for acme lead screws:

$$T_V = W_V \left[r_{mv} \left(\frac{\text{Tan } \alpha + f/\cos \theta_n}{1 - f \text{ Tan } \alpha/\cos \theta_n}\right) + f_c r_{c_v}\right]$$

The description of symbols is similar to the horizontal system as shown on another page.

The term $f_c r_{c_v}$ is omitted since the thrust friction is reduced to a negligible amount by using an antifriction bearing.

The load parallel to the screw axis is first determined. The 90.8 kilogram (200 lb) scanner weight is counter balanced out and doesn't enter the computation, there are six pairs of linear roller bearings with preloads of 90.8 kilograms each.

Approved for Public Release

Contrails

$$W_V = (0.0025) \quad [(45.4)(2) + (90.8)(4)]$$

$$= (0.0025)(454) = \underline{1.135 \text{ kilograms}} \quad (2.5 \text{ lbs})$$

Variation in preload is caused by guideway thickness variations or dust on the guideway. Thickness can increase 5 microns (200 microinches). This variation can increase the load, as follows:

$$W_V = (1.79 \times 10^6)(0.0005)(6)(0.0025)$$

$$= \underline{13.4 \text{ gms}}$$

The mean thread radius is $r_{mv} = 1.59$ cm (0.625 in.)

The Helix Angle $\alpha = 1.4° \begin{array}{l} + 2.6 \\ - 0 \end{array}$ seconds

as previously calculated for the Horizontal System

$$f = 0.2$$

$$\theta_n = 14.5°$$

The Nominal Torque is calculated as follows:

$$T_V = (1135)(1.59) \left[\frac{\text{Tan } 1.4° + (0.2)/\cos 14.5°}{1 - (0.2)(\text{Tan } 1.4)/\cos 14.5°}\right]$$

$$= (1135)(1.59)(0.233) = \underline{420 \text{ gm-cm}} \quad (0.364 \text{ lb-in.})$$

The torque variation is

$$\Delta T_V = (13.4)(1.59) \left[\frac{\text{Tan } 1.4° + 0.2/\cos 14.5°}{1 - 0.2 \text{ Tan } 1.4/\cos 14.5°}\right]$$

$$= (13.4)(1.59)(0.233) = \underline{4.96 \text{ gm-cm}} \quad (0.0043 \text{ lb-in.})$$

Approved for Public Release

Contrails

Vertical Drive System Torque Perturbation

$$T_V = \frac{4.96}{420} \times 100 = \underline{1.18\%}$$

TORQUE ANALYSIS - HEADING CONTROL MOTOR

The actual torque required at the scanner heading control drive motor is dependent on bearing load, seal friction, and slip ring friction. The torque at forward bearing is determined as follows:

$$T_1 = \mu W_1 r_1$$

Where

T_1 = Bearing torque in gm-cm

μ = 0.0015 friction coefficient for angular contact ball bearings

r_1 = 11.4 cm Radius of Bearing Bore

W_1 = 18,300 gram radial bearing load

Therefore,

$$T_1 = (0.0015)(18300)(11.4) = \underline{313 \text{ gm-cm}} \quad (0.271 \text{ lb-in.})$$

At the aft bearing

$$r_2 = 3.81 \text{ cm} \quad \& \quad W_2 = 6100 \text{ gms}$$

Therefore,

$$T_2 = \mu W_2 r_2 = (0.0015)(6100)(3.81) = \underline{35 \text{ gm-cm}} \quad (0.0303 \text{ lb-in.})$$

The seals used in the gas supply swivel coupling utilize graphite filled teflon and are designed to a loose fit allowing a slight leakage with a subsequent low friction load requirement.

The estimated breakaway friction load at an operating pressure of 7 kg/cm^2 (100 psi) is 4100 grams. The normal running load is 2270 grams. The torque is then as follows:

$$T_3 = 2F_s r_3$$

Approved for Public Release

Contrails

Where,

T_3 = Seal friction torque expressed in gm-cm

F_s = 2270 grams operating force

r_3 = 3.81 cm radius of seal contact for two seals

Therefore,

$$T_3 = (2)(2270)(3.81) = \underline{17300 \text{ gm-cm}} \quad (15 \text{ lb-in.})$$

The coin silver slip rings and silver graphite brushes create the following torque load:

$$T_4 = 2\mu F_B \quad [R_4 + R_5 + R_6 + R_7]$$

Where,

T_4 = Slip ring torque expressed in gm-cm

μ = 0.2 coefficient of friction for silver graphite brushes against coin silver rings

F_B = 45 gm brush load

R_4 = 8.1 cm (3.2 in.) Slip Ring Radius

R_5 = 8.9 cm (8.9 in.) " " "

R_6 = 9.7 cm (3.8 in.) " " "

R_7 = 10.5 cm (4.1 in.) " " "

Therefore,

$$T_4 = (2)(0.2)(45) \quad [8.1 + 8.9 + 9.7 + 10.5]$$

$$= \underline{670 \text{ gm-cm} \quad (0.58 \text{ lb-in.})}$$

The minimum torque requirement on the motor is:

$$T_{min} = T_1 + T_2 + T_3 + T_4$$

$$= 313 + 35 + 17300 + 670$$

$$= \underline{18318 \text{ gm-cm} \quad (15.88 \text{ lb-in.})}$$

Approved for Public Release

Contrails

TORQUE LOAD CAUSED BY CENTER OF GRAVITY OFFSET

Each drive screw (x and y systems) is mounted off center for practical reasons. This effect normally imparts torque perturbations on the system or cogging. For instance, the Vertical Drive System is offset from its center of gravity by (2.8 inches). This means that a net moment or torque could result. Taking into account the static balance of the offset cg, this effect is neutralized. However, under dynamic conditions the linear bearing preload comes into play. Each side of the scanner frame bearings impart a total load of 1.135 kilograms (2.5 lbs). The net torque about the lead screw longitudinal axis is,

$$T_{ML} = aR_1 - bR_2$$

Where,

T_{ML} = Net torque due to off center lead screw placement (kg-cm)

a = 8.65 cm Distance from one bearing set to C/L of lead screw

b = 22.8 cm Distance from outer bearing set to C/L of lead screw

$R_1 = R_2$ = 1.135 kg Bearing load reaction parallel to direction of motion.

$$T_{ML} = (8.65)(1.135) - (22.8)(1.135) = \underline{16 \text{ kg-cm}}$$

This torque unbalance is readily removed by adjusting the bearing preload until it is taken out.

The Horizontal Drive System exhibits a similar torque unbalance. This is overcome simply by preloading the lower set of linear roller bearings a greater amount than the upper bearings. The arm attaching the lead screw nut to the base of the transparency support is over hung as shown on Figure 40. The following unbalance load is studied:

$$T_p = FX$$

Where,

T_p = torque due to lead screw centerline offset from transparency centerline

F = friction force parallel to direction of motion = 1.31 kg

X = 6.1 cm (2.4 in.) moment arm

$$T_p = (1.31)(6.1) = \underline{8 \text{ kg-cm}}$$

Force normal to transparency support =

Approved for Public Release

Contrails

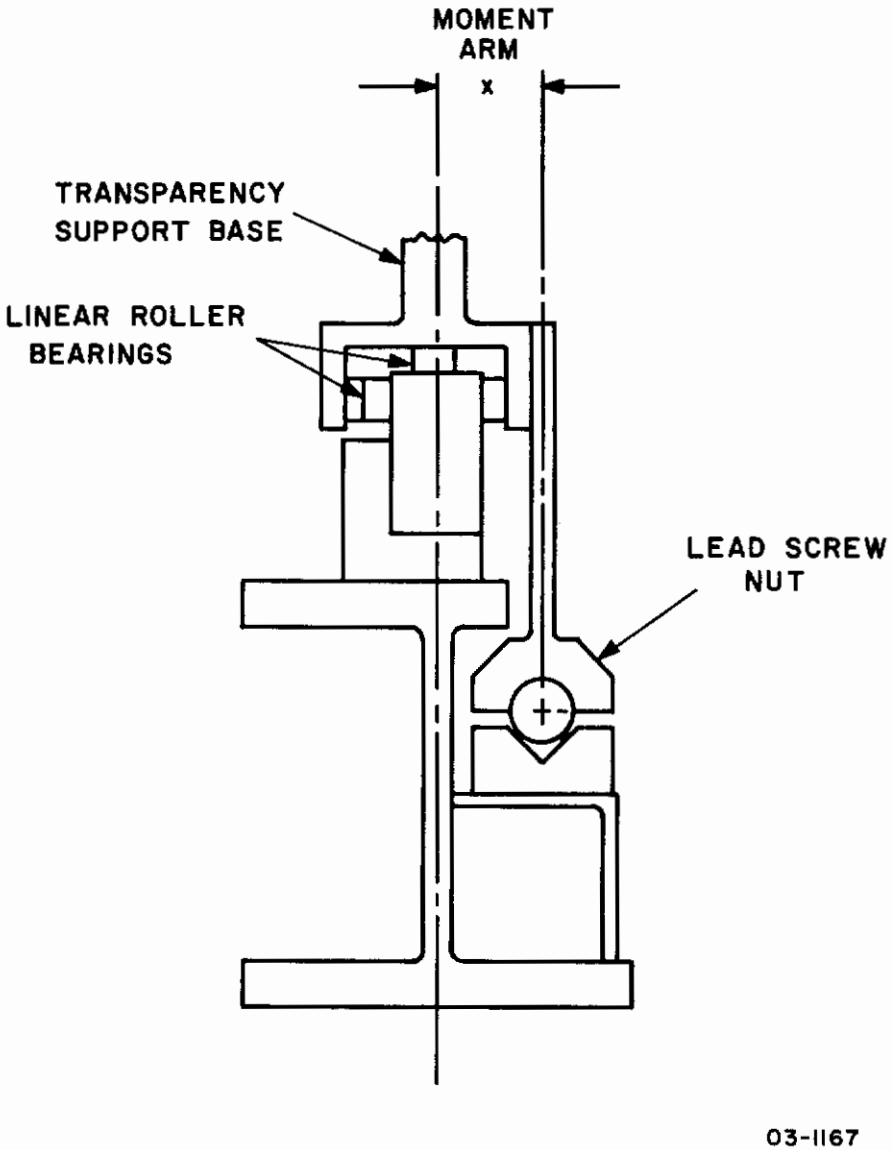

Figure 40 OFF-CENTER LEAD SCREW MOUNTING

Approved for Public Release

Contrails

$$F_N = \frac{T_p}{\ell} = \frac{8}{132} = \underline{0.0606 \text{ kg}}$$

ℓ = 132 cm (54 in.)

The net friction force due to this load acting against motion of lead screw is

$$F' = (0.0606)(0.0025) = \underline{0.0001515 \text{ kg}}$$

The net increase percentage wise

$$\% = \frac{0.0001515}{1.31} \times 100 = \underline{0.01155\%}$$

This small increase in load is negligible, and will not degrade drive system accuracy.

A possible effect on system accuracy, especially in using a split horizontal lead screw nut is the tendency under tooth contact for a small amount of cam action or lift out of the nut with respect to the lead screw. For a Pressure angle θ = 14.5°

The lift out force

$$F_L = \frac{2T_H \operatorname{Tan}\theta}{D}$$

Where,

F_L = Lift out force expressed in grams

T_H = Torque applied to turn screw

= 485 gm-cm

Tan θ = 0.259

D = Mean thread dia 3.18 cm

$$F_L = \frac{(2)(485)(0.259)}{(3.18)} = \underline{79 \text{ gm}}$$

$$= \underline{0.079 \text{ kilograms}}$$

This is $\frac{0.079}{159} \times 100 = \underline{4.96\%}$

Approved for Public Release

Contrails

of the window load and will not effect horizontal drive system accuracy.

WINDAGE TORQUE ON SCANNER DISC

The windage torque is given by

$$T = 2\Pi\mu\omega r_o^2 \ell$$

Where,

μ = 1.85×10^{-7} gm-sec/cm^2 for Air

r_o = 8.9 cm

ω = 523 Radian/sec

ℓ = 0.952 cm

$$T = 2\Pi\ (1.85 \times 10^{-7})(523)(8.9)^2(0.952)$$

$$= \underline{0.046 \text{ gm-cm}}$$

Approved for Public Release

Contrails

APPENDIX II

STRUCTURAL LOADS AND DEFLECTIONS

GENERAL

The following section discusses structure loads and subsequent deflections and elongations. This consists of deflections of the guideways and the supporting vertical (y) and horizontal I-beams. Their respective deflection plots are shown in Figure 16 and 17. The figures derived in these calculations are used to establish system accuracy under dynamic loading. The static weight and deflection are initially accounted for in the alignment and need not enter the calculations outlined here. The effects of scanner bearing preload is further analyzed to see how it effects position accuracy in the amount of give in the upper and lower scanner supporting structure. In addition, the optical window deflection is analyzed to guide in the selection of proper glass thickness and to compare effects of other glass thicknesses. A plot is shown in Figure 41.

DEFLECTION OF HORIZONTAL I-BEAM BY FILM TRANSPARENCY SUPPORT

A Load Schematic of the loaded member is shown on Figure 42. The intent of this analysis is to demonstrate, as simply as possible, the merit of using the I-Beam as a structural member with three-point support. The worst case approach of a simply supported beam, uniformly loaded, illustrates a more severe deflection curve than in actual use. This indicates that a further weight saving can be realized at final design without sacrifice in structural rigidity.

The following deflection analysis is based upon "Formulas for Stress and Strain", by Raymond J. Roark, Fourth Edition, case 14, Page 107.

Where

$$y = \frac{1}{48\ EI} \left\{ 8\ W \frac{d}{\ell} \left(x^3 - \ell^2 x\right) + Wx \left[\frac{8d^3}{\ell} - \frac{2bc^2}{\ell} + \frac{c^3}{\ell} + 2c^2 \right] \right\}$$

y = Deflection expressed in cm

E = Youngs Modulus for steel is 2.11×10^6 kgm per cm^2 (30×10^6 psi)

I = Beam moment of inertia is 11300 cm^4 (271.8 $in.^4$)

W = Total load on beam is 159 kgm (350 lbs)

d = $\ell - \left(\frac{b + a}{2}\right)$ expressed in centimeters

ℓ = distance between spans 132 cm (52 in.)

Approved for Public Release

Contrails

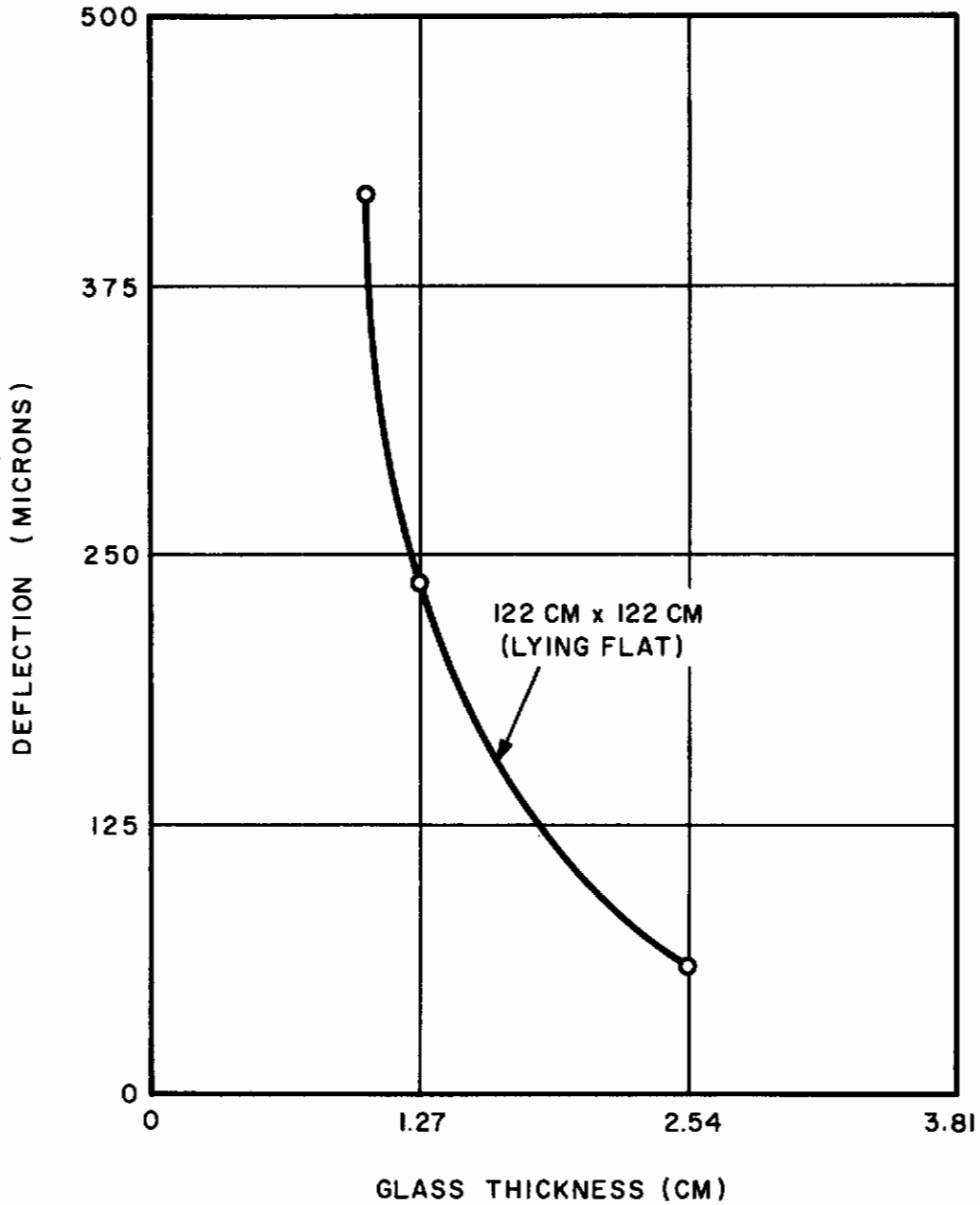

03-1167

Figure 41 OPTICAL WINDOW DEFLECTION

Approved for Public Release

Contrails

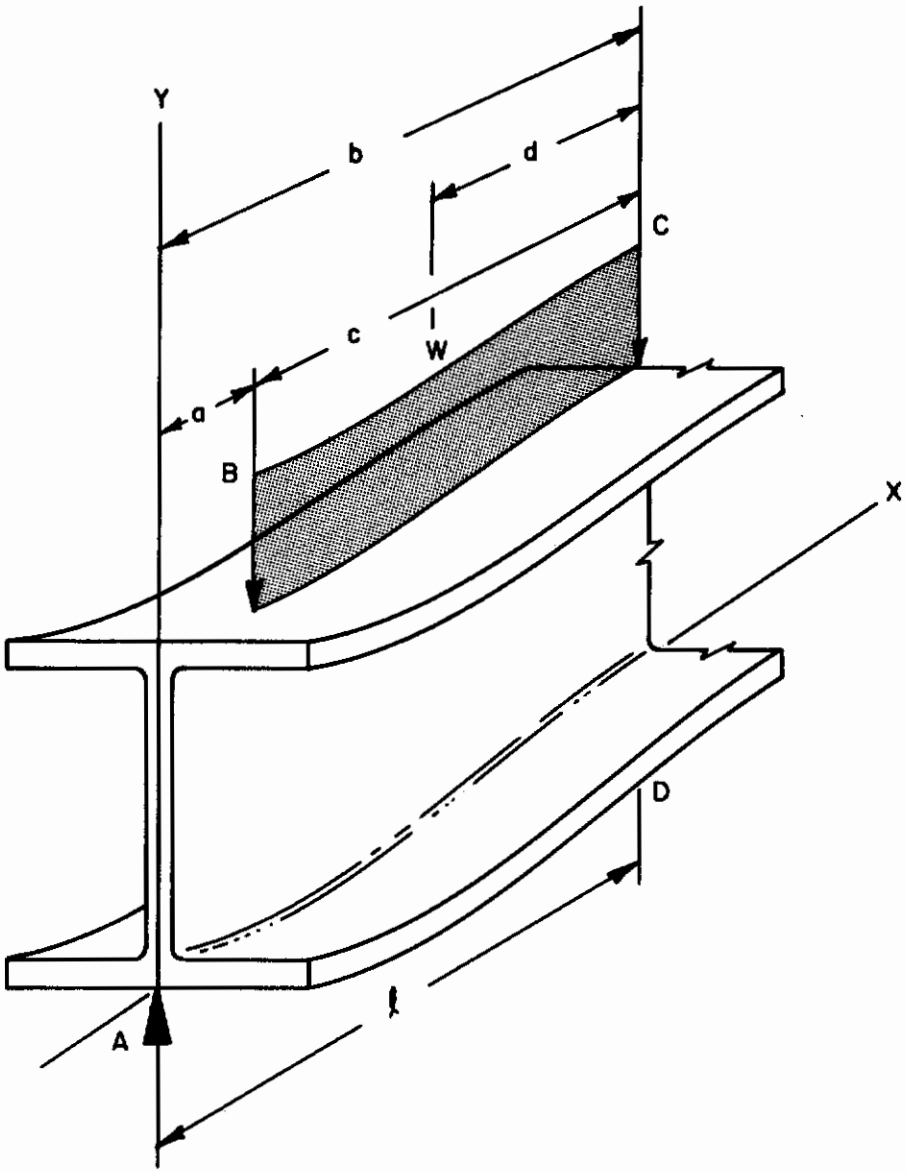

03-1167

Figure 42 HORIZONTAL I-BEAM LOAD DIAGRAM

Approved for Public Release

Contrails

x = coordinate distance where deflection is calculated cm

b = dimension in cm

c = dimension in cm

a = dimension in cm

Therefore,

at a = x = 15.25 cm (6 in.), d = 58.4 cm (23 in.)

b = 132 cm (52 in.), c = 117 cm (46 in.)

$$y_{15.25} = \frac{1}{(48)\ (2.11 \times 10^6)\ (11300)} \left\{ \frac{(8)\ (141)\ (58.4)}{(132)} \left[(15.25)^3 - (132)^2(15.25)\right] \right.$$

$$\left. + \ (141)\ (15.25)\left[\frac{(8)\ (58.4)^3}{(132)} - (2)\ \frac{(132)\ (117)^2}{(132)} + \frac{(117)^3}{(132)} + (2)\ (117)^2\right]\right\}$$

$$= \underline{0.68 \text{ micron}} \quad 27 \text{ (microinches)}$$

at a = x = 30.5 cm, d = 50.8 cm, b = 132 cm, c = 101.6 cm

$$y_{30.5} = \frac{1}{(48)(2.11 \times 10^6)(11300)} \left\{ \frac{(8)(122)(50.8)}{(132)} \left[(30.5)^3 - (132)^2(30.5)\right] \right.$$

$$\left. + \ (122)(30.5) \left[\frac{(8)(50.8)^3}{(132)} - \frac{(2)(132)(101.6)^2}{(132)} + \frac{(101.6)^3}{(132)} + (2)(101.6)^2\right]\right\}$$

$$= \underline{1.13\ \mu} \quad (45\mu\text{-in.})$$

at a = x = 45.75, d = 43.2 cm, b = 132 cm, c = 86.4 cm

$$y_{45.75} = \frac{1}{(48)(2.11 \times 10^6)(11300)} \left\{ \frac{(8)(104)(43.2)}{132} \left[(45.75)^3 - (132)^2(45.75)\right] \right.$$

$$\left. + \ (104)(45.75) \left[\frac{(8)(43.2)^3}{132} - \frac{(2)(132)(86.4)^2}{132} + \frac{(86.4)^3}{132} + (2)(86.4)^2\right]\right\}$$

$$= \underline{1.15\ \mu} \quad (46\ \mu\text{-in.})$$

Approved for Public Release

Contrails

at $a = x = 61$ cm, $d = 35.6$ cm, $b = 132$ cm, $c = 71$ cm

$$y_{61} = \frac{1}{(48)(2.11 \times 10^6)(11300)} \left\{ \frac{(8)(85.5)(35.6)}{132} \left[(61)^3 - (132)^3(61)\right] \right.$$

$$\left. + (85.5)(61) \left[\frac{(8)(35.6)^3}{132} - \frac{(2)(132)(71)^2}{132} + \frac{(71)^3}{132} + (2)(71)^2\right]\right\}$$

$$= \underline{1.07\ \mu} \quad (43\ \mu\text{-in.})$$

at $a = x = 76.2$ cm, $d = 28$ cm, $b = 132$ cm, $c = 56$ cm

$$y_{76.2} = \frac{1}{(48)(2.11 \times 10^6)(11300)} \left\{ \frac{(8)(28)(67)}{132} \left[(76.2)^3 - (132)(76.2)\right] \right.$$

$$\left. + (67)(76.2) \left[\frac{(8)(28)^3}{132} - \frac{(2)(132)(56)^2}{132} + \frac{(56)^3}{132} + (2)(56)^2\right]\right\}$$

$$= \underline{0.75\ \mu} \quad (30\ \mu\text{-in.})$$

at $a = x = 91.5$ cm, $d = 20.3$ cm, $b = 132$ cm, $c = 40.6$ cm

$$y_{91.5} = \frac{1}{(48)(2.11 \times 10^6)(11300)} \left\{ \frac{(8)(48)(20.3)}{132} \left[(91.5)^3 - (132)^2(91.5)\right] \right.$$

$$\left. + (48)(91.5) \left[\frac{(8)(20.3)^3}{132} - \frac{(2)(132)(40.6)^2}{132} + \frac{(40.6)^3}{132} + (2)(40.6)^2\right]\right\}$$

$$= \underline{0.4\ \mu} \quad (16\ \mu\text{-in.})$$

Approved for Public Release

Contrails

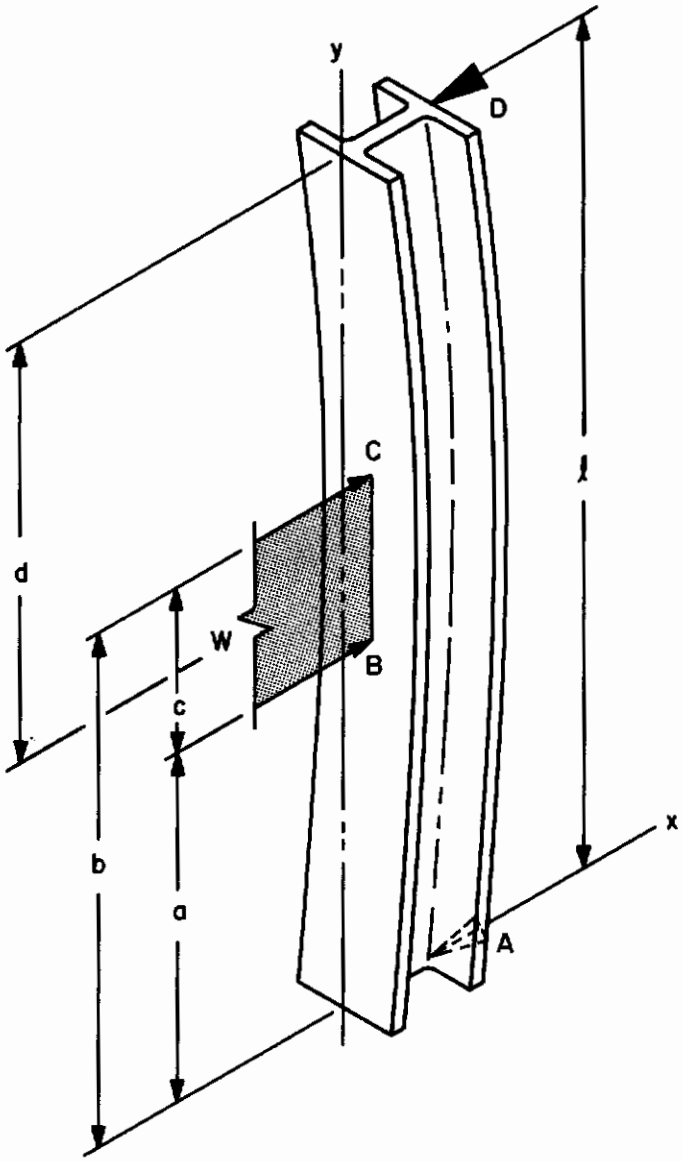

Figure 43 VERTICAL I-BEAM LOAD DIAGRAM

Approved for Public Release

Contrails

at $a = x = 107$ cm, $d = 12.7$ cm, $b = 132$ cm, $c = 25.4$ cm

$$y_{107} = \frac{1}{(48)(2.11 \times 10^6)(11300)} \left\{ \frac{(8)(30.6)(12.7)}{(132)} \left[(107)^3 - (132)^2(107)^2\right] \right.$$

$$\left. + (30.6)(107) \left[\frac{(8)(12.7)^3}{132} - \frac{(2)(132)(25.4)^2}{132} + \frac{(25.4)^3}{132} + (2)(25.4)^2\right]\right\}$$

$$= \underline{0.12\ \mu}\ (5\ \mu\text{-in.})$$

DEFLECTION OF VERTICAL I-BEAM BY SCANNER CARRIAGE

The load schematic is shown in Figure 43. The load in this case is created by the preloaded linear roller bearings mounted in the scanner carriage. This load is transmitted from the vertical guideways uniformly to the vertical I-Beam support. The magnitudes shown in this analysis are high, but does not impose a serious threat since it is systematic and can therefore be compensated for electronically. In addition there are three direct methods of reducing the deflections realizable at final design. First the bearing preload can be reduced, second a larger beam can be used, or third the deflection can be built in at initial alignment to provide zero error in operation. The analysis is based upon "Formulas For Stress and Strain" by Raymond J. Roark, Fourth Edition, case 14, page 107.

$$x = \frac{1}{48EI} \left\{ \frac{8wd}{\ell} (y^3 - \ell^2 y) + wy \left[\frac{8d^3}{\ell} - \frac{2bc^2}{\ell} + \frac{c^3}{\ell} + 2c^2 \right] - 2w \frac{(y-a)^4}{c} \right\}$$

Where,

x = deflection expressed in cm

E = Youngs Modulus 2.11×10^6 kgm/cm^2 (30×10^6 psi)

I = (6 in. WF. 25 lb/ft) Beam moment of inertia

= 2230 cm^4 (53.5 in.^{4})

w = total beam load 90.8 kgm (200 lbs)

d = $\ell - (\frac{b+a}{2})$ expressed in centimeters

= distance between spans 168 cm (66 in.)

y = coordinate distance to point of deflection from base

Approved for Public Release

Contrails

a = dimension in cm

b = dimension in cm See Figure 43

c = dimension in cm = 20.3 cm (8 in.)

@ $y = a + c/2 = 15.25$ cm, $a = 5.15$ cm, $b = a + c = 25.45$ cm,

$d = 153.0$ cm

$$x_{15.25} = \frac{1}{(48)(2.11 \times 10^6)(2230)} \left\{ \frac{(8)(90.8)(153.0)}{(168)} \left[(15.25)^3 - (168)^2(15.25)\right] \right.$$

$$\left. + (91)(15.25) \left[\frac{(8)(153)^3}{(168)} - \frac{(2)(25.45)(20.3)^2}{168} + \frac{(20.3)^3}{168} + (2)(20.3)^2\right]\right\}$$

$$- \frac{(2)(91)(15.25 - 5.15)^4}{20.3}$$

$$= \underline{2.5\ \mu}\ (100\ \mu\text{-in.})$$

@ $y = 30.5$ cm, $a = 15.4$, $b = 35.7$, $d = 142.5$

$$x_{30.5} = \frac{1}{(48)(2.11 \times 10^6)(2230)} \left\{ \frac{(8)(91)(142.5)}{168} \left[(30.5)^3 - (168)^2(30.5)\right] \right.$$

$$\left. + (91)(30.5) \left[\frac{(8)(142.5)^3}{168} - \frac{(2)(35.7)(20.3)^2}{168} + \frac{(20.3)^3}{168} + 2\ (20.3)^2\right]\right\}$$

$$- \frac{(2)(91)(30.5 - 15.4)^4}{20.3}$$

$$= \underline{6.5\ \mu}\ (260\ \mu\text{-in.})$$

Approved for Public Release

Contrails

@ $y = 45.7$ cm, $a = 35.6$ cm, $b = 56$ cm, $d = 122.2$ cm

$$x_{45.7} = \frac{1}{(48)(2.11)(10^6)(2230)} \left\{ \frac{(8)(91)(122)}{168} \left[(45.7)^3 - (168)^2(45.7)\right] \right.$$

$$+ (91)(45.7) \left[\frac{(8)(122.2)^3}{168} - \frac{(2)(56)(20.3)^2}{168} + \frac{(20.3)^3}{168} + (2)(20.3)^2 \right]$$

$$\left. - \frac{(2)(91)(45.7 - 35.6)^4}{(20.3)} \right\}$$

$$= \underline{12\ \mu}\ (480\ \mu\text{-in.})$$

@ $y = 61$ cm, $a = 51$ cm, $b = 61$ cm, $d = 112$ cm

$$x_{61} = \frac{1}{(48)(2.11 \times 10^6)(2230)} \left\{ \frac{(8)(91)(112)}{168} \left[(61)^3 - (168)^2(61)\right] \right.$$

$$+ (91)(61) \left[\frac{(8)(122)^3}{168} - \frac{(2)(61)(20.3)^2}{168} + \frac{(20.3)^3}{168} + (2)(20.3)^2 \right]$$

$$\left. - \frac{(2)(91)(61 - 51)^4}{20.3} \right\}$$

$$= \underline{16.5\ \mu}\ (660\ \mu\text{-in.})$$

@ $y = 76.2$ cm, $a = 66$ cm, $b = 86.3$ cm, $d = 92$ cm

$$x_{76.2} = \frac{1}{(48)(2.11 \times 10^6)(2230)} \left\{ \frac{(8)(91)(92)}{(168)} \left[(76.2)^3 - (168)^2(76.2)\right] \right.$$

Approved for Public Release

Contrails

$$+ \quad (91)(76.2) \left[\frac{(8)(92)^3}{168} - \frac{(2)(86.3)(20.3)^2}{168} + \frac{(20.3)^3}{168} + (2)(20.3)^2 \right]$$

$$- \quad \frac{(2)(91)(76.2 - 66)^4}{20.3} \Bigg\}$$

$$= \underline{17.8\ \mu}\ (710\ \mu\text{-in.})$$

@ $y = 84$ cm, $a = 73.8$ cm, $b = 94$ cm, $d = 84$ cm

$$x_{84} = \frac{1}{(48)(2.11 \times 10^6)(2230)} \left\{ \frac{(8)(91)(84)}{168} \left[(84)^3 - (168)^2(84)\right] \right.$$

$$+ \quad (91)(84) \left[\frac{(8)(84)^3}{168} - \frac{(2)(94)(20.3)^2}{168} + \frac{(20.3)^3}{168} + (2)(20.3)^2 \right]$$

$$- \quad \frac{(2)(91)(84 - 73.8)^4}{20.3} \Bigg\}$$

$$= \underline{18.8\ \mu}\ (750\ \mu\text{-in.})$$

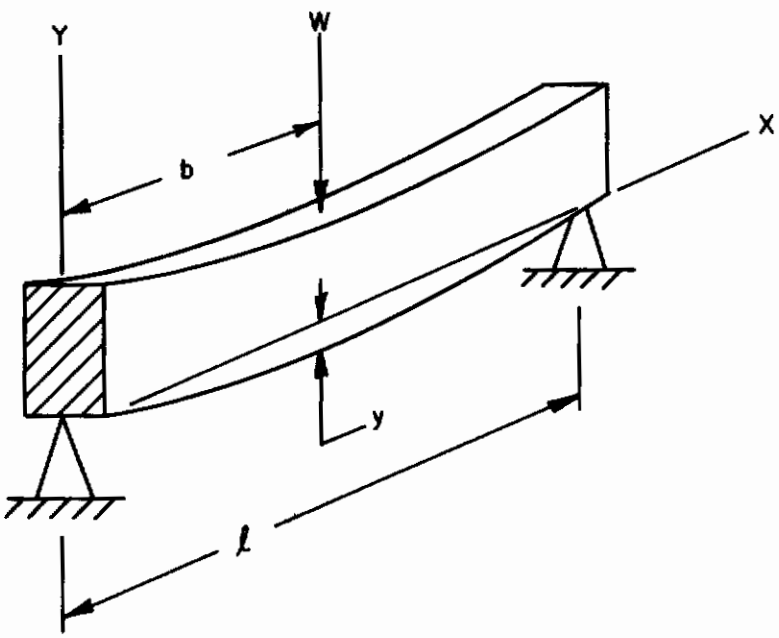

Figure 44 GUIDEWAY SECTION LOAD DIAGRAM

Approved for Public Release

Contrails

HORIZONTAL AND VERTICAL RECTANGULAR GUIDEWAY DEFLECTION

These guideways are attached to structural I-Beams in such a manner that they are adjustable at periodic intervals along their lengths. The horizontal guideways are adjusted with precisely machined gage blocks, and the verticals with screw adjustments. The adjustment feature provides precise positioning of guideways and subsequent high accuracy of scanner spot positioning. This feature allows a small amount of deflection of guideways. Each segment of unsupported guideway is treated as a simply supported beam with a concentrated load as shown on load schematic Figure 44.

Deflection of Horizontal guideway is determined from the following relationship:

$$y = \frac{Wbx}{6EI\ell} \left[2\ell(\ell - x) - b^2 - (\ell - x)^2 \right]$$

Where,

y = deflection expressed in microns

W = 31.8 kgm (70 lbs. per bearing)

E = 2.11×10^6 kgm/cm^2 (30×10^6 psi) Youngs Modulus

I = 76.8 cm^4 (1.84 in.^{4}) Moment of inertia

ℓ = 30.5 cm (12 in.)

b & x are expressed in cm

Therefore, the worst deflection occurs at

$$x = b = \frac{\ell}{2} = 15.25 \text{ cm}$$

$$y_{max} = \frac{(32)(15.25)^2}{(6)(2.11 \times 10^6)(76.8)(15.25)} \left[(30.52)^2 - (15.25)^2 - \frac{(30.5)^2}{4} \right]$$

$$= \underline{1.15 \text{ micron}} \quad (46 \text{ microinch})$$

Approved for Public Release

Contrails

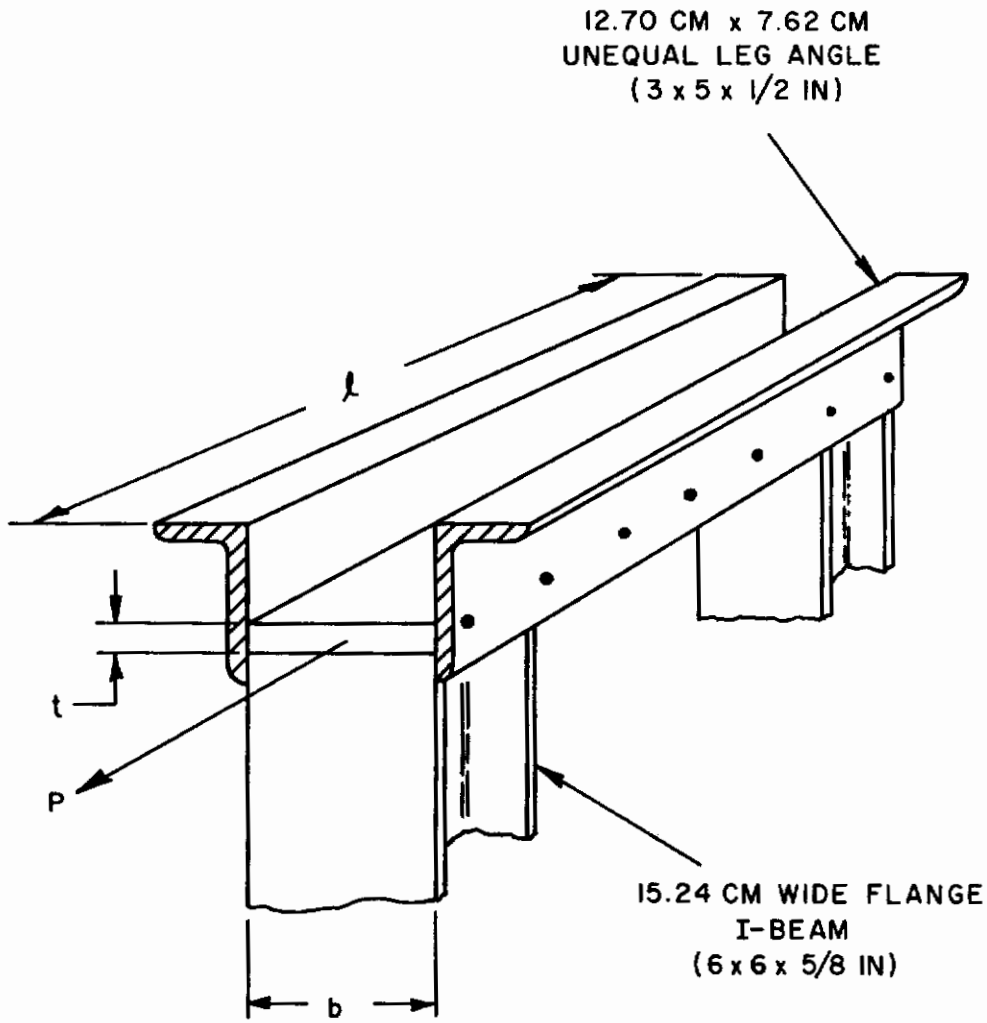

03-1167

Figure 45 SCANNER TOP SUPPORT STRUCTURE LOAD DIAGRAM

Approved for Public Release

Contrails

For the vertical guideway,

$W = 45.4$ kgm (100 lbs)

$I = 76.8\ cm^4$

$\ell = 30.5$ cm (12 in.)

Again, at $x = b\ \ell/2 = 15.25$ cm

$$y_{max} = \frac{(45.4)\ (15.25)}{(6)\ (2.11 \times 10^6)\ (76.8)} \left[(30.5)^2 - (15.25)^2 - \frac{(30.50)^2}{2} \right]$$

$$= \underline{1.65 \text{ micron}} \quad (65 \text{ microinch})$$

ELONGATION OF SCANNER TOP SUPPORT STRUCTURE

Axial elongation of top support structure shown on Figure 45 is determined as follows:

The elongation is determined by the classical equation

$$\zeta_T = \frac{P\ell}{\Delta E}$$

Where

ζ_T = axial elongation expressed in cm

P = 91 kilogram force created by linear bearing preload. (200 lbs)

ℓ = 86.5 cm length of member (34 in.)

$\Delta = bt + 2A_c = (15.25)(2.54) + (2)(24.2) = 87.72\ cm^2$

A_c = crossectional area of (5 in. x 3 in. x 1/2 in.) angle = 24.2 cm^2

$E = 2.11 \times 10^6\ kgm/cm^2$ Youngs Modulus

$$\zeta_T = \frac{(91)(86.5)}{(87.72)(2.11 \times 10^6)} = 42.5 \times 10^{-6} \text{ cm}$$

$$= \underline{0.425 \text{ micron}} \quad (16.8 \text{ microinch})$$

Approved for Public Release

Contrails

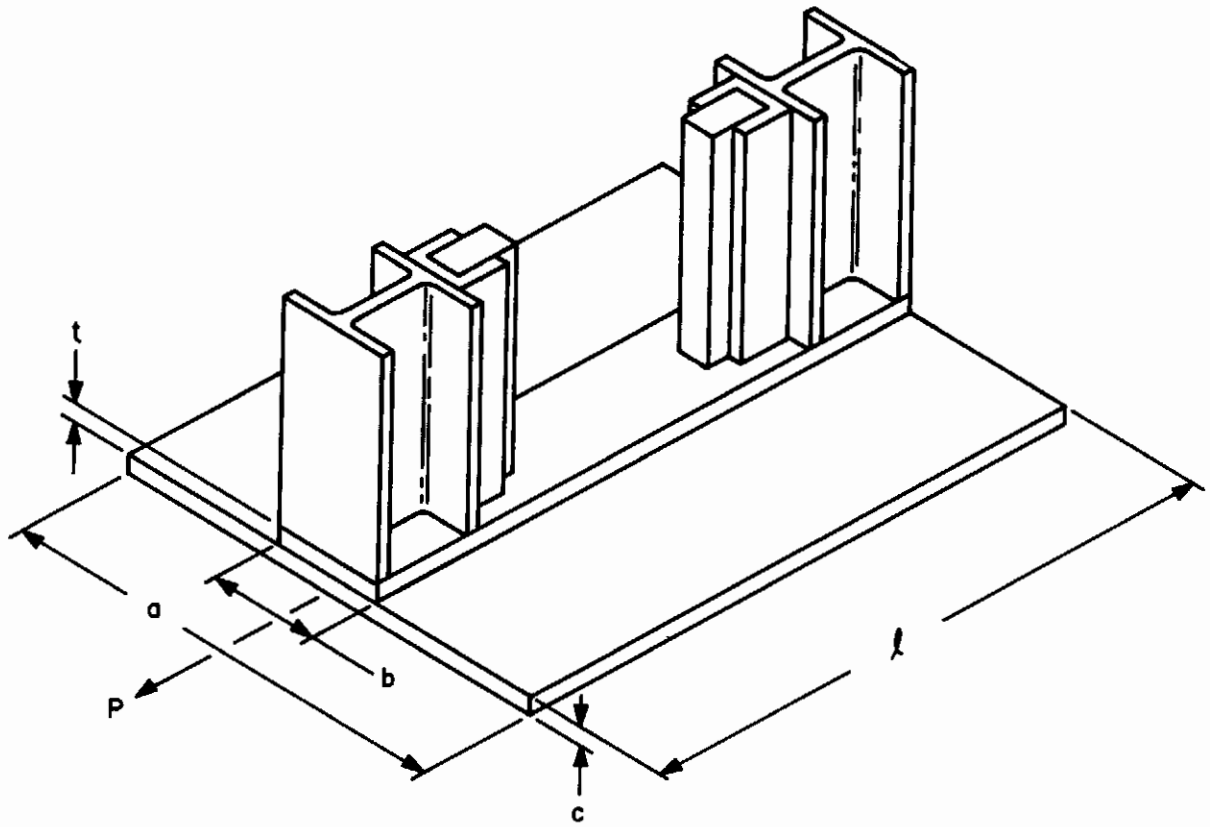

03-1167

Figure 46 SCANNER BOTTOM SUPPORT STRUCTURE LOAD DIAGRAM

Approved for Public Release

Contrails

ELONGATION OF SCANNER LOWER STRUCTURE

A load diagram is shown on Figure 46. The load is caused by the Preloaded Linear Scanner Carriage Support Bearings.

The elongation is determined by the following equation

$$\zeta_T = \frac{P\ell}{\Delta E}$$

Where

ζ_T = axial elongation in cm

P = 91 kgm bearing preload (200 lbs)

ℓ = 86.5 cm Length of Member (34 in.)

A = bt + ac = (15.25)(2.54) + (50.8)(2.54) = 167.8 cm^2

E = 2.11×10^6 kgm/cm^2 Youngs Modulus

$$\zeta_T = \frac{(91)\ (86.5)}{(167.8)\ (2.11 \times 10^6)} = 22.2 \times 10^{-6} \text{ cm}$$

$$= \underline{0.222 \text{ micron}} \quad (8.75 \text{ microinch})$$

LATERAL DEFLECTION OF TOP SCANNER SUPPORT MEMBER

The 6 x 6 x 5/8 inch angles that tie in the scanner support at the top are subjected to lateral forces when the scanner operates in this region. The scanner preload linear bearings transmit approximately a 91 kilogram force on two smaller angles and a flat plate, the elongation of these members is transmitted to the above side members. Based upon this elongation shown, the channel moment of inertia should not exceed this amount. A load schematic is shown on Figure 47. The maximum deflection equation for a simply supported beam with a concentrated load at its center is

$$* \ \zeta_{max} = \frac{P\ell^3}{48EI}$$

to find the size of the beam recommended

$$I = \frac{P\ell^3}{48E\zeta_{max}}$$

---

* Standard equation shown in any text on strength of materials.

Approved for Public Release

Contrails

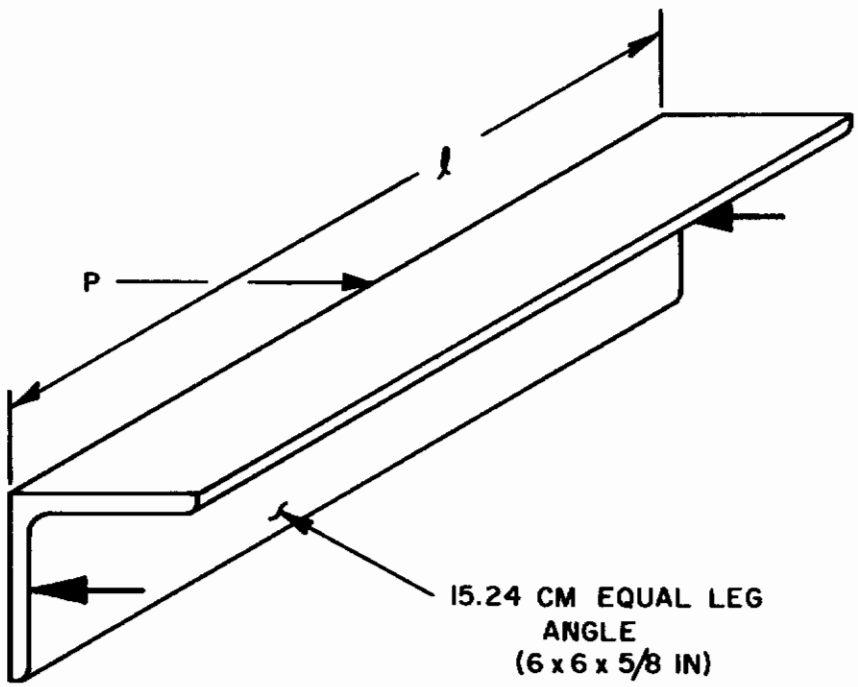

03-1167

Figure 47 SCANNER TOP SUPPORT SIDE MEMBER LOAD DIAGRAM

Approved for Public Release

Contrails

Where,

I = Moment of inertia of channel expressed in cm^4

P = 91 kg load due to bearing preload

ℓ = 50.8 cm beam length

E = 2.11×10^6 kgm/cm^2 (30×10^6 psi) Youngs Modulus

ζ_{max} = $0.425/2 \times 10^{-4}$ cm from another page

$$I = \frac{(91)\ (50.8)^3}{(48)\ (2.11 \times 10^6)\ (21.3 \times 10^{-6})}$$

$$= 5500\ cm^4\ (132\ in.^4)$$

A 6 x 6 x 5/8 in. angle has a moment of inertia of 1010 cm^4 (24.2 $in.^4$) which provides flexibility and avoiding buckling of the channel members tying the scanner assembly to the frame.

DEFLECTION OF OPTICAL WINDOW DURING LOADING

The window is supported in a frame at all four edges. The loading is uniform over the entire window. The analysis is performed in accord with "Formulas for Stress and Strain" by Raymond J. Roark, Table X, Case 30, Page 224, Fourth Edition.

$$y_{max} = -\frac{0.0487\ wa^4\ (m^2 - 1)}{m^2\ E\ t^3}$$

Where,

y_{max} = Maximum Deflection at the center in millimeters

w = Unit applied load in kgm/cm^2

= 2.521×0.953 = 2.40×10^{-3} gm/cm^2

a = Size of square window

m = $1/v$ = Reciprocal of Poissons Ratio = 1/.16 = 6.25

t = Thickness of Glass in centimeter = 0.953 cm

E = Modulus of Elasticity = 705000 gm/cm^2

Approved for Public Release

Contrails

$$y_{max} = -\frac{(0.0487)\ (2.40 \times 10^{-3})\ (122)^4}{(6.25)^2\ (7.05 \times 10^5)\ \ (0.953)^3}\ \ [\ (6.25)^2 - 1\ ]$$

$$= \underline{-\ 0.424\ \text{mm}}\quad (0.0167\ \text{in.})$$

its strength is determined as follows:

$$S_{max} = -\frac{0.2208\ wa^2\ \ (m + 1)}{m\ \ t^2}$$

where

S_{max} = Maximum stress in Glass due to uniform loading in kgm/cm^2

$$S_{max} = -\frac{(-02208)\ (2.40)\ (122)^2\ (6.25\ +\ 1)}{(6.25)\ (0.953)^2}\ \times\ 10^{-3}$$

$$= \frac{(-0.2208)\ (2.40)\ \ (1.48 \times 10^4)\ (7.25)}{(6.25)\ (0.91)}\ \times\ 10^{-3}$$

$$= \underline{10.0\ \text{kilograms/cm}^2}$$

The deflections for 1.27 cm and 2.54 cm thick windows follow

at $t = 1.27$ cm

$$y_{max} = -\frac{(0.0487)\ (2.40 \times 10^{-3})(122)^4}{(6.25)^2\ (7.05 \times 10^5)\ (1.27)^3}\ \ [\ (6.25)^2 - 1\ ]$$

$$= \underline{0.241\ \text{mm}\ \ (0.0095\ \text{in.})}$$

$\underline{t = 2.54\ \text{cm}}$

$$y_{max} = -\frac{(0.0487)\ (2.40 \times 10^{-3})\ (122)^4}{(6.25)^2\ (7.05 \times 10^5)\ (2.54)^3}\ \ [(6.25)^2 - 1]$$

Approved for Public Release

Contrails

APPENDIX III

INERTIA

LEAD SCREW INERTIA

Since the same type lead screw is used both in vertical drive and horizontal drive systems, the inertia is the same for each lead screw.

Since

$$I_\ell = \frac{w}{g}\frac{k^2}{22}$$

Where

I_ℓ = lead screw inertia expressed in gm-cm-sec^2

w = weight of lead screw expressed in grams

k = 1.59 cm (0.625 in.) radius of gyration

g = 980 cm/sec^2 gravitational acceleration

$$w = [\,(4.57)(1.9)^2 + (3.3)(2.79)^2 + (4.82)(3.05)^2 + (7)(3.05)^2 + (5.2)(3.05)^2$$

$$+ (0.71)(4.45)^2 + (2.03)(3.05)^2 + (137)(3.17)^2 + (2.67)(1.52)^2]\ \frac{(0.785)}{(0.126)}$$

$$= 9700 \text{ grams } (21.4 \text{ lbs})$$

Therefore,

$$I_\ell = \frac{(9700)}{(980)}\frac{(1.59)^2}{2} = \underline{12.6 \text{ gm-cm-sec}^2}$$

SCANNER CARRIAGE INERTIA

The Scanner Carriage reflects its translational inertia into rotational inertia at the lead screw and drive motor by the following relationships.

The Kinetic energy in translating the carriage is equal to the kinetic energy in rotation of the lead screw, barring losses.

Approved for Public Release

Contrails

Since

$$KE = \frac{1}{2} mv^2 = \frac{1}{2} I w^2$$

$$I = m \left(\frac{v}{w}\right)^2 = \frac{W}{g} \left(\frac{v}{n}\right)^2 \left(\frac{1}{2\pi}\right)^2$$

Where

W = weight of carriage at 91 kilograms

g = 980 cm/sec^2 acceleration due to gravity

v = 0.254 cm/sec Rectilinear motion of carriage

n = 1.0 rev/sec Rotation of lead screw shaft

$$I = \left(\frac{9100}{980}\right) \left(\frac{0.254}{1.0}\right)^2 \left(\frac{1}{2\pi}\right)^2 = \underline{0.152 \text{ gm-cm-sec}^2} \quad (1.31 \times 10^{-4} \text{ lb-in.-sec}^2)$$

FILM TRANSPARENCY SUPPORT INERTIA

The relationship worked out previously for the scanner carriage, to convert translational inertia into rotational form also works for this case equally well.

Therefore

$$I = \frac{W}{g} \left(\frac{v}{n}\right)^2 \left(\frac{1}{2\pi}\right)^2$$

Where

W = 159 kilograms weight of film transparency support

v = 0.254 cm/sec Rate of Motion of Support

n = 1.0 rev/sec Rate of Rotation of Lead Screw

$$I = \frac{(159000)}{(980)} \frac{(0.254)^2}{(1.0)} \left(\frac{1}{2\pi}\right)^2$$

$$= 0.265 \text{ gm-cm-sec}^2 \quad (2.3 \times 10^{-4} \text{ lb-in.-sec}^2)$$

Approved for Public Release

Contrails

VERTICAL GUIDEWAY ASSEMBLY CENTROID AND INERTIA CALCULATION

The Centroid is calculated as follows:

$$\bar{y} = \frac{A_1Y_1 + A_2Y_2 + \ldots\ldots A_nY_n}{A_1 + A_2 + \ldots\ldots A_n}$$

$$\bar{y} = \frac{(3.18)(5.4)(21.44) + (8.25)(5.72)(19.06) + (15.4)(16.2)(8.1) - (3.18)(3.18)(20.33)}{(3.18)(5.4) + (8.25)(5.72) + (15.4)(16.2) - (3.18)(3.18)}$$

$$- \frac{(7.42)(13.88)(8.1)\ (2)}{(7.42)\ (13.88)\ (2)}$$

$$= \frac{369 + 900 + 2020 - 205 - 1670}{17.2 + 47.2 + 250 - 10.1 - 206}$$

$$= \frac{1414}{98.3} = \underline{14.4\ \text{cm}}$$

The inertia of the vertical guideway assembly is then calculated as follows:

I-Beam = 2230 cm^4

Rect. Guideway = 76.8 cm^4

Channel

$$I = \frac{bh^3}{12}$$

$$= \frac{(8.25)(5.72)^3 - (3.18)(3.18)^3}{12}$$

$$= \frac{1540 - 102}{12} = \frac{1438}{12} = 120$$

$$= \underline{120\ \text{cm}^4}$$

Guideway A_d^2 = $(3.18)(5.4)(7)^2$ = 840 in^4

I-Beam A_d^2 = $[(15.4)(16.2) - (7.42)(13.88)(2)]\ (6.3)$ = 1740

Approved for Public Release

Contrails

$$\text{Channel } A_d^2 = (8.25)(5.72)(4.62) - (3.18)(3.18)(5.89) = 158.5$$

$$\text{Total } I = 2230 + 76.8 + 120 + 840 + 1740 + 158.5$$

$$= \boxed{5165 \text{ cm}^4}$$

HORIZONTAL GUIDEWAY ASSEMBLY CENTROID AND INERTIA CALCULATION

The inertia and centroid of the composite beam is determined by the following two equations:

$$\bar{y} = \frac{A_1y_1 + A_2y_2 - A_3y_3}{A_1 + A_2 - A_3} \quad \ldots, \text{ and } \quad I_T = I_1 + I_2 + A_1\bar{y}_1^2 + A_2\bar{y}_2^2 - A_3\bar{y}_3^2$$

Where

A = Represents section areas in cm^2

y = Represents distance in cm from area centroids to datum

$\bar{y}$ = Distance in cm between area centroids and composite centroid

I = Moment of inertia of sections expressed in cm^4 taken from tables

A	y	Ay	$\bar{y}$	$\bar{y}^2$	Ay^2	I
17.2	28.0	481	14.59	213	3670	76.8
478.0	11.4	5450	2.05	4.2	2010	11300.0
-353.0	11.4	-4020	2.05	4.2	-1480	-
142.2		1911			4200	11376.8

Therefore,

$$\bar{y} = \frac{\Sigma\, Ay}{\Sigma\, A} = \frac{1911}{142.2} = \underline{13.45 \text{ cm}}$$

And

$$I_T = \Sigma\, I + A\bar{y}^2 = 113.76.8 + 4200 = \underline{15576.8 \text{ cm}^4}$$

Approved for Public Release

Contrails

APPENDIX IV

WEIGHT

WEIGHT OF GLASS

$$W_G = \rho_G \ell^2 2t$$

Where

ρ_G = 2.61 gm/cc (0.094 lb/in^3) specific weight of glass

ℓ = 122 cm Length & height of glass

t = 0.95 cm (0.375 in.) glass thick

W_G = $(2.61)(122)^2(2)(0.95)$ = <u>73000 gm</u> (161 lbs)

WEIGHT OF FRAMEWORK

$$W_F = 2\rho_F \; [\, a\ell_1 t_1 + a\ell_2 t_1 \,]$$

Where

ρ_F = 2.61 gm/cc (Aluminum frame)

ℓ_1 = 122 cm Length of side arms

t_1 = 5.08 cm Frame thickness

a = 5.08 cm Frame width

ℓ_2 = 132 cm Length of top & bottom arms

$$W_F = (2)(2.61) \; [\, (5.08)(122)(5.08) + (5.08)(132)(5.08) \,]$$

$$= \frac{34000 \text{ gm}}{(75 \text{ lbs})} = 34 \text{ kgm}$$

WEIGHT OF STEEL CHANNEL

$$W_{CH} = \rho_s \; [bt_2\ell_2 + 2Ct_2\ell_2]$$

Approved for Public Release

Contrails

Where

ρ_s = 8 gm/cc Specific weight of steel

b = 7.6 cm width of channel

t_2 = 1.27 cm Channel thickness

ℓ_2 = 132 cm Length

C = 5.08 cm Depth

$$W_{CH} = (8) \quad [(7.6)(1.27)(132) + (2)(5.08)(1.27)(132)]$$

$$= \underline{23600 \text{ gm}} \quad (52 \text{ lbs})$$

Total Weight of Film Transport

Window	73000 gm
Frame	34000 gm
Steel Channel (2 pcs)	47200 gm
Bearings & Miscellaneous Hardware	4540 gm
TOTAL	158740 gm (350 lbs)

WEIGHT OF HORIZONTAL GUIDEWAY ASSEMBLY

The respective weights of the Horizontal Guideway and I-Beam are computed as follows:

Guideway ....

$$W_G = (3.18)(5.4)(132)(8) = 13200 \text{ grams}$$

$$\text{I-Beam} = 997 \frac{\text{gm}}{\text{cm}} \quad (67 \text{ lb/ft from table})$$

$$W_I = (997)(132) = 131000 \text{ gm}$$

$$\underline{131 \text{ kgm}}$$

$$W_T = 131000 + 18200 = 149200 \text{ gm}$$

$$= \underline{149.2 \text{ kgm}}$$

Approved for Public Release

Contrails

WEIGHT OF VERTICAL GUIDEWAY ASSEMBLY

The weight of the vertical I-Beam and guideway assembly is:
ω = 0.372 kilograms/cm (25 lb/ft) for I-Beam (from tables)

Therefore, total weight

$$W_I = (0.372)(168) = 62.5 \text{ kgm}$$

The guideway weight is

$$W_G = (3.18)(5.4)(168)(8) = 23100 \text{ gm}$$

$$= \underline{23.1 \text{ kgm}}$$

$$\rho_s = 8 \text{ gm/cc}$$

Specific weight of steel

The Channel

$$W_c = [(2.54)(8.25) + (3.18)(2.54)(2)] \quad (168)(8) = 50000 \text{ gm}$$

$$= \underline{50 \text{ kgm}}$$

Total Assembly Weight

$$W_T = 62.5 + 23.1 + 50$$

$$= \underline{135.6 \text{ kgm}}$$

Approved for Public Release

Contrails

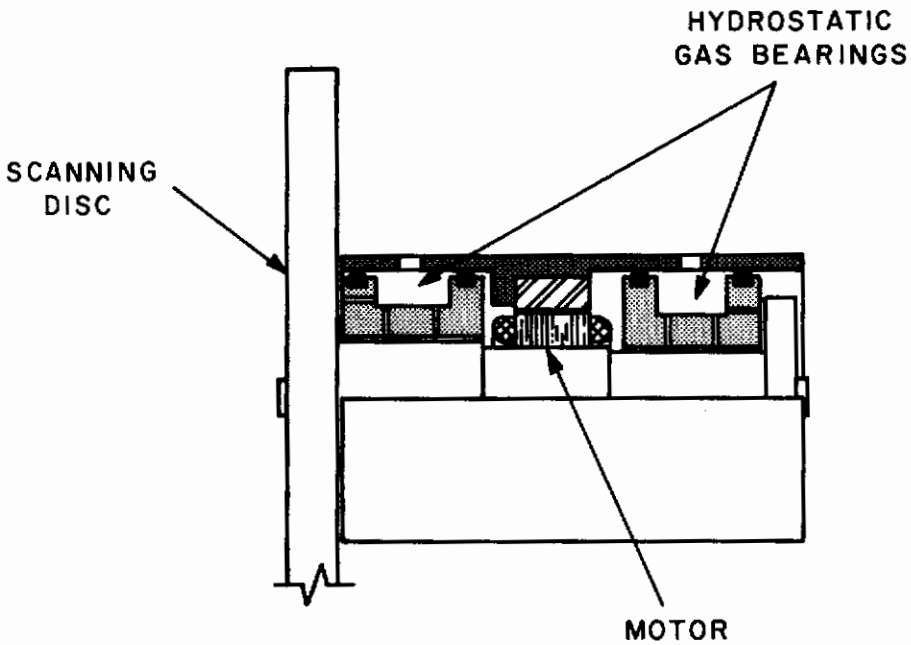

(a) DRIVE MOTOR CONFIGURATION

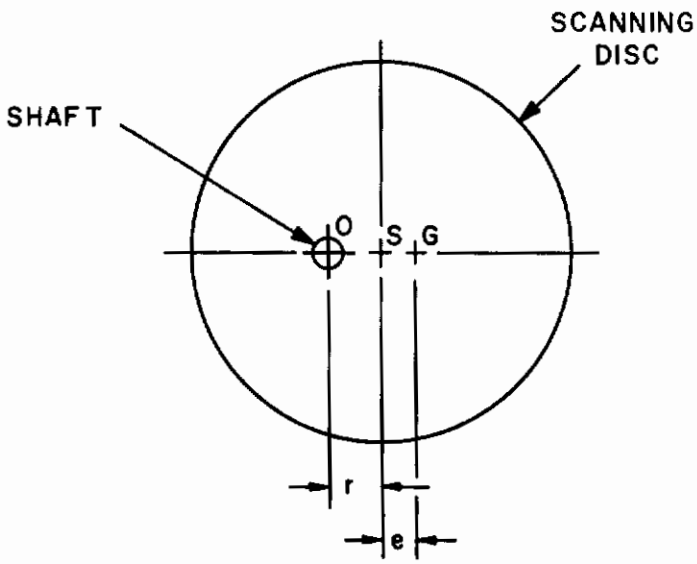

(b) EXAGGERATED VIEW OF SHAFT DISPLACEMENT

03-1167

Figure 48 SCANNER DRIVE MOTOR SHAFT DISPLACEMENT

Approved for Public Release

Contrails

APPENDIX V

SYSTEM VIBRATION

GENERAL

The system configuration illustrated in Figure 6 and discussed in this report exhibits high structural rigidity. A systematic check on the critical drive components and directly affected support components are given in the following analysis. The natural frequencies and drive frequencies are listed in Table IX. A comparison of values shown in this table indicates that the rotary to linear drive systems featuring lead screws have a high natural frequency compared to the maximum simulated aircraft speeds. This indicates that lead screw or drive perturbations will be self dampening due to the high spring rates of components involved. The most serious threat appears to be the scanner disc driven at 5000 revolutions per minute. However, even in this case the shaft critical speed is much higher than the speed shown above. Some loading is transmitted to adjacent structure but is of such a low magnitude that it will not significantly disturb position accuracy. It is therefore concluded that the system is structurally sound and should not suffer any vibration problems.

VIBRATION ANALYSIS OF SCANNER SHAFT AND DISC

Figure 48 depicts the exaggerated displacements of center of gravity "G" of disc and geometric center "S" of disc with respect to bearing centerline "O" as shown in view (b). This analysis is intended to show the amplitude of lateral vibration and force transmitted to the bearings and structure. Neglecting the effect of gravity and friction there are two forces which affect the disc: the restoring force of the shaft tending to straighten itself and centrifugal force acting through center of gravity G. The two forces oppose each other. Therefore equating the two will solve for lateral deflection or amplitude

$$kr = m\omega^2 (r + e)$$

Solving for

r, Since, $\omega_n = \sqrt{K/m}$

$$r = \frac{m\omega^2 e}{k - m\omega^2}$$

$$r = \frac{(\omega/\omega_n)^2 e}{1 - (\omega/\omega_n)^2}$$

Where

r = amplitude of vibration expressed in cm.

Approved for Public Release

Contrails

TABLE IX

SYSTEM NATURAL FREQUENCIES

Components	Frequency in CPS Natural	Drive Frequency
x - lead screw	331	0.01 - 1.0
y - lead screw	313	0.01 - 1.0
x - Guideway Assembly	457	---
y - Guideway Assembly	143	---
Linear Bearing	10,000	0.0016 - 0.16
Scanner Gas Bearing	630	83.3
Scanned Disc and Shaft	505	83.3

Approved for Public Release

Contrails

$$\omega = 5000 \text{ RPM} \times \frac{2\pi}{60} = \underline{523 \text{ Radians/sec}} \text{ shaft speed}$$

$$= \underline{83.3 \text{ CPS}}$$

$$e = 37.5 \times 10^{-6} \text{ cm}$$ Approximate eccentricity after balancing operation

$$\omega_n = \sqrt{K/m} = \sqrt{\frac{g}{\delta}}$$ Shaft lateral natural frequency

The natural frequency is thereby determined from the deflection characteristics of the shaft based upon a simply supported shaft on two gas bearings and with the disc creating a bending moment about its left support. The end loaded cantilever case most nearly approximates this condition.

Therefore,

$$\delta = \frac{P\ell^3}{3EI}$$

Where

$$P = (0.785)(17.8)^2(0.958)(2.77) = \underline{657 \text{ gram Disc load}}$$

$$\ell = 1.77 \text{ cm shaft overhang}$$

$$E = 2.11 \times 10^6 \text{ gm-cm } (30 \times 10^6 \text{ psi})$$ Youngs Modulus

$$I = \frac{\pi D^4}{64} = \frac{(3.31)^4}{64} = 5.94 \text{ cm}^4$$ Moment of inertia

$$\delta = \frac{(657)(1.77)^3}{(3)(2.11 \times 10^6)(5.94)} = 0.000097 \text{ cm}$$

$$\omega_n = \sqrt{\frac{980}{0.000097}} = \underline{3180 \text{ Radian/sec}} \quad (505 \text{ cps})$$

Therefore

r is

$$r = \frac{(\omega/\omega_n)^2 e}{1 - (\omega/\omega_n)^2} = \frac{(523/3180)^2(37.5 \times 10^{-6})}{1 - (523/3180)^2}$$

$$= \underline{1.04 \times 10^{-6} \text{ cm Amplitude}}$$

Approved for Public Release

Contrails

The force transmitted to the gas bearings and structure is

$$F = m(r + e)\omega^2 = \frac{w}{g}(r + e)\omega^2$$

Where

$$W_T = \text{Total weight of disc and shaft}$$

$$W_{Disc} = (0.785)(17.8)^2(0.958)(2.77) = 657 \text{ gm}$$

$$W_{Shaft} = (0.785)(2.54)^2(11.4)(8) = 462 \text{ gm}$$

$$W_T = W_{Disc} + W_{Shaft} = 657 + 462 = \underline{1120 \text{ gm}}$$

$$F = \left(\frac{1120}{980}\right) \quad (1.04 + 37.5)(10^{-6})(523)^2 = \underline{12 \text{ gm}}$$

This force represents

$$\frac{12}{91000} \times 100 = 0.0132\%$$

of the loading imposed on the scanner supporting guideway structure and will not degrade positioning accuracy of scanner drive system. The speed of operation is well below the critical frequency of the scanner drive shaft and the scanner disc drive does not have to cross this critical frequency during stops and starts, thereby avoiding resonance and subsequent destructive vibration.

SCANNER GAS BEARING NATURAL FREQUENCY

The bearing stiffness recommended by the gas bearing supplies is:

$$K = 17900 \text{ kgm/cm}$$

The weight of spindle and scanner disc $W = 1.120$ kgm

$$f_n = \frac{1}{2\pi}\sqrt{\frac{K}{m}} = \frac{1}{2\pi}\sqrt{\frac{KG}{W}}$$

$$= \frac{1}{2\pi}\sqrt{\frac{(17900)(980)}{(1.120)}} = \underline{630 \text{ cps}}$$

NATURAL FREQUENCY OF HORIZONTAL GUIDEWAY ASSEMBLY

The natural frequency of the aforementioned assembly is determined by the following step by step analysis:

Approved for Public Release

Contrails

The Beam Deflection is determined first

$$y = \frac{1}{48EI}\{8P\frac{d}{\ell}(x^3 - \ell^2 x) = Px\left[\frac{8d^3}{\ell} - \frac{2bc^2}{\ell} + \frac{c^3}{\ell} + 2c^2\right]$$

@ a = x = 45.75 cm, d = 43.2 cm, b = 132 cm, c = 86.4 cm

$$y = \frac{1}{(48)(2.11 \times 10^6)(15576.8)}\left\{\frac{(8)(104)(43.2)}{132}\left[(45.75)^3 - (132)^2(45.75)\right]\right.$$

$$\left. + (104)(45.75)\left[\frac{(8)(43.2)^3}{132} - \frac{(2)(132)(86.4)^2}{132} + \frac{(86.4)^3}{132} + (2)(86.4)^2\right]\right\}$$

$$= \underline{0.0000832 \text{ cm}}$$

Since $f_n = \frac{1}{2\pi}\sqrt{\frac{PG}{wy}}$

Where

P = 104 kgm

(See second page of Appendix IV, WEIGHT OF HORIZONTAL GUIDEWAY ASSY)

w = 149 kgm

y = 0.0000832 cm

G = 980 cm/sec^2

$$f_n = \frac{1}{2\pi}\sqrt{\frac{(104)(980)}{(149)(8.32 \times 10^{-5})}} = \underline{457 \text{ cps}}$$

NATURAL FREQUENCY OF VERTICAL GUIDEWAY ASSEMBLY

The natural frequency of the subject assembly is determined by first calculating the beam deflection characteristics as follows:

$$X = \frac{1}{48EI}\left\{\frac{8wd}{\ell}(y^3 - {}^2y) + W_y\left[\frac{8d^3}{\ell} - \frac{2bc^2}{\ell} + \frac{c^3}{\ell} + 2c^2\right] - \frac{2w(y-a)^4}{c}\right\}$$

Approved for Public Release

Contrails

at $y = 84$ cm, $a = 73.8$ cm, $b = 94$ cm, $d == 84$ cm

$$X = \frac{1}{(48)(2.11 \times 10^6)\ (5165)} \left\{ \frac{(8)\ (91)\ (84)}{168} [(84)^3 - (168)^2\ (84)] \right.$$

$$+ (91)\ (84) \left[\frac{(8)\ (84)^3}{168} - \frac{(2)\ (94)\ (20.3)^2}{168} + \frac{(20.3)^3}{168} + (2)\ (20.3)^2 \right]$$

$$\left. - \frac{(2)\ (91)\ (84 - 73.8)^4}{20.3} \right\} = \underline{8.1 \text{ micron}} \quad (324 \text{ microinches})$$

Since

$$f_n = \frac{1}{2\pi} \sqrt{\frac{K}{m}} = \frac{1}{2\pi} \sqrt{\frac{P/X}{W/g}} = \frac{1}{2\pi} \sqrt{\frac{Pg}{Wx}}$$

Where

P = 91 kgm beam loading

g = 980 cm/sec^2 Gravitational acceleration

W = 135.6 kgm weight of assembly. See 3rd page of Appendix IV, Weight of Vertical Guideway Assembly.

X = 8.1×10^{-4} cm beam deflection

$$f_n = \frac{1}{2\pi} \sqrt{\frac{(91)\ (980)}{(135.6)\ \ (8.1 \times 10^{-4})}} = \frac{1}{2\pi} \sqrt{81200}$$

$$= \underline{143 \text{ cps}}$$

LINEAR BEARING NATURAL FREQUENCY

The bearings' natural frequency is determined as follows:

$$f_n = \frac{1}{2\pi} \sqrt{\frac{k}{m}}$$

Where

f_n = Bearing natural frequency expressed in cycles per second

Approved for Public Release

Contrails

$k = 9.12 \times 10^8$ gm/cm (5.1×10^6 lb/in.) Spring Rate

$m = \frac{w}{g} = \frac{227}{980} = 0.232 \frac{\text{gm-sec}^2}{\text{cm}}$

$w = 227$ gm (0.5 lbs)

$g = 980$ cm/sec^2 Gravitational acceleration

Therefore,

$$f_n = \frac{1}{2\pi} \sqrt{\frac{9.12 \times 10^8}{0.232}} = \underline{10{,}000 \text{ cps}}$$

LEAD SCREW NATURAL FREQUENCY

The natural frequency is a function of the following relationship

$$f_n = \frac{1}{2\pi} \sqrt{\frac{R}{I_\ell}}$$

Where,

$R = I =$ Torsional spring constant expressed in θ gm-cm/radians

$I_\ell = 12.6$ gm-cm-sec^2 lead screw inertia as computed in Appendix III, LEAD SCREW INERTIA

$T = 485$ gm-cm load torque on horizontal lead screw shaft

$\theta = \frac{T\ell}{E_s J}$ equals torsional deflection of lead screw expressed in radians.

$\ell =$ Length of lead screw $= 153$ cm

$E_s = 8.45 \times 10^8$ gm/cm^2 Shear modulus for steel (12×10^6 psi)

$J = \frac{\pi D^4}{32} =$ Polar moment of inertia of lead screw

$D = 3.18$ cm nominal dia. of lead screw

Therefore,

$$J = \frac{\pi D^4}{32} = \frac{\pi\ (3.18)^4}{32} = 9.9 \text{ cm}^4 \quad (0.238 \text{ in.}^4)$$

Then,

$$\theta = \frac{T\ell}{E_s J} = \frac{(485)\ (153)}{(8.45 \times 10^8)\ (9.9)} = \underline{8.85 \times 10^{-6} \text{ radians}}$$

Approved for Public Release

Contrails

and,

$$R = \frac{T}{\theta} = \frac{485}{8.85 \times 10^{-6}} = 5.5 \times 10^{7} \ \frac{\text{gm-cm}}{\text{radian}}$$

The Horizontal lead screw natural frequency is therefore,

$$f_n = \frac{1}{2\pi} \sqrt{\frac{R}{I_\ell}} = \frac{1}{2\pi} \sqrt{\frac{5.5 \times 10^{7}}{12.6}} = \underline{\underline{331 \ \frac{\text{Cycles}}{\text{Sec}}}}$$

The vertical lead screw, which is geometrically similar, differs in its loading,

where

$$T = 420 \text{ gm-cm}$$

$$R = \frac{T}{\theta} = \frac{420}{8.85 \times 10^{6}} = 47.5 \times 10^{6} \ \frac{\text{gm-cm}}{\text{radian}}$$

and consequently, vertical screw

$$f_n = \frac{1}{2\pi} \sqrt{\frac{R}{I_\ell}}$$

$$= \frac{1}{2\pi} \sqrt{\frac{47.5 \times 10^{6}}{12.6}} = \underline{\underline{313 \text{ Cycles/Sec}}}$$

Approved for Public Release

Contrails

Security Classification

DOCUMENT CONTROL DATA - R & D

(Security classification of title, body of abstract and indexing annotation must be entered when the overall report is classified)

1. ORIGINATING ACTIVITY *(Corporate author)*
CBS Laboratories
227 Highridge Road
Stamford, Connecticut 06905

2a. REPORT SECURITY CLASSIFICATION
UNCLASSIFIED

2b. GROUP
N/A

3. REPORT TITLE
DESIGN STUDY FOR RADAR LAND MASS SIMULATION SYSTEM

4. DESCRIPTIVE NOTES *(Type of report and inclusive dates)*
Final Report, February 1967 - October 1967

5. AUTHOR(S) *(First name, middle initial, last name)*
Ivan H. Shim
Alfred E. Mletzko
Jon I. Wigby

6. REPORT DATE
May 1968

7a. TOTAL NO. OF PAGES
133

7b. NO. OF REFS
0

8a. CONTRACT OR GRANT NO. F33615-67-C-1400

b. PROJECT NO. 6114

c. Task No. 611414

d.

9a. ORIGINATOR'S REPORT NUMBER(S)

9b. OTHER REPORT NO(S) *(Any other numbers that may be assigned this report)*
AMRL-TR-68-8

10. DISTRIBUTION STATEMENT
Distribution of this document is unlimited. It may be released to the Clearinghouse, Department of Commerce, for sale to the general public.

11. SUPPLEMENTARY NOTES

12. SPONSORING MILITARY ACTIVITY
Aerospace Medical Research Laboratories
Aerospace Medical Div., Air Force Systems Command, Wright-Patterson AFB, OH 45433

13. ABSTRACT

A design study and investigation to determine the requirements for the mechanical and electrical components of a Radar Land Mass Transparency System has been performed. The technique consists of moving a laser beam across a 122 cm square transparency to simulate the side-looking radar system of an aircraft. The most promising system of those considered from accuracy, complexity and cost considerations is shown to be a horizontally driven transparency with a vertically driven flying spot scanner. The spot, in its vertical heading, scans out a strip 5 cm wide. Spot size can be kept to 2.5 microns over the 5 cm scan length at any location on the transparency. Smoothness of motion to simulate an aircraft is achieved through a feedback control system designed to move at constant velocity. An overriding position loop will correct for any accumulated errors which could result from environmental or load condition changes. A position accuracy of $\pm$ 0.00127 cm over the entire transparency is shown to be quite feasible. In addition, the speed range from low flying aircraft to satellites of approximately 100:1 is also shown to be feasible using the same system. Mechanical and electrical components chosen for performance calculations and tolerance determinations are off-the-shelf. These parts are easier to acquire and lower in cost than equivalent custom made components.

DD FORM 1 NOV 65 1473

Security Classification

Approved for Public Release

Contrails

Security Classification

14. KEY WORDS	LINK A ROLE	LINK A WT	LINK B ROLE	LINK B WT	LINK C ROLE	LINK C WT
Side-looking radar						
Simulation						
Mechanical system analysis						
Mechanical system components						
System maintainability						
Dual transparency readout system						
Control system design						
Low-flying aircraft and satellites						

Security Classification

Approved for Public Release